21014

NATIONAL LIBRARY
OTTAWA

BIBLIOTHÈQUE NATIONALE
OTTAWA

NAME OF AUTHOR....Donald James GATES.....

TITLE OF THESIS....On the Mechanism of.....
....Bacteriophage T4 Neutralization.....
.....

UNIVERSITY.....University of Alberta.....

DEGREE FOR WHICH THESIS WAS PRESENTED.....M. Sc.....

YEAR THIS DEGREE GRANTED.....1974.....

Permission is hereby granted to THE NATIONAL LIBRARY OF CANADA to microfilm this thesis and to lend or sell copies of the film.

The author reserves other publication rights, and neither the thesis nor extensive extracts from it may be printed or otherwise reproduced without the author's written permission.

(Signed).....Don Gates.....

PERMANENT ADDRESS:

#8, 10650 - 83rd AVE
EDMONTON, ALTA
.....

DATED.....Feb 8.....1974

NL-91 (10-68)

THE UNIVERSITY OF ALBERTA

ON THE MECHANISM OF BACTERIOPHAGE T4 NEUTRALIZATION.

by

© DONALD JAMES GATES

A THESIS

SUBMITTED TO THE FACULTY OF GRADUATE STUDIES AND RESEARCH

IN PARTIAL FULFILMENT OF THE REQUIREMENTS FOR THE DEGREE

OF MASTER OF SCIENCE.

DEPARTMENT OF MICROBIOLOGY

EDMONTON, ALBERTA

SPRING, 1974

THE UNIVERSITY OF ALBERTA

FACULTY OF GRADUATE STUDIES AND RESEARCH

The undersigned certify that they have read, and recommend to the Faculty of Graduate Studies and Research, for acceptance, a thesis entitled

"On The Mechanism Of Bacteriophage T4 Neutralization."

submitted by Donald James Gates

in partial fulfillment of the requirements for the degree of Master of Science.

.....
Supervisor

.....

.....

.....

Date January 29, 1974

ABSTRACT

Neutralization of bacteriophage T4 with monovalent antibody fragments proceeds with apparent two-target kinetics. The effect of such neutralization on the normal adsorption characteristics of phage suggests the formation of a slower adsorbing class results from a single tail fiber-Fab' interaction. The resulting adsorption profiles are consistent with those predicted for a mixture of fast (P^0) and slow (P^1) adsorbers. The concentrations of each class are predictable from a Poisson distribution of the different neutralizing Fab' dosages over the input phage population. These changes in adsorption are not due to reformation of the fast adsorbing class through dissociation of the [Fab'-phage] complex, since the observed rate of dissociation could not account for adsorption of the P^1 class.

Evidence further supporting this model arises from changes in adsorption characteristics of <u>in vitro</u> complemented fiberless T4 particles. Adsorption characteristics of particles in different stages of activation again suggest a mixture of fast and slow adsorbing phage, each possessing identical adsorption characteristics of the P^0 and P^1 classes, respectively.

These observations are compatible with the concept of functional inactivation of a single fiber imposed by one "hit". Although further insight into the molecular basis of this "hit" was not obtained from blocking experiments, the tail fiber antigens coded in genes 34 and 37 appear to play the largest role in blocking specific neutralizing antisera.

ACKNOWLEDGEMENTS

I wish to thank Dr. Gerry Stemke for his patient guidance and direction throughout the course of this work. Our many informative and stimulating discussions have been invaluable in the development of the ideas in this thesis.

I owe a great debt to Dr. Bill Knight, who kindly provided the computer programs for the adsorption model. A special thanks also goes to Dr. Ed Butz for the calculations involving Fab' dissociation, and to "Charlie" Huneycutt for the Calcomp programs used for most of the plots on adsorption and neutralization.

I am most grateful to the other members of my committee for their assistance in the preparation of this thesis, notably to Drs. K.L. Roy and Doug Scraba, who laboured over numerous unclear passages. To Mrs. Wilma Melnychuk, I owe a special thanks for her excellent technical assistance.

Financial support for this work has been provided through Graduate Teaching and Research Assistantships by the University of Alberta, from grants awarded to Dr. Stemke by N.I.H. and N.R.C., and by my loving wife, Janet, who has also provided the kind and gentle encouragement needed so often.

TABLE OF CONTENTS

PAGE

INTRODUCTION 1

MATERIALS AND METHODS 14

a. Phage and Bacterial Stocks 14

b. Terminology and Definitions 14

c. Media and Growth Conditions 20

d. Chemicals 21

e. Phage Preparations 22

f. Purification of Fiberless T4 Particles 24

g. Antiserum and Neutralization Assays 26

h. Calculation of Titer and Fragment Dosage 27

i. Phage Adsorption Assays 30

j. *In Vitro* Complementation Assays 30

k. Serum Blocking Assays 31

l. Lysozyme Assays 32

m. Electron Microscopy 33

n. Column Chromatography and Sedimentation Characteristics of Ferritin-Labelled IgG 34

o. Computing Facilities and Programs 38

RESULTS-PART I 39

A. Phage Adsorption: Effect of Fab' Treatment ...39

i. Adsorption Profiles of Untreated Phage .40

ii. Bacterial Concentration Effects 43

iii. Fab' Treatment 45

PART I (cont'd)

B. [Fab'-Phage] Dissociation 47

i. Aging of the [Fab'-Phage] Complex 48

ii. Experimental Kd Value 49

iii. Fitting of Kd 53

C. Activation of Fiberless Particles 56

i. Titer Increase With Time 58

ii. Changes in Adsorption Profiles 61

iii. C^0 Generation 63

D. Adsorption Profiles of Amber Mutants 65

E. Electron Microscopy 69

RESULTS-PART II 71

A. Normalization of Mutant Lysates 72

i. Uniform Infected Centers 72

ii. Burst Size Comparisons 74

iii. Lysozyme Activities 75

B. Serum Blocking Power of Mutant Lysates 77

DISCUSSION 87

SUMMARY 114

BIBLIOGRAPHY 116

APPENDIX A 123

LIST OF TABLES

TABLE	DESCRIPTION	PAGE
I	Stock Phage Descriptions	15
II	Adsorption Rate Constants for amN122	42
III	Fitting of Dissociation Constant, Kd	57
IV	Rate Constants For Amber Mutants	68
V	Normalization of Lysates for Serum Blocking Experiments	73

LIST OF FIGURES

FIGURE PAGE

1. Sedimentation Profiles of PEG and Perritin 35
2. Elution Profile of Commercial PEG 36
3. Adsorption Profiles of Untreated Phage (amN122) on *E. Coli* B/1 41
4. Effect of Bacterial Concentration on Kinetics of Phage Adsorption 44
5. Fab' Treatment: Effect on Adsorption Profile of amN122 46
6. Dissociation of Fab' at 22°C:Changes in Adsorption Profile of "0.4-Hit Phage" 50
7. Dissociation of Fab' at 37°C:Changes in Adsorption Profile of "0.8-Hit Phage" 51
8. Apparent Dissociation of Fab'-Phage Complex at 22°C and 37°C:Residual Hits v/s Incubation Time 52
9. Effect of Varying Kd Values on Simulated Phage Adsorption Profiles: 0.4 and 0.5 Hit Data 54
10. Effect of Varying Kd Values on Simulated Phage Adsorption Profiles: 0.8 and 1.2 Hit Data 55
11. *In Vitro* Complementation of Fiberless T4 Particles With N23-10 Lysate 59
12. Adsorption Profiles of *In Vitro* Complemented Phage at Various Times in the Activation Process 62
13. Activation of Fiberless T4 Particles:Rate of C^0 Production 64
14. Adsorption Characteristics of Amber Mutants (Normal Adsorbers) 66
15. Adsorption Characteristics of Amber Mutants (Slow Adsorbers) 67

16. Residual Neutralizing Activity of Anti-T4 Blocked with M34 Lysate 78

17. Residual Neutralizing Activity of Anti-T4 Blocked with M35 Lysate 79

18. Residual Neutralizing Activity of AntiT4 Blocked with Double Mutant (DM) Lysate 80

19. Residual Anti-T4 Activity After Blocking With Wild Type T4 Control Lysate 82

20. Residual Anti-T4 Activity After Blocking With Wild Type T4 "Blank" Lysate Control 83

21. Summary of Serum Blocking Activities of Amber Mutant Lysates 86

22. Predicted Survival Curves of One-Hit, Multi-Hit and Multi-Target Phage Neutralization Models 90

23. Dosage Effects on Phage Class Concentrations and Ratio of [P^0:(P^0+P^1)] 93

INTRODUCTION

Bacterial viruses, by virtue of their biological "simplicity", have proven invaluable in numerous types of investigations. Antibody neutralization of bacteriophages has provided many versatile models with which to study biological multi-component reactions. The model for neutralization of T4 is one of the more complex, because of the numerous antigenically and functionally different structures of this particular phage. The importance of understanding not only the kinetics, but the mechanisms involved in phage neutralization can be evidenced by its use as an extremely sensitive biological assay of specific antibody concentrations (Makela, 1966; Haimovich and Sela, 1969; Blakeslee, et.al. , 1973; Hornick and Karush, 1969; Barber and Rittenberg, 1969).

Inactivation of phage by antibodies normally proceeds via a first order or single-hit mechanism (Hershey, 1941; Cann and Clark, 1954; Jerne and Skovsted, 1953). The importance of antibody bivalence, together with the monogamous interaction of IgG with phage, offers the most satisfactory explanation for this first order process of inactivation to date (Blank, et. al. , 1972; Dudley, et. al. , 1970; Klinman, et.al. , 1967; Witte and Slobin, 1972).

Recent advances in molecular biology and immunochemistry have led to a greater understanding of not

only the basic kinetic interpretations of the system, but also to the deviations from first order which accompany extremes in phage or antibody concentrations (Hale, et.al. 1969). Vargues and Vollet (1973) have reviewed the development of immunological kinetics, outlining chronologically the significant ideas and proposals concerning phage neutralization. Observations ranging from initial pseudo-first order kinetics to collision theory and critical binding site predictions are correlated with the mathematical derivations in their review.

Deviations from first order neutralization kinetics (in the case of the T-even phage) have previously been attributed to phage and antibody heterogeneity. Such deviations are not usually evident over several orders of magnitude of antibody concentration, as neutralization curves are reproducibly proportional over such limits. A significant reduction in the complexity of the system (neutralization of the T-even phages) was established upon finding that only anti-tail fiber activity was responsible for all or most inactivation (Franklin, 1961; Edgar and Lielausis, 1965; Stemke, et.al. , in press). Antibodies to other antigenic structures on the phage do not play a significant role in neutralization.

Numerous workers have used monovalent antibody fragments produced from enzymatic digestion of IgG to elucidate further the mechanism of phage neutralization

(Dudley, et. al. , 1970; Goodman and Donch, 1964, Stemke, 1969; Klinman et.al. , 1967). These monovalent fragments demonstrate very different neutralization kinetics, and have lead to an hypothesis in which inactivation results from multiple independent interactions between phage and neutralizing agent. These kinetics are distinct from the monogamous binding effects evident from neutralizing studies employing divalent IgG (Goodman and Donch ,1964; Stemke, 1969, Karush, 1970).

One notable difference in this system is the decreased effectiveness of the monovalent fragments in neutralizing phage as compared to that of divalent antibodies. Only 10 to 20% of the neutralizing activity of IgG remains after digestion and reduction, but no significant change is observed in affinity of the individual combining sites (Goodman and Donch, 1964; Stemke, 1969).

Characteristic of these studies employing monovalent fragments in neutralization is the observation of a distinct lag in the inactivation curve. This lag preceeds the typical exponential decrease in phage titer in the kinetic assay normally used. Such a lag is a result of multiple combinations of fragment with phage being required for neutralization, and has led to a two-target hypothesis for neutralization of phage by monovalent antibody molecules (Stemke, 1969).

The interaction of T4 with neutralizing antibodies presumably affects the adsorption of the phage to its host, thus preventing infection of the bacterium (Lanni and Lanni, 1953; Franklin, 1961; Nagano, et.al. , 1956). Adsorption kinetics of untreated phage indicate an initial first order reaction, characteristic of diffusion controlled processes, but the adsorption curve rapidly deviates from linear exponential kinetics.

Several models for the mechanism of adsorption of T4 have been proposed (Gamow, 1969). Evidence supports the idea that formation of an initial reversible complex between phage and host, followed by irreversible decay of the complex to an infected bacterium are the major steps in the mechanism. The question still remains as to the precise number of fibers required for adsorption, however.

This [reversible-complex] model for adsorption offers a means to examine the Fab'-effected neutralization process by allowing the prediction of an intermediate adsorbing class of phage which exhibits less efficient adsorption characteristics than the untreated phage. Further explanations outlining this adsorption and neutralization model will follow in various parts of the text.

One important question imposed by the multi-target hypothesis of Fab' neutralization is that of the actual target of the inactivating molecule. In divalent IgG

neutralization, the role of bridging of two fibers or inactivation of only a single fiber as the explanation for inactivation has not been clarified. Binding of the monovalent antibody to a single fiber would possibly interfere with the functional integrity of that fiber with respect to its role in adsorption.

It has been established that the effects of dissociation of the divalent agent are insignificant in the neutralization of phage (Bowman and Patnode, 1964; Krummel and Uhr, 1969). Thus, the divalent nature of IgG contributes significantly to the stability of the phage-antibody complex (Karush, 1970). Use of the monovalent fragment would result in an increase in the rate of dissociation of the complex. This dissociation would further complicate any mathematical solutions to the kinetics.

Since neutralization of phage by either divalent antibody or monovalent antibody fragments presumably is due to impairment of phage-bacterial adsorption, one should examine the state of knowledge of the "organs" of such interactions, the tail fibers. Much of this knowledge has been acquired by the use of conditional lethal mutants of the T-even phages (Epstein, et. al., 1963). A further explanation of this portion of the study will follow a brief explanation of nonsense mutations and their use in deriving the different antigenic regions of the tail fibers of T4.

The mechanism of such conditional lethal nonsense mutations has been well documented (Garen, 1968; Zipser, 1969). Chain termination at the site of the mutation in the phage genome arises from the non-translatable nature of the nonsense codons in these conditional lethals. The presence of suppressor genes in the permissive (i.e., non-lethal) host bacteria, however, permits these codons to be translated. The nature of the suppression of the nonsense codon involves the synthesis of altered tRNA molecules in the Su+ host. These altered tRNA's can recognize the nonsense triplet.

In amber mutants, the nonsense codon consists of the UAG triplet. This triplet can only be read in the Su+ host (*E. coli* CR63 in this study), whose suppressor tRNA can insert an amino acid (e.g., serine) at the site of the mutation. Such an insertion does not normally alter the function of the gene product significantly, unless the insertion is at a highly critical site in the polypeptide. Thus, near normal burst size and viability is maintained on the permissive host. Under Su- conditions (*E. coli* B/1), the mutant gene product is essentially absent in lysates (for example, a specific enzyme or structural component of the phage).

There are, however, secondary effects imposed on this interpretation of amber mutants. Some of these are

characteristic of most amber mutations, and some are highly specific to the fiber cluster of the T4 genome. These secondary effects are paramount to the questions asked in this thesis concerning the blocking power of lysates prepared from tail fiber mutants, grown on the restrictive host. Further explanations and interpretations will be left for the discussion of observations of serum blocking power of the lysates examined.

A great deal of work has been carried out on phage T4 tail fiber structure and function in the past decade. Initially, the aim of such research was to understand the overall morphological nature of fiber morphogenesis and fiber addition to precursors. Serological analysis has proven invaluable in the majority of these investigations, and the fiber antigenic structure, even to gene product subdivision, has been well documented in the past few years (Yanagida and Ahmed-Zadeh, 1970; Beckendorf, 1973; Ward, et.al. , 1970; King and Wood, 1969).

Edgar and Lielausis (1965) showed the existence of three antigenic components of T4 tail fibers, and postulated their importance in neutralization. This classification of the A, B and C antigens has been maintained since then, and correlated further to include gene product identification, characterization, and, most recently, complete isolation (Eiserling, et.al. , 1967; Imada and Tsugita, 1970,1972a,b; Beckendorf, 1973). The composition of the fiber will be

reviewed briefly to establish a basis for further examination of the neutralization process at the gene product level.

Each of the six fibers is composed of two rod-shaped half-fibers, each about 700 Angstroms long and 45 Angstroms in diameter, joined end to end at an angle of 160 degrees (Ward, et.al. , 1970). Each half-fiber is under different multigenic control. The genes directing the synthesis and composition of the whole fiber are located within a cluster, except for gene 57 (required for synthesis of all three antigens located on the whole fiber, but its product is not included structurally). (Edgar and Lielausis, 1965; Wilhelm and Haselkorn, 1971b). The genes found within the cluster are numbered 34 through 38, inclusive, and have been shown to be co-transcribed in two divisions, genes 34 and 35 and genes 36 through 38 (Stahl, et.al. , 1970). The proximal half-fiber contains the A antigen, and is composed of two copies of the product of gene 34 (Takata and Tsugita, 1970). It is characterized as rod-shaped, with a small knob or protrusion on one end, supposedly which plays a role in binding the half fiber to the baseplate. This proximal half contains the largest single antigenic structure of the tail fiber. The gene 34 product has a molecular weight of about 130,000.

The distal half-fiber is antigenically more complex than the A half-fiber. The largest antigen in this half is

the C antigen, composed of two copies of the gene 37 product (molecular weight 105,000), but requiring genes 57 and 38 for its synthesis (King and Laemmli, 1971; Ward and Dickson, 1971). The gene 37 product has been identified and isolated either as a 425 Angstom fragment (King and Laemmli, 1971) or as a 560 Angstrom fragment (Imada and Tsugita, 1970; Ward, et. al., 1970). Such differences appear to be of importance in the final morphogenic pathway of the distal half-fiber. The C antigen has been further categorized into 4 functionally and antigenically distinct sub-components, each being well-defined to the T4 system alone or cross-reacting with T2 (Beckendorf, 1973). Its primary function prior to completion of the whole fiber is to act as a substrate for the B antigen (gene 36 product, molecular weight 24,000) to form the BC antigen (Wood, et. al., 1968; King and Laemmli, 1971).

This BC antigen, although structurally and antigenically complete as the half fiber, must be further activated by interaction with the gene 35 product (40,000) to form the BC' antigen (King and Wood, 1969; Eislering and Dickson, 1972). This completed half-fiber, the BC' half, can then join spontaneously with the A half-fiber to form the completed fiber. This completed fiber requires the action of gene 63 prior to its binding to the baseplate of the phage particle (Wood and Henninger, 1969).

Of significance in this description are the functions

of some of the structural components of the fibers, in both morphological and adsorption processes. The gene 37 product appears to be the site of host range mutations. Specifically, a small portion of the gene 37 product, the d portion, appears as the primary site of these host range mutations, since these mutations map at tightly linked sites within this segment (Beckendorf, 1973). The function of segment d is two-fold; interaction with the specific receptor on the bacterial surface, and interaction with gene product 38 in the morphogenisis of the half fiber. The other 3 segments of gene product 37 in T4 are cross-reacting with T2, and indicate a lack of divergence of the amino-terminal region of this gene product polypeptide between the two phage strains (Beckendorf, 1973).

Orientation of the gene 37 product within the distal half fiber is thought to be linear with its amino-terminus near the fiber joint and its carboxy-terminus near the distal tip. The B antigen is located near the junction of the proximal and distal half fibers. This B antigen, however, must be assymetric due to its bifunctional nature as well. These two functions include its proximal end interaction with the distal half fiber, and its distal end interaction with the gene 37 products. The gene 35 product, though required for half-fiber completion prior to junction, adds no discernible antigenic activity to the distil-half fiber.

Numerous complexities are apparent as to the specific roles of each of the fiber antigens in neutralization due to their roles in the adsorption process. In opposition to their roles in adsorption, thus limiting their individual contribution to neutralization, is the immunogenicity of each antigen. This term implies the availability and capacity of each fiber antigen to induce antibody formation. Also in question for each of the antigens is the ease of accessibility for competition in the specific antibody-antigen reaction. Thus, to fully understand the complete neutralization phenomenon, examination of the antigenic and structural complexities of each of the antigens, together with characterization of their respective antibody populations will be required.

Indirect evidence in support of the multi-target model of phage neutralization by Fab' and its effect on adsorption of partially neutralized phage could possibly arise from the duplication of such changes by a different method. Since binding of a single Fab' molecule to a fiber might be expected to inactivate that fiber, an opposite approach to the problem offered an opportunity to impose similiar restrictions on phage adsorption. Therefore, by adding active fibers to fiberless T4 phage particles, prepared from an amber conditional lethal mutant, one would obtain a mixed population of phages which possessed different numbers of fibers. The two final stages in fiber attachment would then

represent the classes of phage produced by Fab' neutralization; the second last stage being comparable to those phage with one Fab' molecule bound, and the final activated phage being comparable to those phage with no fragments bound.

In addition to the mutant used in the preparation of fiberless particles, this study has made use of several other amber mutants. These mutants have facilitated the examination of the adsorption characteristics of both modified and unmodified phage, by permitting the use of a kinetic assay of phage remaining free in solution in the presence of host bacteria. Such a scheme will be fully explained later, but essentially the adsorption of the amber mutant onto its restrictive host permits differentiation of phage adsorbed at any given time from those phage either remaining free at the time of sampling, or arising from the dissociation of the phage-bacterial complex. Any phage reaching the infected non-permissive bacterium stage is lost to the assay, since plaque formation cannot ensue.

The investigations described here should be summarized briefly to indicate which level of the phenomenon has been examined. Of primary significance is the interaction of the monovalent antibody fragment, Fab', with phage T4, and its interference with normal adsorption of the phage to the host bacterium. A model has been established for such a modification, and consistent values for rate constants

describing the model were found from experimental data examining several basic parameters. These parameters include the effects of bacterial concentration, fragment dosage, and fragment dissociation. Further support for the hypothesized model was established by examining incomplete phage with respect to their adsorption characteristics. These experiments are presented in part I of the Results section which follow, together with electron microscopic attempts to validate some of these ideas upon which the model was based. Also presented in part I of the results are the adsorption characteristics of the amber mutants used in the second section.

Experiments which examined the roles of individual fiber antigens in the neutralization process are included in part II of the results. Such experiments attempted to correlate fiber antigen concentration with individual sera-neutralization blocking ability. Results of this portion of the study indicate no major differences in such blocking activity, but limitations of the techniques used in these experiments can account for the similiarities observed for most blocking antigens.

MATERIALS AND METHODS

a. PHAGE AND BACTERIAL STOCKS

Wild type bacteriophage T4 was a laboratory strain. Amber mutants were obtained from Dr. E. Kellenberger and Dr. R.S. Edgar, and are described in Table I. Amber mutants are able to form plaques on the permissive host Escherichia coli CR63 but not on the restrictive host E. coli B/1. These hosts have been described elsewhere (Wood, et. al. ,1968). Amber mutant stocks not associated with fiber antigen studies are marked "N/A" under the "POSITION" column in Table I.

Double and triple amber mutants were constructed by Ms. A. Rogers from defined single amber mutants by recombination. Their compositions were checked by simple complementation of plaque isolates on the restrictive host. Complementation tests on the laboratory stocks were carried out using parental amber mutants stored in phage buffer under chloroform, and were checked every few months for reversion rates.

b. TERMINOLOGY AND DEFINITIONS.

Amber mutants are designated by the number of the gene which carries the mutation. Defective mutant lysates are identified in the same manner. Mutant lysates always infer phage production on the restrictive host. They are also

TABLE I

STOCK PHAGE DESCRIPTIONS

STOCK	SITE(S)	GENE(S)	POSITION[1]	REVERSION ($\times 10^7$)	REMARKS
am N122	N122	42	N/A	4.3	Defective in early DNA synthesis. Adsorption profile similiarity to wild type T_4 facilitates restrictive host assay system.
M23-10	H11-B255	23, 10	N/A	4.9	Deficient in head-tail formation. Source of fibers for *in vitro* complementation of fiberless particles.
M34	B25	34	mid-early	4.4	Proximal half-fiber (A antigen) missing from *E. coli* B/1 lysate.
M35	B252	35	mid-late	3.6	Missing gene 35 product prepares distal half-fiber for union with proximal half. Converts BC to BC'.
M36	E1	36	middle	0.4	Proximal region of distal half-fiber missing from B/1 lysate (hinge region or B antigen).
M37	N91	37	not found	0.4	Major structural protein of distal half-fiber missing from B/1 lysate (C antigen).
DM	N91-B262	37,38	same as in single ambers	0.4	Gene 38 product adds no structural antigens to distal half, but is required for C antigen production.
TM	B25-N91-B262	34,37,38		6.1	Best yield of fiberless particles. B antigen does not associate with particles in lysate.
X4E	as published[2]	(34,35,37,38)	.....	34	Fails to produce any fiber antigens, as previously reported.[2]
WT T_4	-	-	-	-	Used to measure 'control' tail fiber antigen levels in *E. coli* B/1 lysate.

1- within gene indicated.
2- Edgar and Wood, 1966.

referred to as phenotypic lysates , or lysates which lack the gene product in which the amber mutation lies. Phage grown on permissive host are sometimes termed genotypic mutants, indicating they still are not viable on restrictive host conditions.

Multiplicity of Infection (M.O.I.) in reference to infection schemes indicates the ratio of phage to bacteria, rather than the classical definition of the number of phage adsorbed per bacterium. The terms adsorption and absorption are used throughout the text and require clarification as to their meanings. Adsorption infers a surface phenomenon or interaction, as in "phage adsorption to bacterial cell walls". Absorption differs from its regular meaning in that it infers a removal of specific material from a suspension or solution, rather than the distinction of the material becoming an integral part of the structure. Two examples of its use in the text would be " E. coli were used to absorb contaminating fibered particles from a suspension of partially purified fiberless particles", and, " Anti-T4 antiserum was absorbed with a phage lysate".

Complementation in reference to phage stock assays indicates complementation at the in vivo level (simultaneous infection of a cell by phage mutants of two or more different genotypes). Complementation of non-viable phage particles infers in vitro complementation (structural components interacting prior to infection of a permissive

host). Complemented phage in both senses of the word carry the original amber genotypes. A few progeny in the first case carry wild type genotypes, since recombination can occur to a limited degree.

Titer can also be used in two frames of reference. With respect to phage neutralization, it is normally associated with an exponential process of phage inactivation by antiserum and is indicative of the activity associated with a given antiserum. Titer is also used to indicate the number of viable plaque forming phage (PFU's), normally expressed as concentration in PFU's/ml.

IgG is a divalent immunoglobulin of molecular weight 150,000. It can be degraded by proteolytic enzymes to yield Fab and Fc, or $F(ab')^2$. Fab and Fab' contain a single combining site of the IgG molecule, differing only in a few amino acids due to the point of fragmentation specified by the enzymes used in IgG degradation. $F(ab')^2$, produced by pepsin digestion, must be reduced and alkylated to yield the monovalent Fab' molecule. Fab, on the other hand, is produced along with the Fc fragment directly by degradation with papain.

The term hit indicates one combination of a fragment and phage at a critical site with respect to the adsorption process. When the term ratio is used in reference to Fab' inactivation of phage, it infers the ratio $\{P^0:(P^0+P^1)\}$.

P^0 represents the zero-hit fraction of phage and P^1 represents those phage with one hit.

When ratio is used in conjunction with in vitro complementation of fiberless T4 particles, the ratio $\{C^0:(C^0+C^1)\}$ is inferred. C^0 represents the fully activated particles, or those particles with a full complement of fibers. C^1 represents those particles which behave as if they possess one less fiber than the fully-activated fraction of complemented phage.

Each mechanism infers only two adsorbing classes of phage being involved in plaque formation. P^0 and C^0 represent phage which are "normal" adsorbers with the same adsorption characteristics as the amber mutant am N122. This mutant has been shown to adsorb like wild type T4 by Stemke, et. al., (in press). P^1 and C^1 represent slower classes of adsorbers, whose adsorbing characteristics will be presented in Results.

The term hit-equivalent is useful, therefore, only for the correlation of the two mechanisms in that it determines the relative concentration of fast and slow adsorbers in the viable phage in both the Fab' inactivating process and the fiberless particle activation process. Both mechanisms involve modification to the normal adsorption characteristics of phage.

Two other classes of adsorbers are defined in the

general characteristics of the amber stocks. These are used only to normalize the infection schemes of the different ambers to quantitate the fiber-antigen deficient lysates in Part II of the results.

Rate constants describing each of the adsorption schemes (either Fab'-treatment or in vitro complemented phage) are identified by their superscripts; the first superscript distinguishes which class of adsorber is being referenced, and the second indicates which rate constant in the process is implied. As an example, K^{23} represents the rate constant for the irreversible decay of the Fab'-phage-bacterial complex to an infected bacterium.

This designation does not imply the first class rate constants (i.e., K^{11}, K^{12}, and K^{13}) being those of the P^1 or C^1 class, nor the second class rate constants (i.e., K^{21}, K^{22} and K^{23}) being those of the P^2 or C^2 class of adsorbers. Superscripts ^{1} and ^{2}, in describing the rate constants of the two classes, are used for simplification of rate constant designation, not in identifying the first class as a one-hit class (or incomplete phage in the fiber addition model), nor the second as a neutralized (two-hit) phage class.

C. MEDIA AND GROWTH CONDITIONS

Media and buffers used were:

1. Nutrient broth-phosphate (NB-P).
2. Tryptic soy broth-yeast extract (TSB-YE).
3. Fraser Medium.
4. M-9 Medium.
5. Phage buffer.
6. Phosphate buffered saline (PBS).
7. Phosphate buffer, various molarities and pH's.

These have been described elsewhere (Adams, 1959; Tsugita, et. al., 1968). Bacto-peptone agar plates (1.2%) and NB soft agar overlay (0.7%) were used throughout. Liquid media used for growth were TSB-YE or NB-P. Dilution broth consisted of NB medium containing 0.8% NB (Difco) and 0.5% NaCl in aqueous solution.

Bacterial stocks were maintained on screw-capped agar slants (NB) at 4° C and were transferred twice yearly. These culture slants were used to prepare working stocks every few weeks by inoculating a NB-P or TSB-YE culture flask and incubating overnight with shaking at 37° C. Overnight cultures were prepared by inoculating fresh media with 0.01 ml of the working stocks, and growing under the same conditions overnight. Cultures were then freshly diluted (1:25) and grown for a few hours for use as indicator bacteria, for adsorption experiments, or for inocula for phage preparations. Growth curves were

established by correlating absorbance at 660 nanometers (A^{660}) with cell counts on a Petroff-Hauser bacteria counter. A linear relationship between cell count and absorbance was found between 10^8 and 10^9 bacteria/ml (i.e., from early to late log phase).

Cells used for adsorption experiments were grown to mid-log phase, then diluted to $2x10^8$ cells/ml., unless otherwise indicated. Cells used for phage lysate preparation were grown to mid-log phase as well, but adjusted to $5.5x10^8$ cells/ml.

Bacteria used in lysozyme assays were grown on M-9 medium, centrifuged, frozen for 1 week, then lyophilized at -60° C and $5x10^{-3}$ Torr. Cells in which T4 was to be grown for lysozyme production measurements were grown on Fraser medium.

d. CHEMICALS

DNase I (Bovine Pancreatic, 1X Crystallized) was obtained from Sigma Chemical Company. Dow Corning Antifoam A was used as an anti-foaming agent in all growth media. Bio-gel A 1.5 (200-400 mesh) from Bio-Rad Laboratories was used in purifying ferritin-labelled goat anti-rabbit IgG (FEG) obtained from Cappel Laboratories, Inc. Sodium dextran sulphate 500 was from Pharmacia, polyethylene glycol 6000 from Matheson, Coleman, and Bell. Chloroform was Fisher analytical grade. All other chemicals were reagent

grade.

e. PHAGE PREPARATIONS.

All stocks (except wild type T4) were grown on E. coli CR63 from single plaque isolates through several reinfection cycles. A single plaque was used to infect early-log phase CR63 cells in 25 ml of liquid culture medium, and allowed to grow for 6 hours. Chloroform and DNase were then added to the crude lysates, followed by a low speed centrifugation of 1500xg for 10 minutes. The supernatant was then used to reinfect new bacteria at mid-log phase, and the process repeated. Normally, 3 to 4 of these cycles were required to yield stocks of about 10^{12} PFU's/ml. The later purification stages included a high-speed centrifugation (12,000xg for 90 minutes) to pellet the phage, followed by resuspension overnight in phage buffer.

A highly purified wild type preparation employed in electron microscopy was obtained without the high-speed centrifugations used in normal stock preparations. An aqueous, two-phase system was used to separate complete phage from bacterial debris on the basis of different surface activities (Yamamoto, et. al. , 1970). One liter of E. coli B/1 was grown to early log phase, then infected with WT T4 at a low multiplicity and allowed to grow for 6 hours. Chloroform and DNase were added as before, and allowed to stand for 20 minutes, then 20 grams of NaCl, 2 grams of sodium dextran sulphate 500, and 80 grams of

polyethylene glycol 6000 were added to each liter of lysate. The mixture , upon standing for 12 hours at 2° C, formed 2 distinct layers. The upper layer, comprising about 99% of the volume, was removed and discarded. The creamy bottom phase was resuspended in the residual top phase and centrifuged 10 minutes at 1000xg. The pellet was resuspended in 0.05 volumes distilled water, chilled to 2°C, and 0.05 volumes of cold 3 Molar KCl were added dropwise to precipitate residual dextran sulphate. Following 2 hours at 2° C, the suspension was centrifuged for 10 minutes at 1000xg, and the pellet discarded. About 50 ml of highly purified phage (at $5x10^{11}$ PFU's/ml) were obtained.

Electron microscopy of these phage indicated very little debris, few empty heads, and few contracted sheaths. Normally, high speed preparations appeared to have up to 50% empty capsids and broken tails, along with excess debris in the background.

Phenotypic lysates of the amber mutants were prepared by a one-step growth protocol on the restrictive host, E. coli B/1. Cells were grown to mid-log phase at 37° C, then infected at M.O.I.'s of 0.5 to 5, accompanied by a temperature shift to 30°C. Shaking was continued in a 30° C waterbath for 40 minutes, at which time the cells were treated with chloroform and DNase, then cooled immediately in ice water. Bacterial debris was normally removed by a 10 minute low speed centrifugation. Such lysates were used for

serum blocking characteristics of the fiber antigen-deficient mutants. The same protocol without the addition of chloroform and DNase was used for the preparation of lysates for lysozyme activity determinations.

f. PURIFICATION OF FIBERLESS T4 PARTICLES.

Particles of T4 lacking tail fibers were prepared by one-step growth of the triple amber mutant on its restrictive host, E. coli B/1.

Fiberless particles were concentrated by high and low speed centrifugations of the triple amber mutant lysates (of volumes up to 1 liter). Partial removal of contaminating fibered particles was achieved by absorption of the preparation with E. coli B/1 cells grown for 2 hours to 10^9 cells/ml. Fiberless particles were added to the cells at the same time as 10^{-3} M $MgSO_4$. Thirty seconds later, KCN was added to 10^{-3} M; the mixture was shaken once and left for 2 hours, shaking only to resuspend cells and ensure uniform distribution of materials. The culture was then centrifuged at 1500xg for 10 minutes, and the supernatant centrifuged at 10,000xg for 90 minutes. A further centrifugation at 1000xg for 10 minutes followed resuspension of the high speed pellet in phage buffer.

Purity of fiberless particles was assayed by three methods:

1. Optical density at two wavelengths.

2. Background viable phage on CR63.

3. Serum Blocking Power.

Concentration of the particles was determined by multiplying the absorbance at the two wavelengths by their respective factors,

1.2×10^{12} for 405 nm, and

2.62×10^{12} for 265 nm.

The ratio of the two values gave an estimate for purity of the preparation; the closer the value to 1.0, the more pure the particle preparation (Edgar and Wood, 1966; Sabelnikov, 1972).

Values obtained for the 'fiberless particles before absorption with B/1 cells were :

1.09×10^{12} at 405 nm,

9.80×10^{11} at 265 nm.

Viable phage in this initial preparation amounted to 0.4% of the total particles by titer on CR63.

For the fiberless particles finally used in the in vitro experiments, an absorbance ratio of 1.1 was found, with the concentration of background phage found to be 2×10^{8} PFU's/ml compared to an estimated particle concentration of 7.4×10^{11}/ml (less than 0.03% phenotypic contamination). Genotypic wild type contaminants were assayed on E. coli B/1 to be 5×10^{5}.

Blocking curves of WT T4 and the initial preparation of the fiberless particles showed that a 1% level of contaminating fiber antigens was present in the unabsorbed fiberless particles (i.e., 0.01 phage equivalents). The serum blocking curve of the absorbed preparation showed a 5-fold purification over the unabsorbed fiberless particles, with about 0.2% residual fiber antigenicity remaining with the final preparation. Fiber antigens were possibly present as incomplete fiber complements (i.e. < 4 or 5 fibers), on a small percentage of the particles. This is suggested by greater than a 1000-fold difference between the O.D. measurements of concentration and viable count. Viable count and serum blocking power measurements should agree if contaminating fibers were only on viable phage.

q. ANTISERUM AND NEUTRALIZATION ASSAYS.

Antisera to T4 were raised in rabbits as previously described (Stemke, 1969). IgG was prepared from the immune sera by ammonium-sulphate precipitation followed by DEAE-cellulose chromatography. Monovalent Fab' was prepared by pepsin digestion of IgG followed by reduction and alkylation, also as previously described (Stemke, 1969). The criteria for purity of this Fab' have been described before, and include non-agglutination characteristics as well as thin layer and preparative gel filtration of Sephadex G-200 (Stemke, 1969).

Neutralization assays were carried out at 37° C. Phage were added to antiserum and samples taken at various times were diluted 100-fold prior to plating on indicator bacteria. Normally, exponential rates of killing were used to calculate the titers of antisera, IgG, and Fab', as described in the following section.

h. CALCULATION OF TITER AND FRAGMENT DOSAGE.

An example would best describe the methodology used in calculating anti-T4 titers.

1. IgG and Serum.

Neutralization by these agents can be described in terms of the surviving fraction (S), by the one-hit equation,

$$S = 1 - e^{-KT/D} \quad (1)$$

If a 10-fold decrease in phage titer was effected in 23 minutes by a 1:5000 dilution of anti-T4, the titer of that preparation can be found from the equation

$$K=[\ln(P/P^0)xD/T] \quad (2)$$

, where P = phage survivors at time T,

P^0 = phage at time 0,

and D = dilution

From this equation,

$$K = \frac{2.303 \times 5000}{23 \text{ min.}} = 500/\text{min.}$$

2. Fab'.

Fab' neutralizes according to the multi-target equation,

$$S = 1 - (1 - e^{-KT/D})^n \qquad (3)$$

, where n is the number of fragments required to inactivate the phage. "K" was calculated from the linear portion of the fragment neutralization curve (i.e., after the shoulder), from the equation

$$K=[\ln (P/mP^0) \times D/T] \qquad (4)$$

where m is the ordinate extrapolate of the linear portion of the curve (equal to 2 for Fab').

Fragment dosage is determined from this K value and the time allowed for neutralization (i.e., K/D x time). Using the same values for time and dilution given for IgG and serum, one hit would require phage reacting for 1 minute with a 1:500 dilution of the Fab' (i.e., 500 min^{-1} x 1 min./500). If the dilution was 1:5000, then 1 hit would have involved 10 minutes reaction time. Similiarly, treatment for 5 minutes would yield 0.5 hits.

From the Fab' hit value so derived, different concentrations of P^0 and P^1 classes can be calculated from an assumed Poisson distribution of the fragment dosage over the phage population.

Such a distribution can be represented by the equation

(from Stent, 1963, p75)

$$P(r) = \frac{x^r \cdot e^{-x}}{r!} \qquad (5)$$

where P(r) is that fraction of phage that will bind r fragments each, if an average of x fragments per phage is distributed at random over the entire population.

Although no direct evidence supports the use of this equation, under the dilute conditions employed in the assay system it is most likely this type of distribution which is obtained. Such a distribution is based on the probability (of antibody molecules combining with critical sites on the phage) being derived from the binomial distribution function (Vargues and Vollet, 1973). Again, the multi-target equation with the different class inferences only applies to the fragment neutralizing scheme.

Use of the linear portion of the neutralizing curve of Fab' greatly facilitates calculation of the "K" of Fab' preparations. This apparent discrepancy, of utilizing a multi-target "K" rather than a multi-hit "K" is explained as follows.

The multi-hit "K" arises from the equation,

$$S = 1 - e^{-KT/D} + \frac{KT}{D} \cdot e^{-KT/D} \qquad (6)$$

, for the case of two hits being required for neutralization. The Poisson distribution of fragments over

the phage is based on this equation (6) rather than the multi-target equation (3). However, for significant errors to develop in calculation of the predicted survivors from the number of hits delivered, phage would require from 1.5 to 2 hits, well below most experimental dosages. Hence, this distinction is of minor importance under the experimental conditions used.

i. PHAGE ADSORPTION ASSAYS.

E. coli B/1 cells were grown to mid-log phase then diluted to 2×10^8 cells/ml. KCN was added to 1mM to hinder further cell growth and to prevent any phage replication. These bacterial preparations were used only for 2 hours after addition of the KCN, since adsorption properties of *am* N122 appeared to slow using cells older than this. In experiments of longer duration than two hours, fresh bacteria were prepared for each time sample, then diluted 15 to 30 minutes before the adsorption assay was begun.

Adsorption kinetics were followed by adding phage to the bacteria , then assaying for viable phage left in solution by plating samples on CR63 following 100-fold dilutions. *Am* N122 was used in Fab' treatment and Fab' dissociation experiments. Other amber mutants and *in vitro* complemented phage were used in their respective experiments. From the infection scheme outlined in Appendix A, any phage reaching the irreversibly infected bacterium

stage would be lost to the assay, since it is an amber mutant infecting its restrictive host.

i. IN VITRO COMPLEMENTATION ASSAYS.

Purified fiberless particles at roughly 10^{10}/ml were pre-incubated at 35° C for 10 minutes, then a crude fiber preparation (phenotypic lysate of M23-10) was added. Titer increase of the incubation mixture was followed for about 10 hours on CR63, with the adsorption profile of each time sample being determined on B/1. E. coli CR63 was used as the indicator bacteria for both the titer increase and adsorption assay since the genotype of the complemented phage would still be that of the amber mutant.

The lysate from M23-10 was prepared as described in Section e, and residual contaminating phage were found to be about 5x 10^5 viable counts on CR63. These counts were ignored since they amounted to less than 1% of the plaques on the plates involved in the assays.

k. SERUM BLOCKING ASSAYS.

Serum blocking power of samples was assayed as follows. Samples were added to pre-incubated (37° C, 10 minutes) aliquots of antiserum and allowed to react for 1 hour at 37°C. Reaction mixtures were then incubated at 0 to 4° C for 24 hours . The sample was then centrifuged at 35,000 rpm in a type-SW50.1 rotor in a Model L2-65B Beckman Ultracentrifuge to remove any antibody-phage complexes.

Supernatants were removed immediately and assayed for anti-T4 activity either the same day or the next. Where impossible to do this, samples were frozen at -20° C, and assayed within one week.

Fiberless particles were assayed for contaminating fibers by adding various concentrations to anti-T4, then determining the residual anti-T4 activity following the treatment given above. Controls were carried out to establish a standard curve for fiber antigens associated with similiar wild type concentrations as those used in the fiberless particle blocking curve.

Serum blocking assays on amber lysates were carried out with preparations described in Section e of these methods. Residual blocking activities were calculated assuming single-hit neutralization kinetics.

l. LYSOZYME ASSAYS

Lysozyme concentrations for the amber mutants were determined by the method of Tsugita, et. al. , (1968). Different flasks of E. coli B/1 cells were grown to mid-log phase and infected with the various mutants to be tested for lysozyme production. The O.D.$_{660}$ of each growth flask was checked and adjusted to 0.55, and the same effective multiplicities were used for each mutant. Cells were then incubated for 40 minutes at 30° C, and chilled in ice water immediately. Debris was removed by a 1000xg centrifugation

for 10 minutes. Lysozyme concentrations were determined from samples of these lysates. Assays of the samples were carried out in 3.0 ml of resuspended, lyophilized B/1 cells (0.05%) in 0.05 M phosphate buffer, pH 7.4, as described previously (Tsugita, et. al. , 1968).

Decrease in absorbance at 350 nm. was followed and concentrations in International Unit Equivalents were determined from the initial linear portions of the curves. I.U.E. were determined from standards run using egg white lysozyme at 0.05 mg./ml. One International Unit is defined as a 0.001 min^{-1} decrease in A^{450} at pH 7.0 and 25° C of a 0.3 mg/ml. suspension of dried M. lysodiecticus cells in 0.1 M phosphate buffer. See Results, Part II-A, for the standarization values of egg white lysozyme on E. coli B/1 vs. M. lysodiecticus .

m. ELECTRON MICROSCOPY

Grids used were 300 mesh copper screen which were coated with Formvar and shadowed with a thin carbon film. Specimens were observed in a Philips EM 300 under double condensor illumination with 300 micron condensor apertures and an anti-contamination cold-trap affixed. Most work was carried out under accelerating voltages of 80 and 100 KV with a 50 micron objective aperture.

Phage samples were applied to grids dropwise and

allowed to adsorb for one minute, then washed with one drop of distilled water. Grids were then floated onto antiserum and allowed to react for one half hour to 4 hours, then negatively stained. At times, antibody fragments and phage were mixed first, allowed to adsorb for various times, then stained. Negative staining was carried out using a 1% solution of sodium phosphotungstic acid (PTA) for 1 minute.

A ferritin-labelled antibody "sandwich" technique was utilized to attempt to locate various neutralizable antigens on the fibers. Little success was met using this method, even in locating the fibers with unabsorbed anti-T4 serum. Ferritin labelled goat anti-rabbit IgG (FEG) was diluted 10 to 100-fold in phosphate buffer prior to use on the grids. Phage were adsorbed to the grids, reacted with varying concentrations of antibody, then allowed to react with varying concentrations of FEG. Samples were then washed with a few drops of distilled water, and negatively stained as before.

n. COLUMN CHROMATOGRAPHY AND SEDIMENTATION VELOCITY STUDIES OF FEG.

FEG was further purified by column chromatography after sedimentation velocity observations indicated contaminating unbound ferritin, apo-ferritin, and possibly unbound IgG were present in the supposedly pure FEG obtained commercially (Figure 1). Sedimentation velocity was carried

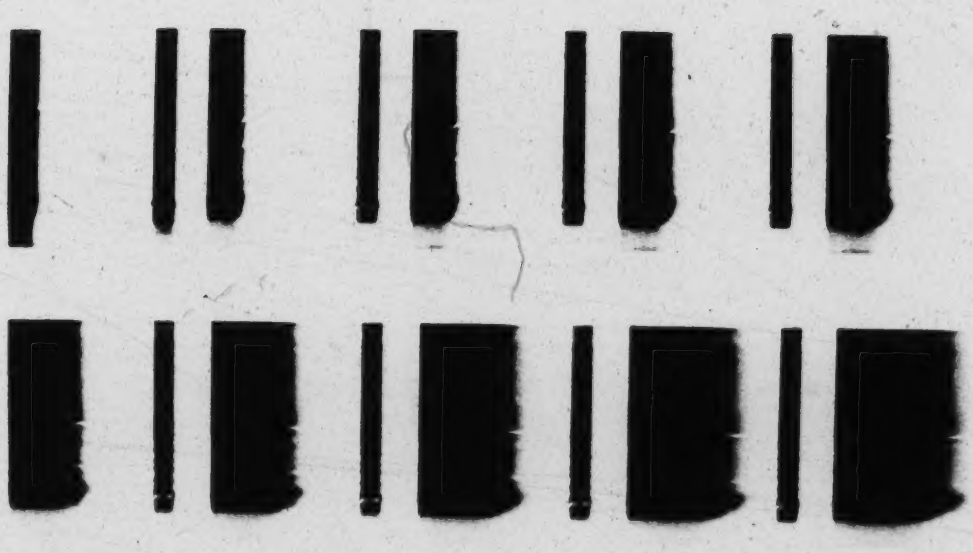

FIGURE 1. Sedimentation profiles of ferritin-labelled goat anti-rabbit IgG (FEG) and normal horse ferritin, centrifuged at 44,000 rpm (D rotor, Beckman Model E Ultracentrifuge) in 0.15 M phosphate buffer, pH 7.2. Upper profile shows contaminating band at 16.7 S and rapid diffusion of main peak at 55 S. Rapid diffusion of peak coincident with normal ferritin (lower band) indicates heterogeneity in FEG, most likely unconjugated ferritin. Underexposed regions coincident with larger S peaks arise from color displacement imposed on optical system by ferritin iron groups.

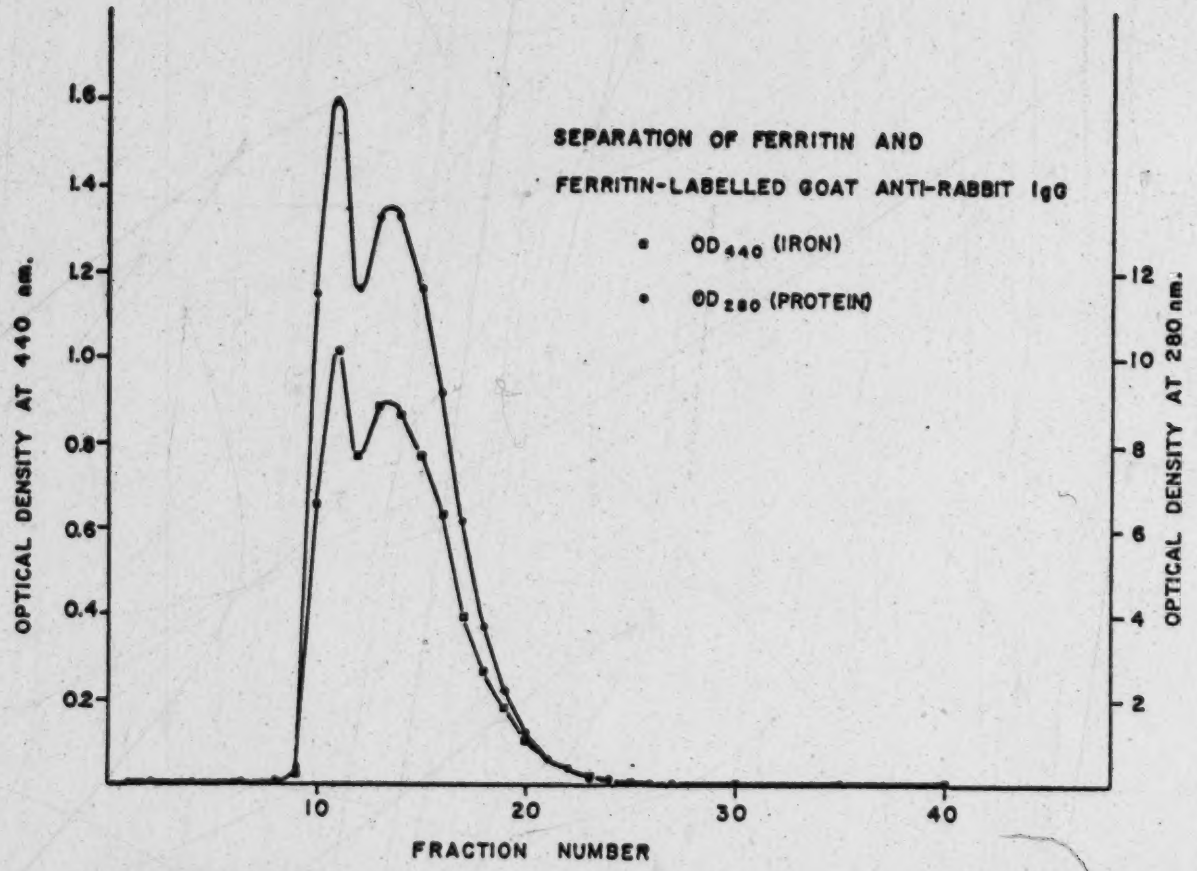

FIGURE 2. Elution profile of Biogel A-1.5 column, 0.05 M phosphate, pH 7.2, showing separation of ferritin and ferritin-conjugated IgG (FEG). Fractions 10 and 11 were pooled and used as the purified FEG in electron microscopy. One-ml fractions were collected.

out at 44,000 rpm at 20 ° C for 1 hour in a D-type rotor in a Beckman Model E Ultracentifuge. A FEG concentration of 0.7 mg/ml in 0.15 M phosphate buffer was used. Rapid diffusion of the main peak in Figure 1 indicated extreme heterogeneity in the iron-containing proteins. A single band sedimented at 16.7 S, indicating apo-ferritin to be present in the commercial preparation. Normal horse ferritin was run as a standard in the second well of the rotor, and is seen as the lower band in Figure 1. Differences in intensity accompaning the major peak in both wells are due to a color displacement in the optical system induced by the iron-containing proteins.

About 15 $O.D._{440}$ units of FEG were layered onto a Biogel A 1.5 (200-400 mesh) column approximately 1 x 30 cm. which had previously been equilibrated and washed twice with 0.05 M phosphate, pH 7.5. The column was eluted with 0.05 M phosphate buffer, pH 7.5, at a flow rate of about 0.05 ml/min (see Figure 2). Exclusion limit of the column was 10,000 Daltons. Recovery was about 95% by $O.D._{440}$.

The initial peak fractions were pooled and used as the purified ferritin-labelled reagent for EM work. The second peak contained the unconjugated ferritin, and most likely the apo-ferritin and unconjugated IgG contaminants.

Further work with the ferritin-labelled anti-rabbit IgG was terminated because of the extremely high degree of non-

specific interactions observed on both phage and background supporting film.

o. COMPUTING FACILITIES AND PROGRAMS.

An IBM 360 Model 67 computer under the Michigan Terminal System in use at the University of Alberta was employed for all work reported here. Programs for adsorption profiles and neutralization assays were written in Fortran IV by Dr. Bill Knight. The program for estimating the contribution of Fab' dissociation was written by Dr. Ed Butz. All best-fitting subroutines of adsorption profiles involved a non-linear regression basis of least squares differentials (see Appendix A).

Plots of the adsorption profiles and neutralization kinetics were drawn using the software available for the Model 770/663 Calcomp Plotter at the University of Alberta Computing Center. A 3-point parabolic curve fitting subroutine was used on the Calcomp plotter for curves associated with best fits of the data points. Programs for the Calcomp Plotter were written by Mr. C.W. Huneycutt.

A second independent set of fitting subroutines was used for the linear neutralization assays which employed a simple regression analysis of the data. No significant differences were observed in using either the linear or non-linear systems in analysis of the neutralization data with regards to best fit obtainable.

RESULTS

PART I. THE BASIC ADSORPTION SCHEME AND ITS MODIFICATIONS

A. Fab' TREATMENT.

The basic premise of the multi-target equation describing phage neutralization by Fab' is that the initial phage-Fab' complex formed is still infective. Such an infective complex might exhibit less efficient adsorption kinetics.

The simplest equations describing the adsorption scheme and its modification are:

$$P + B \underset{K^{12}}{\overset{K^{11}}{\rightleftarrows}} P.B \xrightarrow{K^{13}} B^* \qquad (7)$$

and

$$P1 + B \underset{K^{22}}{\overset{K^{21}}{\rightleftarrows}} P1.B \xrightarrow{K^{23}} B^* \qquad (8)$$

Where P represents the untreated phage

B , the uninfected bacterium

P.B , the reversible phage-bacteria complex

B* , the irreversibly-infected bacterium

P1 , the single-hit phage (phage-Fab' complex)

and P1.B, the phage-Fab'-bacteria complex.

The rate constants have been previously defined.

By examining changes in the adsorption characteristics

of phage upon treatment with Fab', it is possible to obtain results consistent with those predicted by modification of the basic two-stage obligatory reversible complex adsorption scheme of Puck, Garen and Cline (1951).

i. Adsorption Characteristics of Untreated Phage.

It was previously shown that an amber mutant of T4D, am N122, had adsorption and neutralizing characteristics similiar to those of wild type T4 (Stemke, et.al., in press). As outlined in Materials and Methods, the use of such an amber mutant adsorbing onto its non-permissive host permits certain observations that are not possible using the infected cell method originally employed in observing the Fab' effects on phage adsorption (Stemke, et.al., in press).

Results of three independent adsorption assays of am N122 on E. coli B/1 are shown in Figure 3. They represent the controls used in the major experiments to be described in following sections. As can be seen from these survival curves, adsorption appears first-order only in the early stages.

Values of the three rate constants for equation (7) were adjusted until best fits of the data were obtained, and these values (table II) used for the stock untreated phage. The values given in Table II represent average values of the rate constants obtained from about 20 independent adsorption

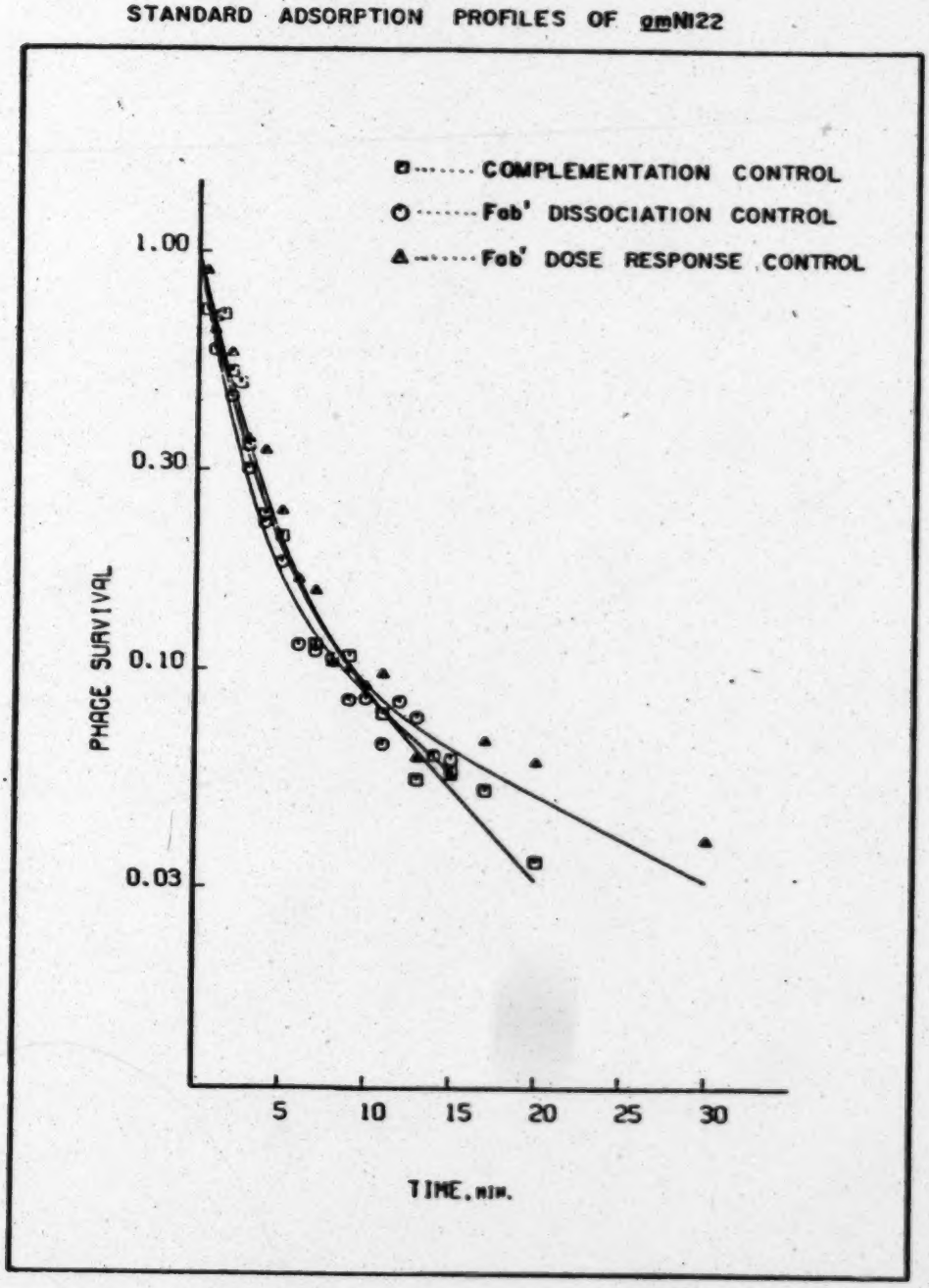

FIGURE 3. Adsorption profiles of untreated am N122 on E. coli B/1. Phage were incubated at 37°C with bacteria at 2 x 10^8/ml., then diluted and plated for free phage on the permissive host, E. coli CR63. Curves were generated from equations given in the text, independently fitting each set of data by the method given in Appendix A.

TABLE II

BEST FIT VALUES FOR ADSORPTION RATE CONSTANTS

RATE CONSTANT	BEST FIT VALUES		UNITS
	A.	B.	
K^{11*}	3.47×10^{-11}	2.87×10^{-11}	$(\text{Bact.} \times \text{sec./ml.})^{-1}$
K^{12}	5.10×10^{-4}	4.00×10^{-3}	sec.^{-1}
K^{13}	2.50×10^{-3}	2.50×10^{-3}	sec.^{-1}
K^{21}	3.47×10^{-11}	N/A	$(\text{Bact.} \times \text{sec./ml.})^{-1}$
K^{22}	1.30×10^{-1}	N/A	sec.^{-1}
K^{23}	2.5×10^{-3}	N/A	sec.^{-1}

A. Values in agreement for Fab' treatment at a bacterial concentration of 2×10^8 cells/ml., and all bacterial concentration determinations except 1×10^9 cells/ml.

B. Values required to fit data of highest bacterial concentration. Hence, no P^1 class of adsorbers since no Fab' treatments were carried out at this concentration.

* Superscipts indicate rate constant of individual population. For example, K^{21} represents K^1 of second population, K^{13} represents K^3 of first population.

assays of am N122 on E. coli B/1. Figure 3 also shows the experimental scatter which can be expected from this technique.

ii. Bacterial Concentration Effects.

As seen from equations (7) and (8), and from a more detailed explanation presented in Appendix A, adsorption kinetics are highly dependent on bacterial concentration. The large number of adsorbing sites per bacterium (200-400 each; Bayer, 1968) and the two-log-fold difference of bacteria over phage concentrations (10^8 vs. 10^6) represents a very large excess of "B", which therefore can be regarded as constant. Consistent values for the rate constants in equation (7), therefore, should fit the adsorption profiles over bacterial concentration extremes if the model is to be consistent.

Data from experiments in which bacterial concentrations were varied are presented in Figure 4. Bacterial concentrations were established by absorbance as described in Materials and Methods. As outlined in Table II, good fits of the data to the predicted survival curves (coincident solid lines for each bacterial concentration) can be obtained using the same rate constants, except for the highest bacterial concentration examined. These data have been presented elsewhere (Stemke, et.al. , in press).

Discrepancies in consistency of this adsorption model

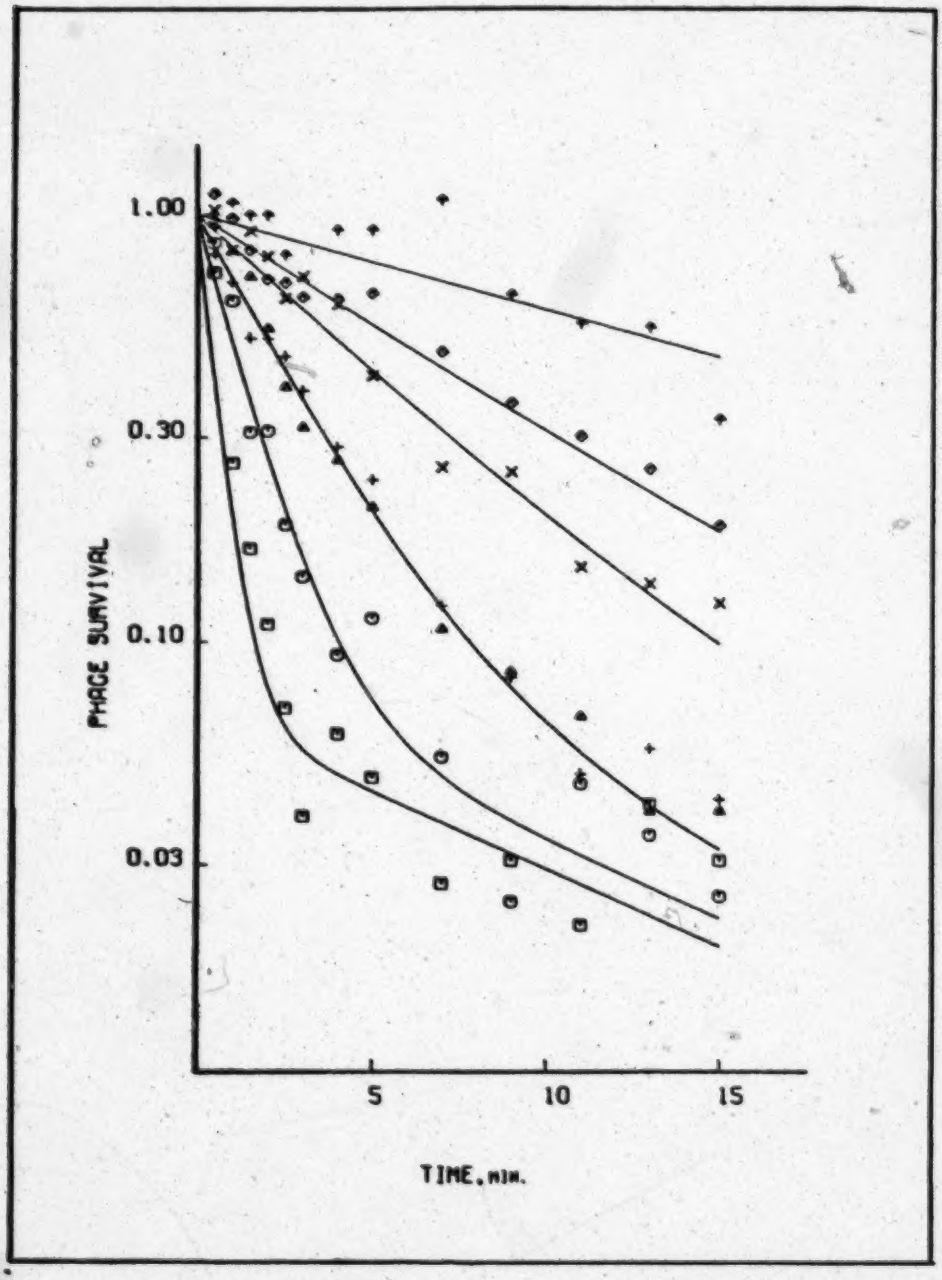

FIGURE 4. Effect of bacterial concentration on phage am N122 adsorption. Assays were carried out as in Figure 3, except different cell concentrations were used. Curves were generated using rate constants given in text. Cell concentrations were 3 x 10^7/ml.(◆), 7 x 10^7/ml.(◇), 1 x 10^8/ml.(x), 2 x 10^8/ml.(+,Δ), 5 x 10^8/ml.(o), and 1 x 10^9/ml.(□).

at this high bacterial concentration can be overlooked since the routine experimental protocol employs much lower bacterial concentrations in determining adsorption characteristics. These discrepancies have been observed in other models as well (Gamow, 1969).

iii. Effect of Fab' Treatment on Phage Adsorption.

Results showing the changes in phage adsorption upon treatment with varying Fab' dosages given to am N122 are shown in Figure 5. Best fits of the adsorption data are coincident with solid lines generated in the following manner.

A different ratio of $\{P^0:(P^0+P^1)\}$ at each dosage is predicted from a Poisson distribution of the Fab' over the initial phage population, as explained in Materials and Methods. The fitting procedure for these data was to adjust the rate constants of the slow adsorbers (K^{21}, K^{22}, and K^{23}) and the ratio of $\{P^0:(P^0+P^1)\}$ independently.

Consistently, the same values of the rate constants for the adsorption of the P^1 class (given also in Table II) and the predicted ratio value were obtained. A uniform increase in K^{22} in all experiments was observed, indicating the data could be fit to the model by increasing the rate of dissociation of the Fab'-phage from the bacterial complex. Such an increase in the dissociation rate would be consistent with less efficient binding of the Fab'-phage to

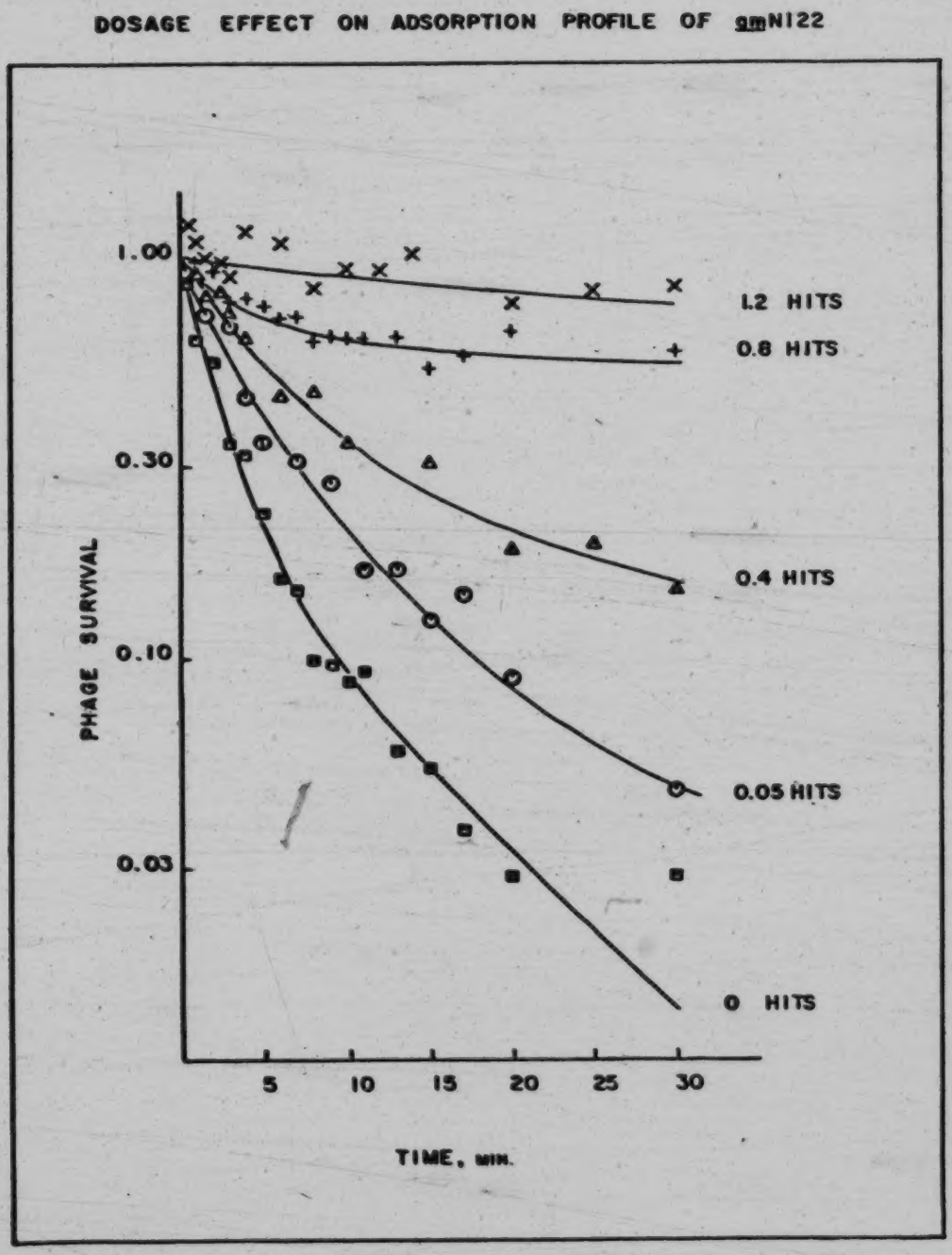

FIGURE 5. Adsorption of am N122 to E. coli B/1: Effect of varying Fab' dosage. Best fit curves were generated from equations and rate constants given in text.

the bacterium caused by modification of a single fiber by the Fab' fragment.

B. Fab' DISSOCIATION.

Other workers have found evidence indicating Fab'-phage dissociation occurs (Krummel and Uhr, 1969). This experimental possibility has been overlooked in treatment of the data in Section A to facilitate the mathematical solutions of multi-target kinetics. However, dissociation of Fab' should be considered in the model since the monovalent fragment does not exhibit the increased efficiency of neutralization characterized by the monogamous binding of the divalent IgG (Blank, et. al., 1972; Hornick and Karush, 1969).

An hypothesis that Fab' dissociation can account fully for the adsorption characteristics of the treated phage can be represented by the scheme:

$$\begin{array}{ccccc} P & + & B & \underset{K^{12}}{\overset{K^{11}}{\rightleftarrows}} & P.B \xrightarrow{K^{13}} B^{*} \\ \uparrow Kd & & & & \\ P\text{-Fab}' & & & & \end{array} \qquad (9)$$

where P-Fab' represents the single hit phage (which are not able to adsorb in this scheme, unlike the P^1 class introduced in Section A). Kd represents the dissociation constant of the Fab'-phage complex. Further mathematical derivations of this system are explained in Appendix A.

The observation that wild type phage given about 3 hits with Fab' and incubated at different temperatures gave increases in titers suggested dissociation did, in fact, occur (Stemke, et.al. , in press). Fragment dissociation, however, could not be measured directly with this technique, since a dilution of the neutralizing agent, followed by incubation of the phage with indicator bacteria, could allow unmeasured dissociation to occur over a two-hour period. The following results, based on changes in irreversible phage adsorption characteristics rather than titer increase, show that dissociation of the Fab'-phage complex occurs. The rate of dissociation found experimentally, however, could not explain the kinetics of Fab'-treated phage adsorption.

i. Effect of Aging of Fab'-Phage.

Am N122 phage were given 0.4 and 0.8 hits in two different experiments to determine the dissociation constant, Kd. Both neutralization schemes were carried out at 37°C, but further incubations of the Fab'-phage reaction mixtures for 10 hours were at 22°C and 37°C, respectively.

Immediately upon receiving the indicated dosages (see Methods, section h.), phage were diluted 1000-fold (thus stopping further hits), and assayed for their adsorption characteristics. Both initial profiles agreed with those predicted for the experiments.

Aliquots taken during the 10 hour incubations were assayed immediately for their adsorption characteristics. Since various dilutions were required to maintain proper phage:Pab' ratios, it was necessary to dilute 5-fold rather than 100-fold in the adsorption assay. The excess non-permissive host bacteria present on the plate did not affect the plaque scoring of controls significantly.

Results of the first experiment, carried out at 22°C after phage had been given 0.4 hits, are shown in Figure 6. Using the same rate constants as calculated in Section A, it was possible to generate best fits of the data by varying the ratio $\{P^0:(P^0+P^1)\}$. From these ratios of each time sample, the residual hit value, or hit-equivalent, was calculated , again using the Poisson function .

The results for the 37° C incubation (0.8 hits) are shown in Figure 7. The ratios of $\{P^0:(P^0+P^1)\}$ were calculated for each of the adsorption profiles , and a residual hit value calculated for each time sample as in the 22°C experiment.

ii. Estimation of Kd.

Results of the aging of the Pab'-phage complexes are shown in Figure 8. When the log of the residual number of apparent hits (derived from the adsorption profiles) was plotted against time of incubation of the complex, an experimental value for the rate of dissociation of Pab' was

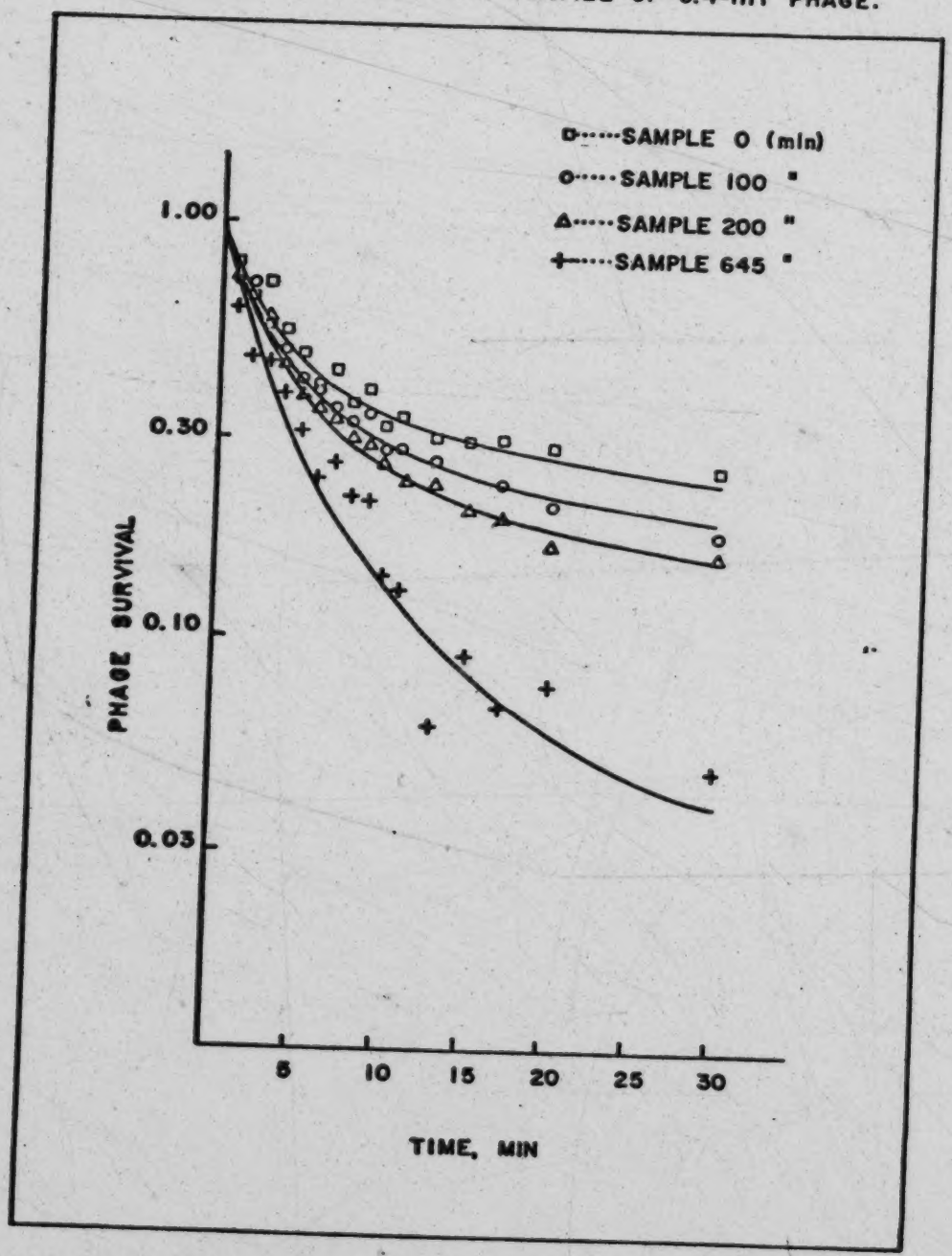

FIGURE 6. Phage-Fab' dissociation: Changes in adsorption profile of phage given 0.4 hits, then incubated at 22°C for up to 10 hours. Sample indicates time of incubation at which adsorption assays were carried out. Curves fit by varying only the ratio of $[P^o:(P^o+P')]$; the adsorption rate constants of the P^o and P' classes were not adjusted to fit the data.

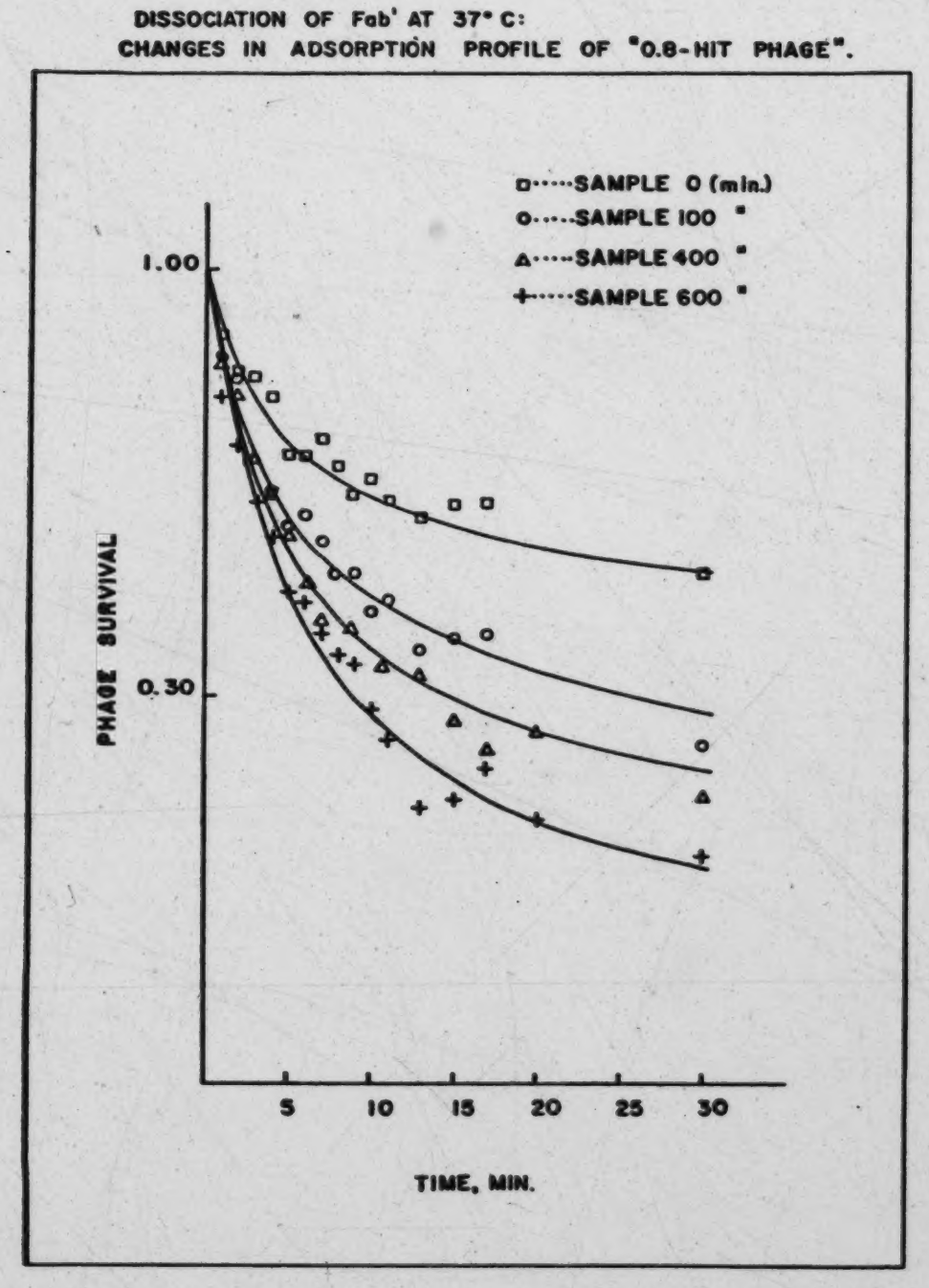

FIGURE 7. Phage-Fab' dissociation: Changes in adsorption profile of phage given 0.8 hits, then incubated at 37°C for up to 10 hours. Samples assayed and curves generated as in Figure 6.

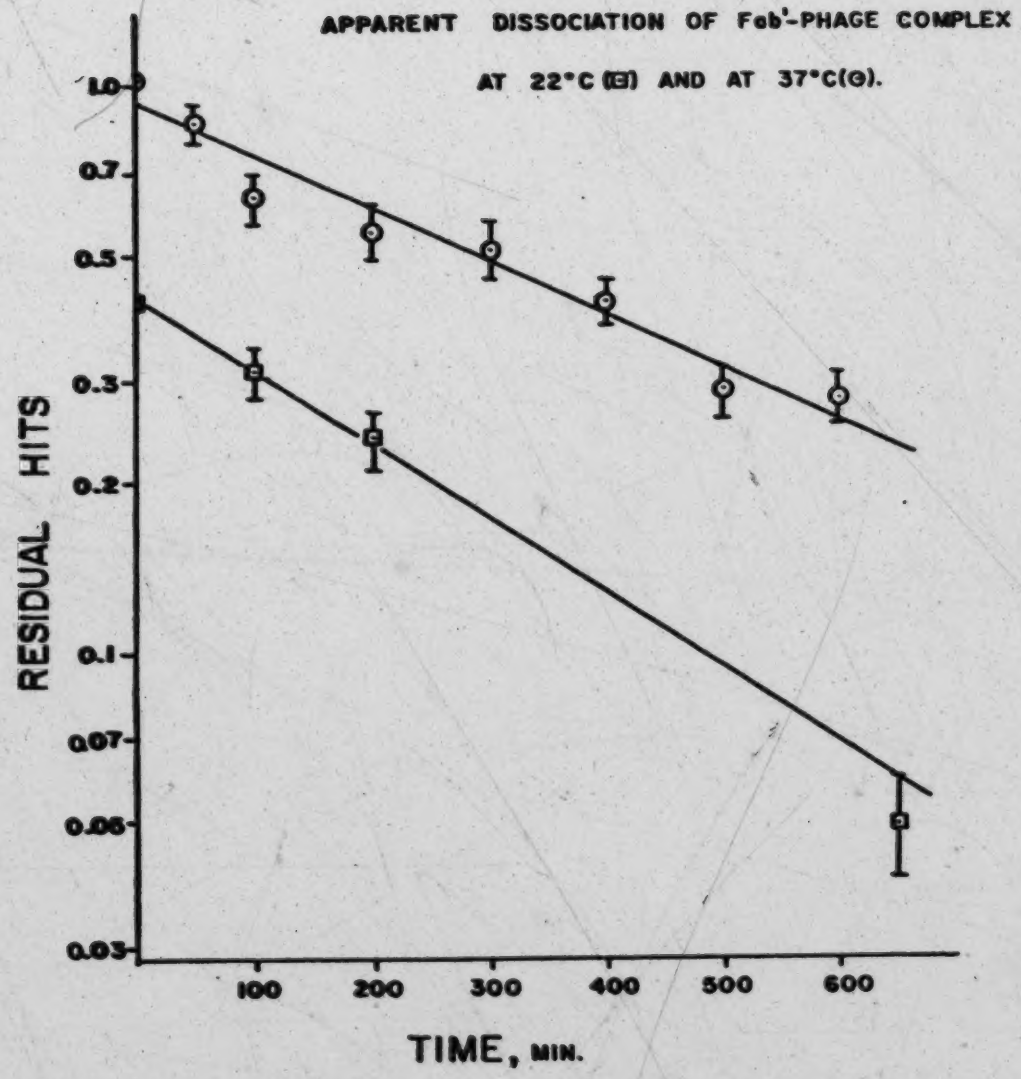

FIGURE 8. Apparent dissociation of Phage-Fab' complex. Residual hit values calculated from adsorption profiles given in Figures 6 and 7, as outlined in text. The slopes drawn though the data points were best fit by linear regression analysis, and represent the dissociation constant Kd. Relative uncertainty of each point indicates precision of calculation of residual hit value, not experimental uncertainty.

determined from the slope of the best fit of the data. This slope should represent a dissociation constant, Kd. The 37°C and the 22°C incubations gave very similiar results in this estimation. The value obtained from the 22° C experiment was calculated to be 2.8×10^{-5} sec^{-1}, that obtained from the 37° C data was 3.0×10^{-5} sec^{-1}.

It must be emphasized that, although this treatment of the data has employed a rather arbitrary and circuitous procedure, deviations indicated on the plot are generated mainly by mathematical manipulations, rather than experimental imprecision. Nevertheless, one would predict exponential dissociation of univalent fragments.

iii Kd fitting.

Using the experimental Kd so calculated, predicted adsorption curves of phage given different dosages were generated using the model outlined at the beginning of this section. Mathematical details are explained in Appendix A.

When these predicted adsorption curves were compared to the best fit curves of the actual adsorption data at any given dosage, significant differences were noted. These are shown in Figures 9 and 10 for 0.4, 0.5, 0.8, and 1.2 hits. The experimental value for Kd used in the calculations was 3.0×10^{-5} sec^{-1}.

Different artificial values of Kd were then chosen and hypothetical survival curves generated for each dosage until

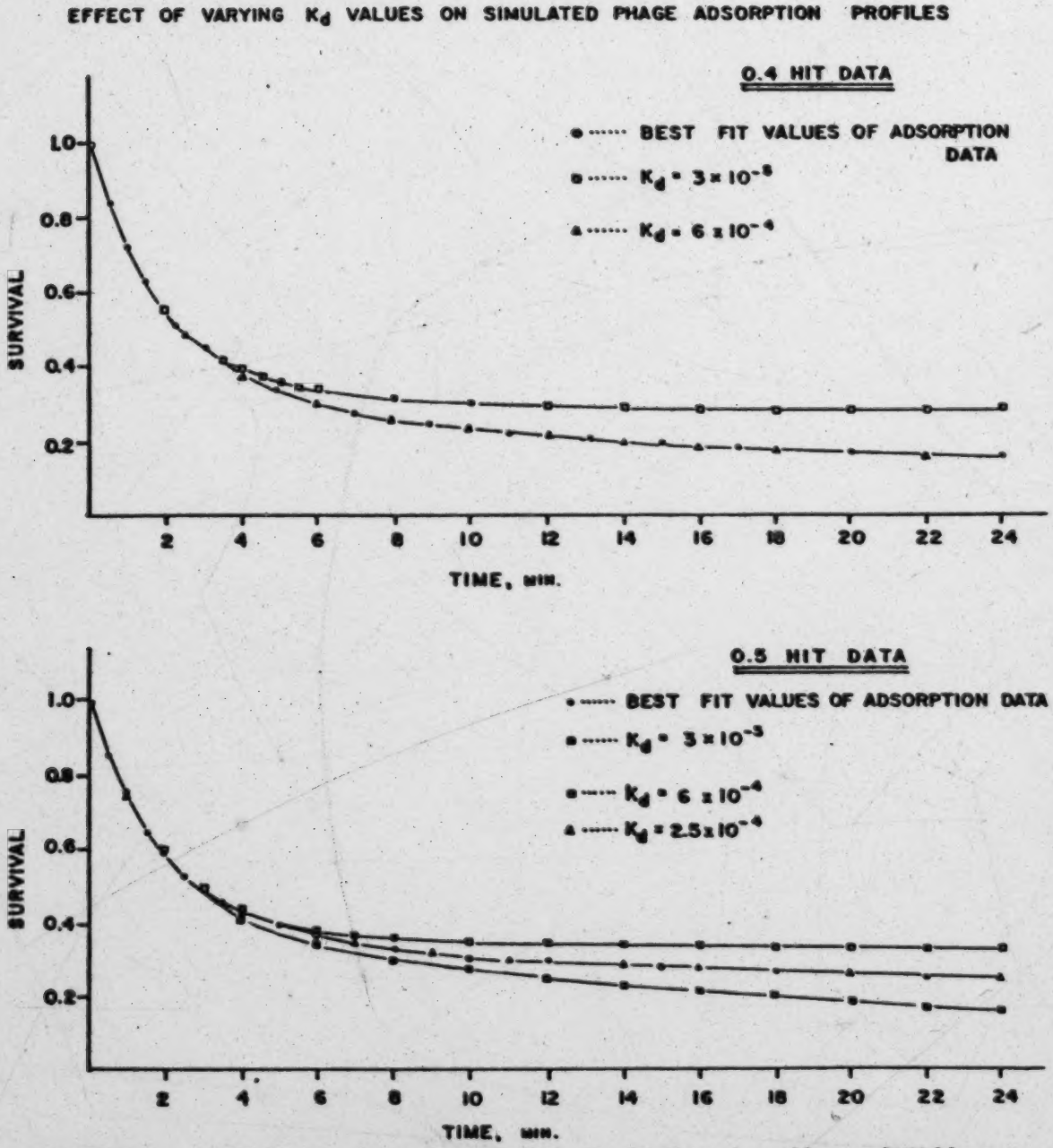
EFFECT OF VARYING K_d VALUES ON SIMULATED PHAGE ADSORPTION PROFILES
0.4 HIT DATA
BEST FIT VALUES OF ADSORPTION DATA
$K_d = 3 \times 10^{-5}$
$K_d = 6 \times 10^{-4}$
SURVIVAL
TIME, MIN.
0.5 HIT DATA
BEST FIT VALUES OF ADSORPTION DATA
$K_d = 3 \times 10^{-5}$
$K_d = 6 \times 10^{-4}$
$K_d = 2.5 \times 10^{-4}$
SURVIVAL
TIME, MIN.

FIGURE 9. Simulated adsorption profiles, showing the effect of different values of K_d. TOP: 0.4 hit data. The experimental value for K_d (determined from slopes in Figure 8 to be 3×10^{-5} sec.$^{-1}$) was used to generate an adsorption curve (□) from the equations given in Appendix A. K_d was varied until coincident curves of best fit values of the actual adsorption data (o) and hypothetical K_d adsorption profile (▵) were obtained.
BOTTOM: 0.5 hit data, same fitting procedure.

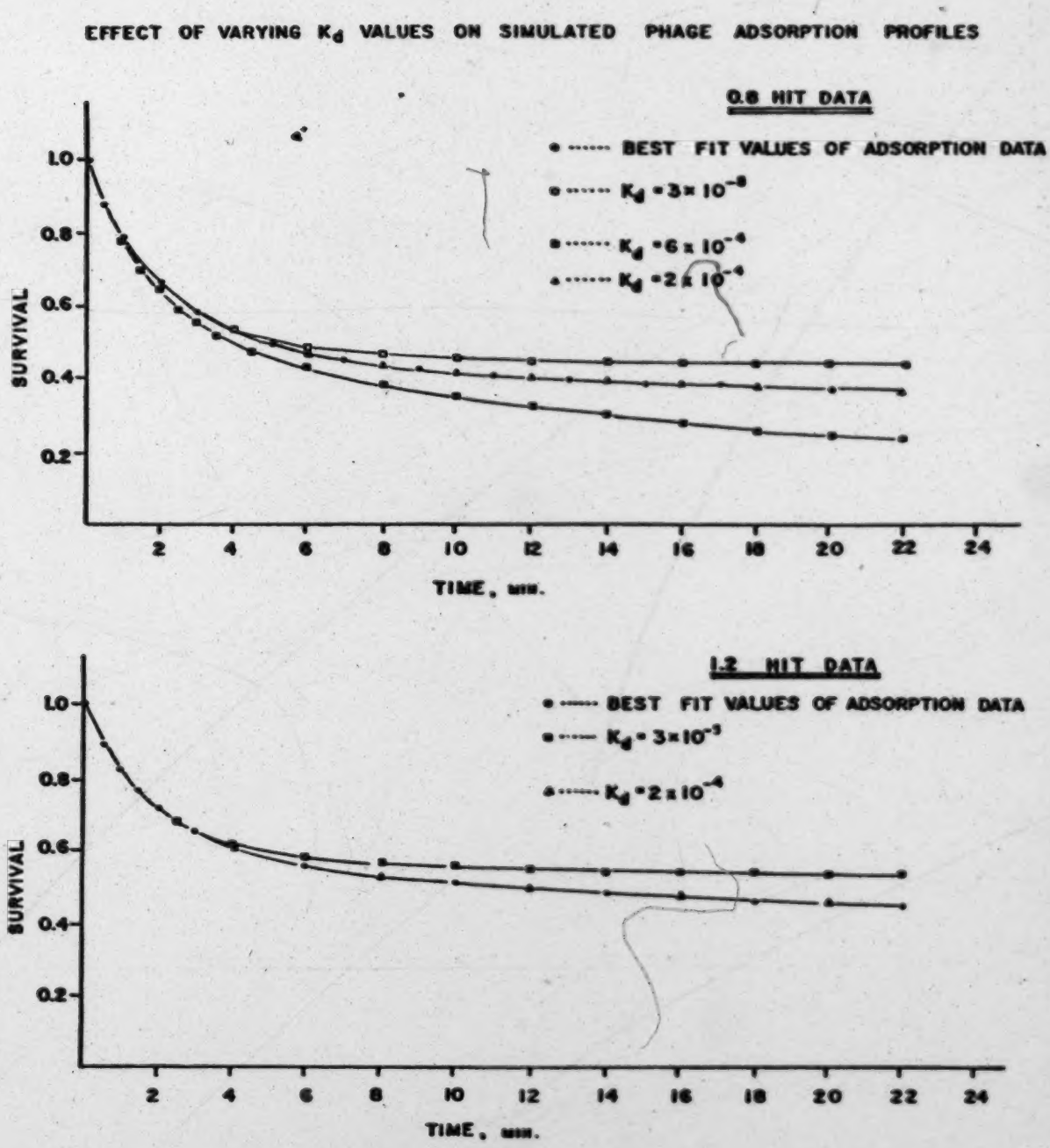

FIGURE 10. Simulated adsorption profiles, showing the effect of different values of K_d. Fitting procedure for 0.8 hit data (top) and 1.2 hit data (bottom) as in Figure 9.

the two survival curves, best fit of the data and adjusted Kd, coincided. Although results are not totally consistent with a unique Kd value, the experimental Kd value was in all cases much lower than would be required to explain the observed adsorption curves of Fab' treated phage. Table III summarizes the values of Kd found necessary to explain the data on such a basis as was outlined in equation (9).

C. ACTIVATION OF FIBERLESS PARTICLES.

Since treatment with Fab' modified the adsorption characteristics of the phage in a manner consistent with generation of a slower adsorbing class of phage, attempts were made to modify the phage in some other manner to yield a similiar class of phage with respect to adsorption characteristics. Wood and Henniger (1969) found that fiberless particles could be activated *in vitro* by the addition of a tail fiber preparation. Although their results were primarily concerned with the mechanism of fiber attachment in morphogenesis, their study offered a system which could be utilized to examine the problem of Fab' inactivation of phage.

Their results were consistent with a mechanism whereby fibers were added one at a time. The feasibility existed, therefore, of producing different classes of phage, each with a different number of tail fibers. Since one implication of the Fab' binding proposal suggests the complete

TABLE III

FITTING OF DISSOCIATION CONSTANT, K_d

HITS	K_d(exp.)*	K_d(fit)**	K_d(fit)/K_d(exp.)***
0.4	2.8×10^{-6}	6.0×10^{-5}	21.4
0.5	-	2.5×10^{-5}	8.3
0.8	3.0×10^{-6}	2.0×10^{-5}	6.7
1.2	-	2.0×10^{-5}	6.7

* K_d(exp.) determined from observed changes in adsorption profile of treated phage for 600 minutes.

** K_d(fit) is that value required to generate survival curve identical to best fit of observed data for each dosage.

*** This ratio indicates to what degree K_d(exp.) would have to be in error to fully explain neutralization by Fab' on a single hit basis.

inactivation of the fiber, a phage particle missing that fiber should have the same or nearly the same adsorption characteristics as the one-hit phage. Results of this section suggest such classes are produced in the *in vitro* complementation of fiberless particles.

i. Titer Increase of Fiberless Particles.

Purified fiberless particles at a concentration yielding $3x10^7$ PFU's/ml (on CR63) were activated by the addition of a lysate which had wild type fibers but lacked phage head and tail structures. The M23-10 lysate was chosen as described in Materials and Methods. This crude lysate of M23-10 used in the *in vitro* activation scheme had a background titer of $5x10^5$ PFU's/ml on CR63, which was ignored since it gave rise to only 1% of the plaques on the initial plates, and less than 0.01% of the plaques on the final plates.

Results of the activation process are shown in Figure 11. The first experiment (o) carried out using fibers prepared only 30 minutes beforehand shows activation kinetics similiar to Wood and Henninger's results. In agreement with their results, no significant increase in titer was observed after 60 minutes.

Adsorption assays of each time sample were carried out promptly using *E. coli* CR63 as indicator bacteria.

The second activation curve (□) represents results of a

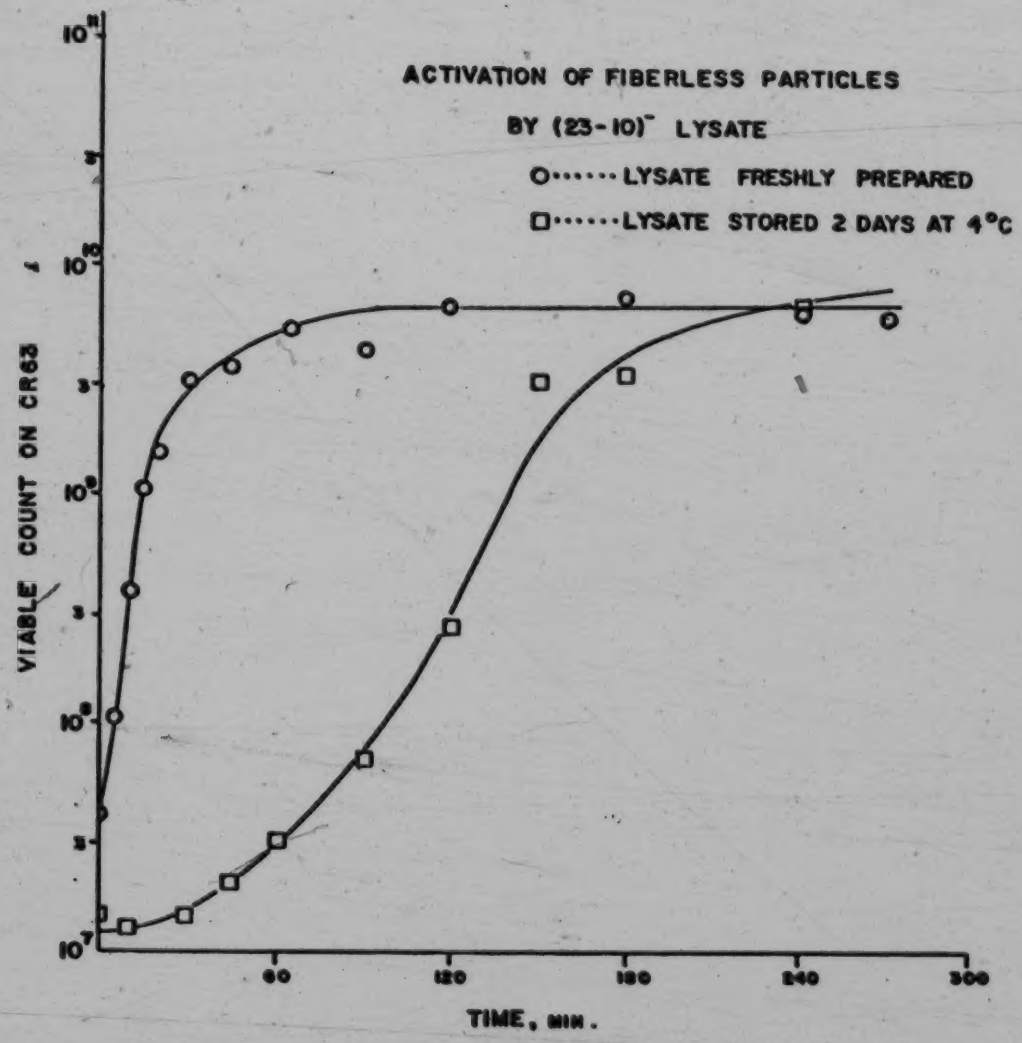

FIGURE 11. In vitro complementation of fiberless T4 particles with M23-10 lysate. 1. Fresh M23-10 lysate was added to fiberless particles and increase in titer was followed by plating on E. coli CR63 (o). 2. Activation repeated using two-day old lysate and one-fourth the number of input fiberless particles (□). Adsorption assays were carried out on samples taken in the first activation experiment only.

2-day old fiber preparation used in the above scheme. The fiber lysate used in the first experiment was stored at 0° C for 2 days, and the activation experiment repeated. One-fourth the initial number of fiberless particles were used in this second experiment, but final titers appeared to reach the same levels as before. This suggests the final level in the first experiment did not reflect the level of complementable particles added. Calculations for the first activation scheme indicate about 20-fold more particles were added than were finally complemented.

A distinct lag of longer duration than that observed in some of Wood and Henninger's results was seen in the second activation process. Total activity of the lysate did not seem to be affected, however, since the final titer was the same as before, even with only one-fourth the number of particles added. Aggregation of the fibers could explain these results; dissociation of the aggregates could be rate limiting in the second experiment. Structural denaturation of fibers is also a distinct possibility, since results would still be in agreement if fibers had not reached final yield-limiting concentrations after such denaturation. The activation curve is also very dependent on a labile cofactor, the gene 63 product (Wood and Henninger, 1969). Concentration and activity of this cofactor could influence this lag formation as well.

Activation experiments were carried out at 35° C, as

outlined in Wood and Henninger's protocol. From other workers' observations of rapid loss of activity of the gene 35 product at 37° C (Imada and Tsugita, 1972a; Ward, et. al., 1970), denaturation of this extremely sensitive product is also a distinct possibility in the second activation experiment.

The possibility of fibers being in yield-limiting concentration was ruled out by using fresh lysates in concentrations approaching near in vivo conditions. Other experiments showed fibers were not yield-limiting in concentration by the addition of fresh fibers at the 180 minute stage. No significant increase in the final titer was noted, but a linear increase in titer of less than 10% was observed within 10 minutes of fiber addition.

No adsorption assays were carried out during the second activation experiment since loss of activity of the fibers was anticipated.

ii. Adsorption Profiles of Complemented Phage.

Only four samples were selected to show the adsorption profiles of complemented phage (see Figure 12). Samples were assayed and kinetic manipulations carried out, however, for the majority of the time points shown on the activation curve of the initial experiment (o-o, Figure 11). Even though the titer does not rise after 60 minutes of activation, the adsorption profiles of the samples change

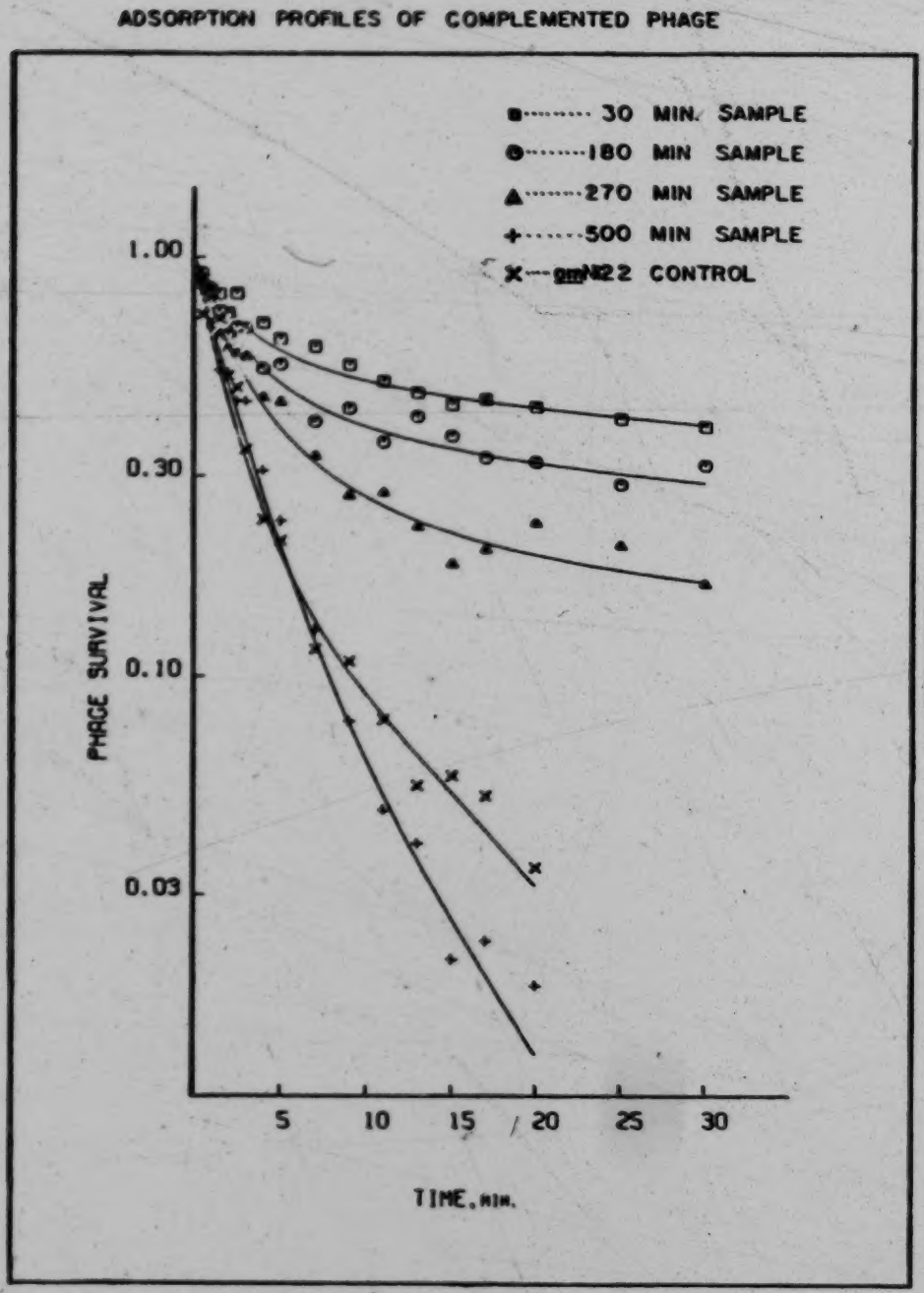

FIGURE 12. Adsorption profiles of <u>in vitro</u> complemented phage at various times in the activation process. Sample indicates time in activation experiment 1 (Figure 11) at which the adsorption assay was carried out. Bacterial concentration used in adsorption assays was 2×10^8 cells/ml. Curves were best fit by adjusting the ratio only; adsorption rate constants and equations are given in the text.

significantly from an obviously slow to a fast adsorbing population.

The curves drawn through the data points shown in Figure 12 represent the best fit of the data. These curves have been generated by the identical solutions to the equations describing the inactivation of phage by Fab' given in Section A. Using the same differential equations and rate constants of the Fab' treatment, the ratio $\{C^0:(C^0+C^1)\}$ was adjusted to fit the data.

iii. Rate of C^0 Generation in Particle Activation.

The differences in adsorption profiles shown in Figure 12 can be attributed to changes in ratios of fast and slow adsorbing classes of phage if the proposals of Wood and Henninger are taken into account. Although exact fiber counts were not established as thought possible by electron microscopy, hypothetical situations of particles having 4,5 or 6 fibers are easily justified. From the adsorption profile, it is possible to calculate a "hit equivalent" value for the incompletely activated phage.

Such a representation of the generation of fully activated phage is shown in Figure 13. Early samples were ignored due to differences in input phage. The low titers of these early time samples , along with the normalization of all curves to the same input value, does not permit valid interpretation at the early times of the activation process.

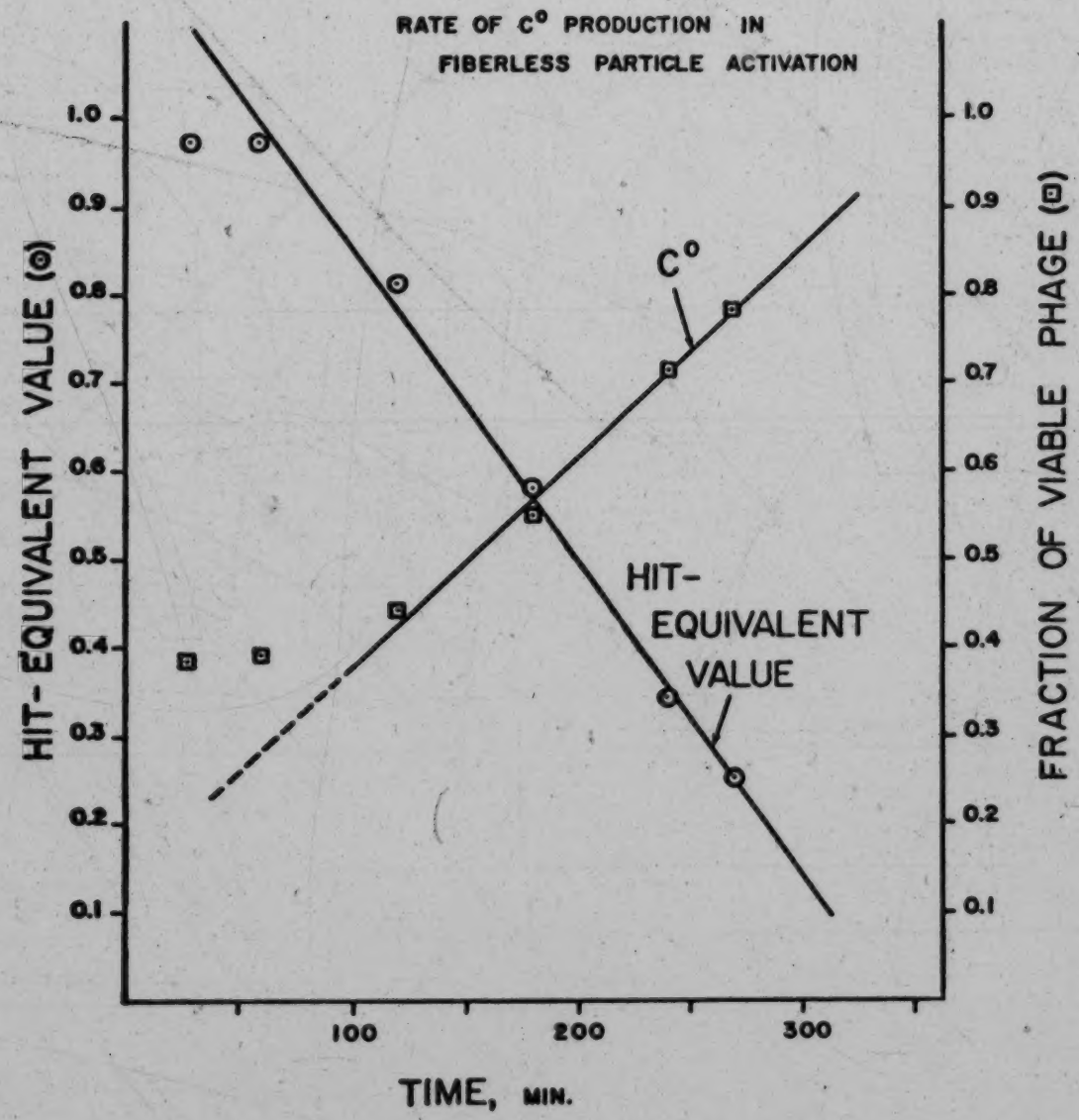

FIGURE 13. Activation of fiberless T4 particles: rate of activation according to changes in adsorption profiles. Hit-equivalent values (o) were derived from the ratio values used to best fit the data shown in Figure 12. C^o values were calculated assuming the Poisson distribution of C^o and C' classes in viable phage.

D. ADSORPTION PROFILES OF AMBER STOCKS.

Before looking at levels of antigens being produced by the different amber mutants (Part II Results), it was necessary to examine the adsorption kinetics of each mutant for two reasons. The first of these was to gain insight into the adsorption rates of the ambers to be able to predict an effective multiplicity to use for constant conditions of infection associated with antigen production. The second was to associate amber mutations with effective roles in the adsorption process at the level of the antigens involved in neutralization.

The adsorption characteristics of the ambers in question are shown in Figures 14 and 15. The adsorption rates for each amber (according to the reversible complex model presented in the preceding results) are given in Table IV. Further reference to the computer solutions will be made in the discussion.

Significant differences are noted in most of the mutants, but generally they can be divided into two different classes . Over 90% of phage in the first class adsorbed in less than 10 minutes (see Fig. 14); the second took about 20 minutes to decrease one-half log (see Fig. 15). The latter type can be described as inefficient adsorbers, the former as normal adsorbers in comparison with <u>am</u> N122. These classes comprise the untreated stock amber

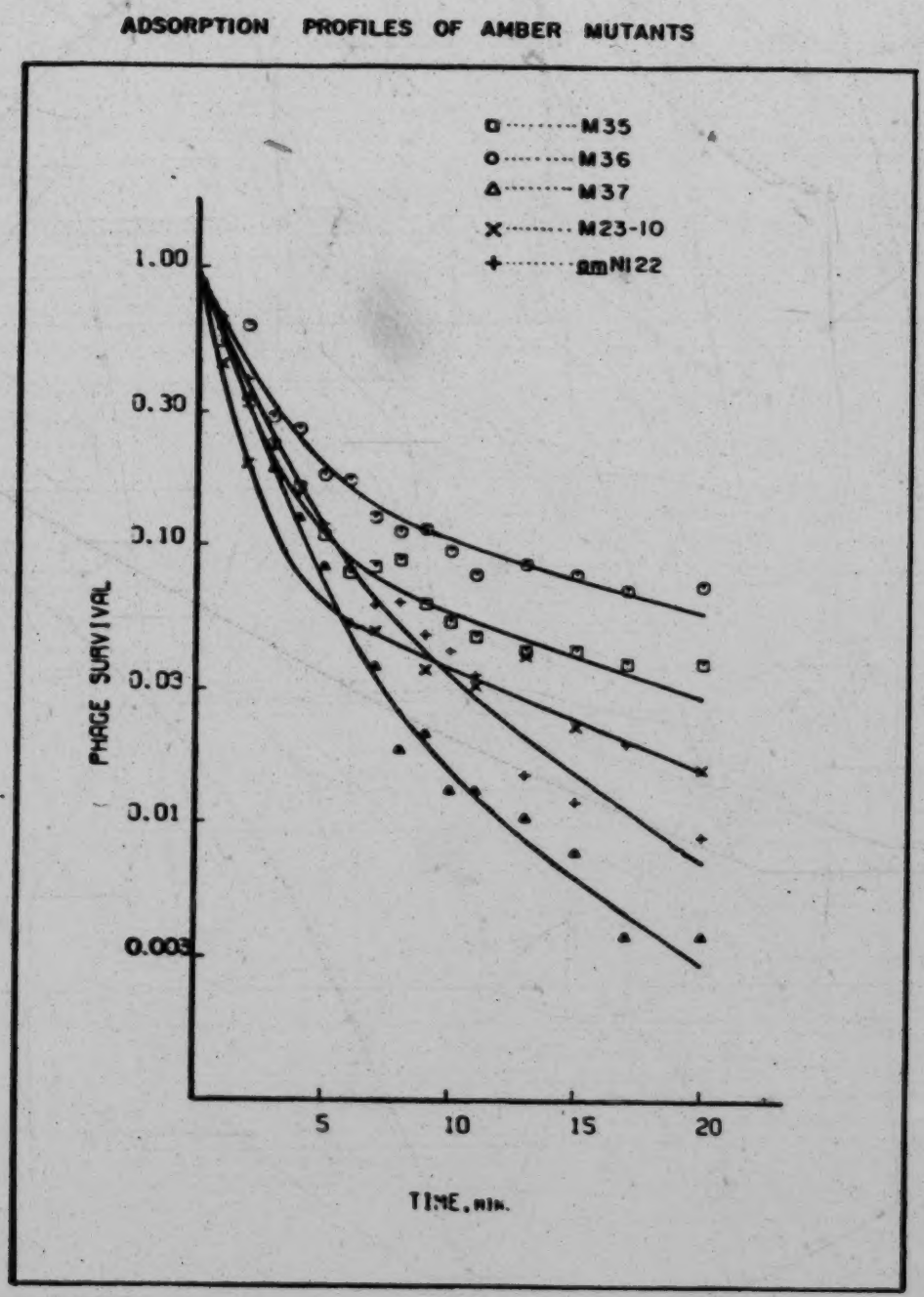

FIGURE 14. Adsorption characteristics of amber mutants. Adsorption profiles determined as in Figure 3, with bacteria at 2×10^8 cells/ml. Best fit curves generated by adjusting adsorption rate constants independently.

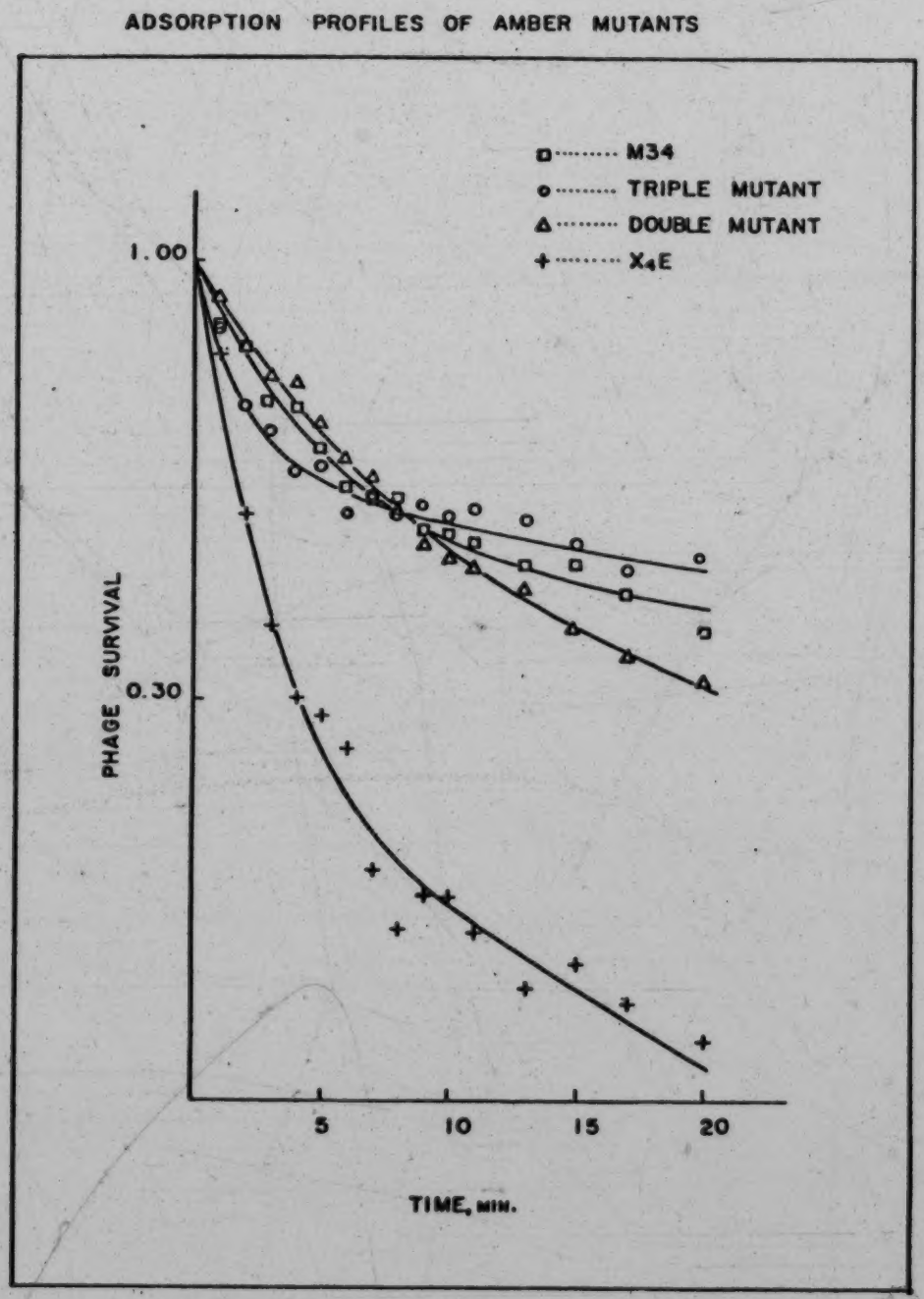

FIGURE 15. Adsorption characteristics of amber mutants. Adsorption profiles and best fits of data were determined as in Figure 14. Double and Triple Mutants have been defined in the text

TABLE IV

ADSORPTION RATE CONSTANTS OF AMBER MUTANTS*

MUTANT	K^1 **	K^2 **	K^3 **
amN122	3.47	5.10	2.5
M34	0.42	5.10	2.6
M35	4.78	1.16	1.2
M36	4.36	1.53	1.0
M37	4.96	0.78	2.4
DM	0.58	4.89	2.5
TM	0.32	7.23	1.6
X4E	4.32	2.04	0.7

*Adsorption model of obligatory reversible complex formation.

** $K^1 \times 10^{11}$ $(\text{Bacteria-sec/ml})^{-1}$

$K^2 \times 10^4$ (sec.^{-1})

$K^3 \times 10^3$ (sec.^{-1})

mutants, and should not be confused with the slow and fast adsorbers introduced in the Fab' treatment or *in vitro* complementation work. Mutants M36 (Fig. 14) and X4E (Fig. 15) have similiar adsorption profiles, and may be used to compare the curves drawn on the two different log scales.

E. ELECTRON MICROSCOPY.

Various attempts were made to correlate the evidence presented in the previous sections with physical observations of such structures. Correlations in fiber counts between wild type T4 and fiberless particles would have supported serum blocking evidence of the purity of fiberless particles. Fiber counts on the *am* N122 mutant used in the adsorption assays would have been of assistance in validating the concentrations of the C^0 class from the *in vitro* experiments.

As well, observations of neutralized phage would have provided evidence for the hypothetical situation of Fab' interaction with a single fiber to modify adsorption properties. Statistical counts correlated with the various dosages of Fab' used to inactivate the phage could have justified use of the Poisson distribution in the calculation of the various classes.

One technique thought to have excellent application to this study was the use of ferritin-labelled anti-rabbit IgG (FEG) as a marker locating antibody molecules bound to the

phage at both neutralizing and non-neutralizing positions.

The system protocol consisted of reacting purified wild type T4 with anti-T4 IgG or Fab' fragments, then reacting, in a "sandwich" fashion, anti-rabbit IgG which had been labelled with electron-dense ferritin. Initially, no success was achieved due to high backgrounds of PEG (even at low concentrations) and non-specific staining by the ferritin. Attempts were made to purify each component of the system, beginning with the gentle purification technique of the two-phase separation of wild-type phage. Purification of the PEG was considered because non-labelled anti-IgG and unconjugated ferritin could contribute to the high background and non-specificity of the samples examined.

Further work with a purified conjugate (see Materials and Methods) showed no better results, again due to high background levels of non-specifically bound ferritin. This stage of the project was then terminated since tail fibers could not be resolved using this technique.

PART II. FIBER ANTIGENS AND THEIR ROLES IN NEUTRALIZATION

Selection of the amber lysates to absorb anti-T4 as opposed to purified antigens themselves arose from the non-trivial purification techniques required to obtain fiber antigens in the necessary quantities (Imada and Tsugita, 1970, 1972a). It was felt that the lysates, being deficient in specific fiber antigens, could be as useful as the purified antigens in establishing their discreet roles in neutralization. Such methodology in obtaining specific antisera has proved useful to other workers (Edgar and Lielausis, 1965; King, 1968; King and Wood, 1969).

Prior to using the deficient lysates in the serum blocking experiments, it was necessary to establish some means of normalizing antigen concentration in the lysates so their relative effectiveness in blocking neutralization could be determined.

Two factors are involved in the serum blocking ability of the antigens in question. The first is obviously the effect of concentration on increasing the blocking power of a lysate. The second, more subtle inference, is that of differences in antigenicity of the individual fiber antigens. Differences in size, accessibility, and immunogenicity contribute to the differences in possible roles of the antigens in fiber neutralization.

It was necessary, then, to examine or detect by

biological and biochemical means any differences of the mutants with respect to their overall infection efficiencies, in particular any differences which might contribute to differential rates of antigen synthesis.

A. CORRELATION OF ANTIGEN CONCENTRATIONS.

Comparative biosynthetic processes and their efficiencies in amber mutants were examined by measuring differences in adsorption properties, burst size, and lysozyme concentrations of each of the mutants to be used in blocking studies.

1. Normalization of multiplicities on the non-permissive host resulting in effectively adsorbed phage.

Normalizing the ratios of input phage to bacteria was not sufficient to ensure uniform infective center formation, due primarily to the differences in the adsorption kinetics of the amber mutants (presented in Part I-D). Uniform infective multiplicities (i.e., formation of actual infected centers, rather than input ratios) were predicted by varying the input phage and adsorption times for each mutant, as shown in Table V. In other words, an attempt was made to allow adsorption of equal numbers of each mutant prior to addition of antiserum. Bacterial concentrations were adjusted to the same absorbance values (within 5%). Dilution adjustments were made using media warmed to 37° C.

TABLE V

PARAMETERS FOR NORMALIZATION OF LYSATES

TO BE USED IN SERUM BLOCKING EXPERIMENTS

MUTANT	INFECTION PARAMETERS[1]				BURST[2]	LYSOZYME[3]
	M.O.I.	TIME	K'	I.C.F.		
M34	4.0	5	0.12	40	75	18.5
M35	0.6	3	1.37	ND	66	17.5
M36	0.6	3	1.25	ND	ND	18.5
M37	0.6	3	1.40	100	170	18.3
DM	4.0	5	0.17	40	70	19.2
TM	5.0	5	0.10	33	47	18.3
X4E	0.6	3	1.25	ND	45	21.4
Wild Type Control	0.8	3	1.00	70	160	16.8

1. M.O.I. represents input multiplicity by titer. TIME, in minutes, is for adsorption before addition of anti-T_4 ($K=1.3$ min.$^{-1}$). K' represents relative first-order adsorption rate on E. coli B/1. I.C.F. is infective center formation, or successful infection on E. coli CR63.
2. Burst size from I.C.F. determinations on E. coli CR63.
3. Lysozyme concentrations are in International Unit Equivalents.

Such adjustments were rarely over 10% of the volume, however.

Infection parameters listed in Table V were adjusted primarily to the initial rate of adsorption of each mutant compared to an N122. A multiplicity of 0.8 for the wild type lysates was selected for dilution controls, as will be presented in the serum blocking results. The three slow adsorbers were given a high multiplicity to compensate for their slow adsorption rates to yield uniform infective center formation. Early linearity of the adsorption profiles indicated dissociation of phage-bacteria complexes' could be ignored in estimating such infective center formation (I.C.F.), but differences noted in I.C.F. values are most likely due to complex decay not accounted for in using only the initial adsorption rate constants of the mutants.

ii. Burst Size Comparisons.

As shown in Table V, burst sizes of the various ambers indicated relatively uniform efficiencies of overall transcriptional and biosynthetic processes. One exception in the burst size is the N37 mutant, whose burst is closer to that of the wild type than the other ambers. This mutant adsorbs more efficiently than wild type. Latent periods of the amber mutants were all about the same when the various adsorption times were taken into account.

The generally lower values of the burst sizes of the mutants, however, suggest lower biosynthetic efficiencies of the mutants when compared to the wild type. This may be of importance in interpretation of the serum blocking capabilities of the phenotypic lysates, presented later in section B.

iii. Relative Lysozyme Concentrations.

Phage-specified lysozyme activity was used as the internal marker to measure phage protein synthesis. Since all other experimental conditions were as uniform as possible, any differences in rates of protein synthesis (indicated from differences in lysozyme concentrations) could be used to imply different fiber antigen concentrations, and adjustments made for such differences in the interpretations of the blocking data.

E. coli B/1 growing at 37° C was infected under the scheme outlined in Table V (i.e., using identical bacterial concentrations and effective multiplicities). Upon infection with the mutants, the cultures were downshifted to 30° C and grown for a further 40 minutes, then chilled immediately in ice water. A 10 minute, 1000xg centrifugation followed immediately, and lysates, kept on ice, were assayed usually within a few hours for activity. No samples were assayed after 4 hours .

Due to the possible effects chloroform would have on

the lysozyme assay system, it was not used in the natural lysate preparation. Observations with early standardizations indicated clearing of the top half of the reaction mixture if chloroform had been used in the lysate preparation.

Initially, lysozyme assays were carried out using dried M. lysodiecticus cells as outlined in Worthington's Enzyme Catalog (1972). No activities were found with any of the lysates, so the modified technique of Tsugita et. al. (1968) was used.

Lyophilized E. coli cells at 0.5 mg/ml were used and absorbancy changes at 350 nm. were followed. Standard egg white lysozyme activity was 3-fold higher using this latter assay as compared to results using the method described in Worthington's Catalog (1972). The activity of standard egg white lysozyme increased from 5.95 units/microgm. on M. lysodiecticus to 15.85 units/microgm. on E. coli. Two-hundred microliters of a T4 wild type lysate had about the same activity as 1 microgram egg white lysozyme in this assay (16.83 units/200 microliters of lysate).

Controls of $6x10^8$ WT T4 PFU's/ml added to the E. coli cells, along with a control of E. coli cells alone, gave no change in absorbance in 30 minutes. Concentrations are given in International Unit Equivalents, calculated from the $O.D._{350}$ changes under the conditions given in Materials and

Methods.

Results of lysozyme production by the various mutants are also shown in Table V. Again, fairly uniform lysozyme activities indicated biosynthetic efficiencies for this late synthesized protein to be approximately equal in all of the phage examined.

B. SERUM BLOCKING CHARACTERISTICS OF AMBER MUTANTS.

Absorption of anti-T4 antiserum with all of the antigens except one would yield an antibody preparation specific for that missing antigen. Knowing the relative concentrations of the fiber antigens from the results presented in the previous section (assuming perhaps equal translation of all fiber genes), it would then be possible to assign a relative role of importance to the fiber antigens involved in neutralization. These roles would depend on each of the absorbed antiserum's neutralization kinetics.

Therefore, serum blocking characteristics were examined for each of the amber deficient lysates, and characteristics were established for the residual neutralizing antibodies left after such absorptions.

Examples of the individual serum blocking experiments of the lysates are presented in Figures 16, 17 and 18. Controls included uninfected E. coli B/1,'lysates' (i.e., cells uninfected, but taken through the same steps as used

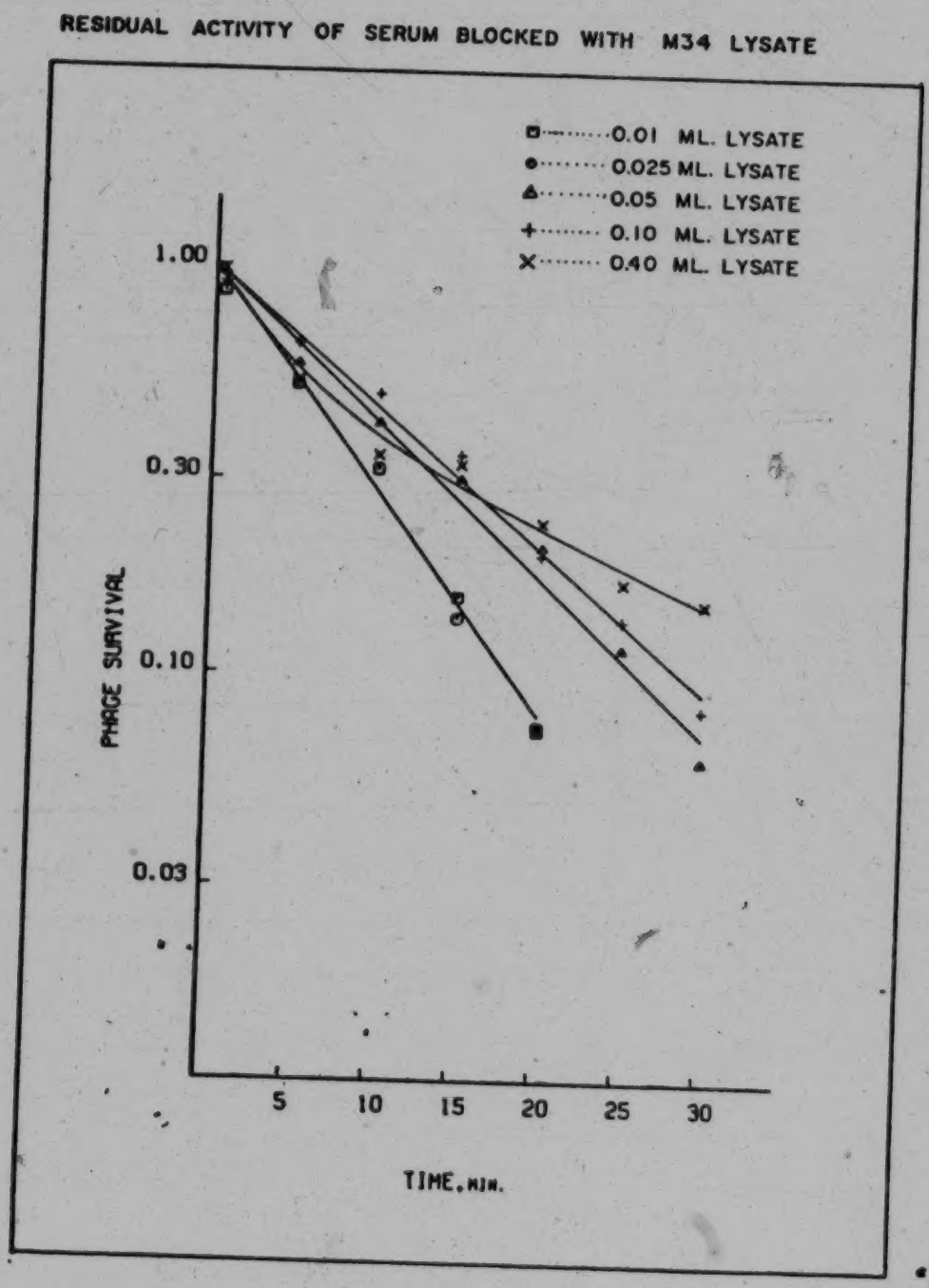

FIGURE 16. Residual neutralizing activity of Anti-T4 blocked with M34 lysate. Anti-T4 and indicated volumes of M34 lysate were incubated under conditions outlined in Materials and Methods. Fitting of data was by non-linear regression analysis for all curves.

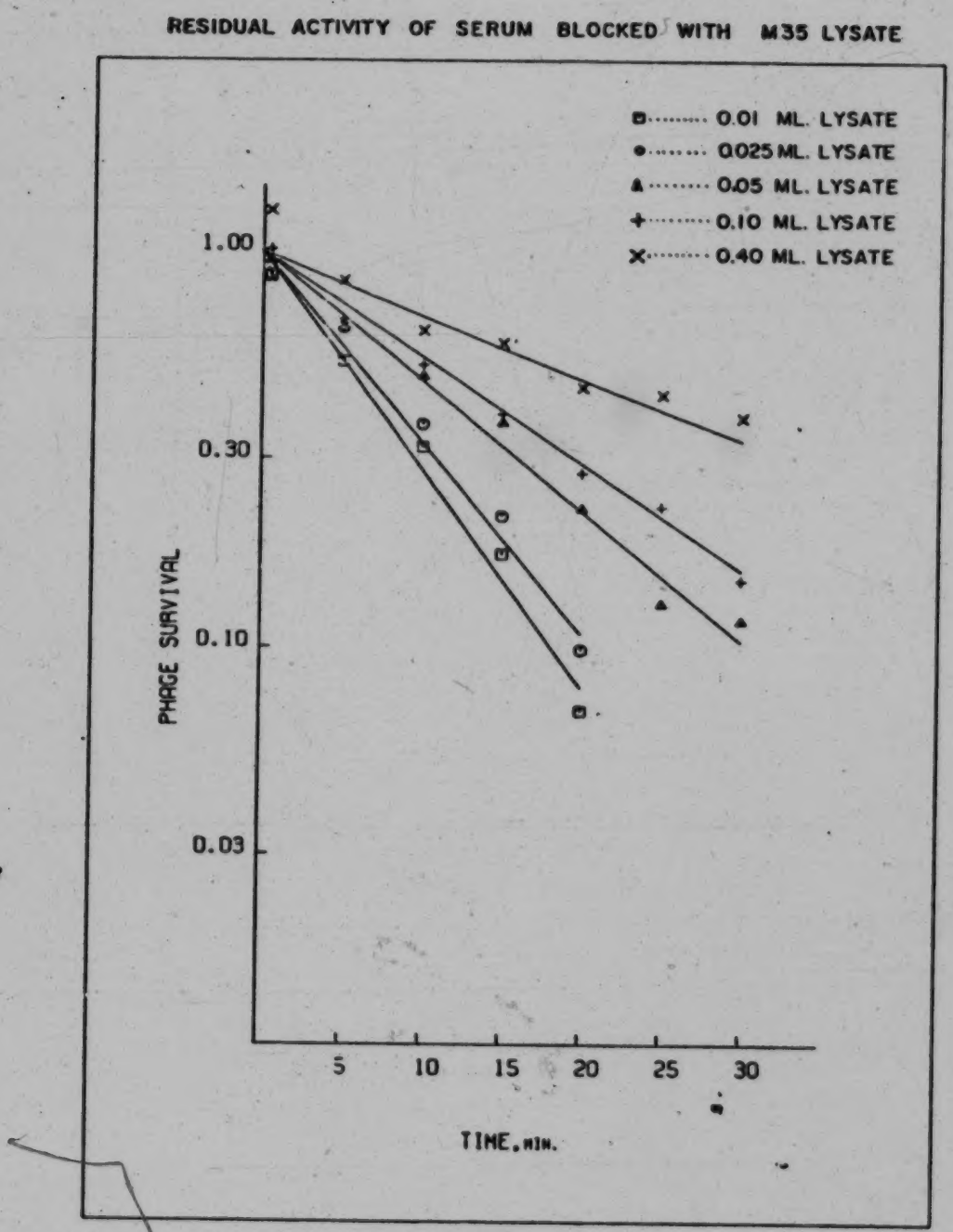

FIGURE 17. Residual neutralizing activity of anti-T4 blocked with M35 lysate. Conditions as in Figure 16. Fitting of data was by linear regression analysis for all curves.

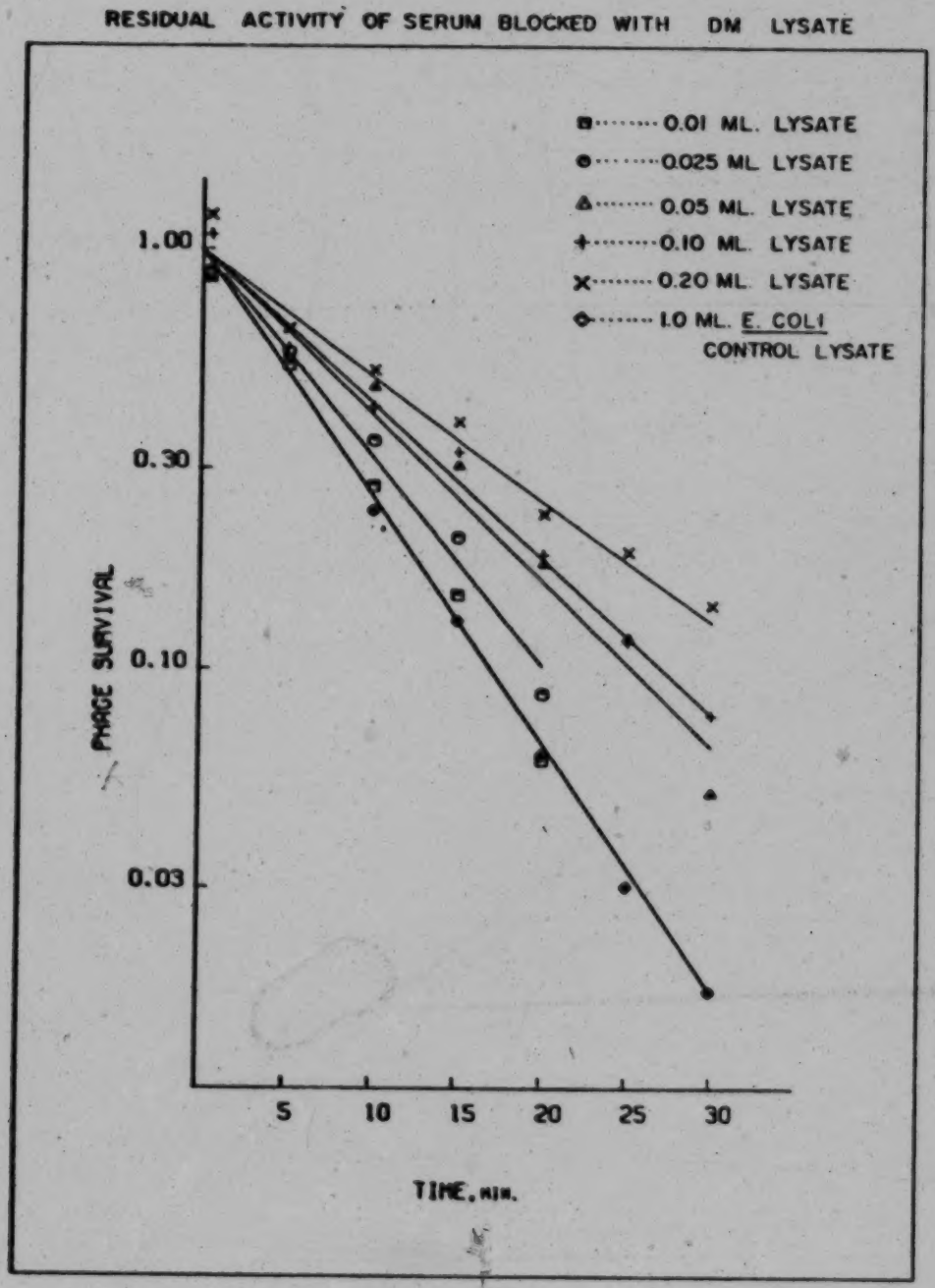

FIGURE 18. Residual neutralizing activity of anti-T4 blocked with DM lysate. Conditions as in Figure 16. E. coli "lysate" (see text) is shown for comparison of residual activity. Curves fit as for Figure 17.

in mutant lysate preparation), T4 WT at the same multiplicity as used for the lysozyme lysates, and that same multiplicity of T4 into a growth flask containing no E. coli.

The results of the T4 WT blocking experiments are shown in Figures 19 and 20. The blocking power of the phage diluted from a blank growth flask (Figure 20) is in close agreement with the standards run in the assays for purity of the fiberless particles. Phage numbers were calculated from the input multiplicity of 0.8 times the dilution factors for medium volume and volume taken for the absorption. Fifty microliters of "blank lysate" were equivalent to 5×10^6 phage particles. This T4 control was used as a measure of the maximum residual fiber antigen concentration remaining in solution after phage adsorption.

One ml of uninfected E. coli lysate failed to block the neutralizing activity of the diluted antiserum. This control is shown with the Double Mutant blocking results, Figure 18. Dilution errors introduced by using different volumes of lysates were insignificant as all controls of this parameter agreed to within 5% (K values from 650 $min.^{-1}$ to 675 $min.^{-1}$). Possible discrepancies in the data were also kept to a minimum by running all lysates at the same time using the same volumes for each run number. Reaction mixtures, then, had a double label to prevent confusion in the ensuing neutralization assays.

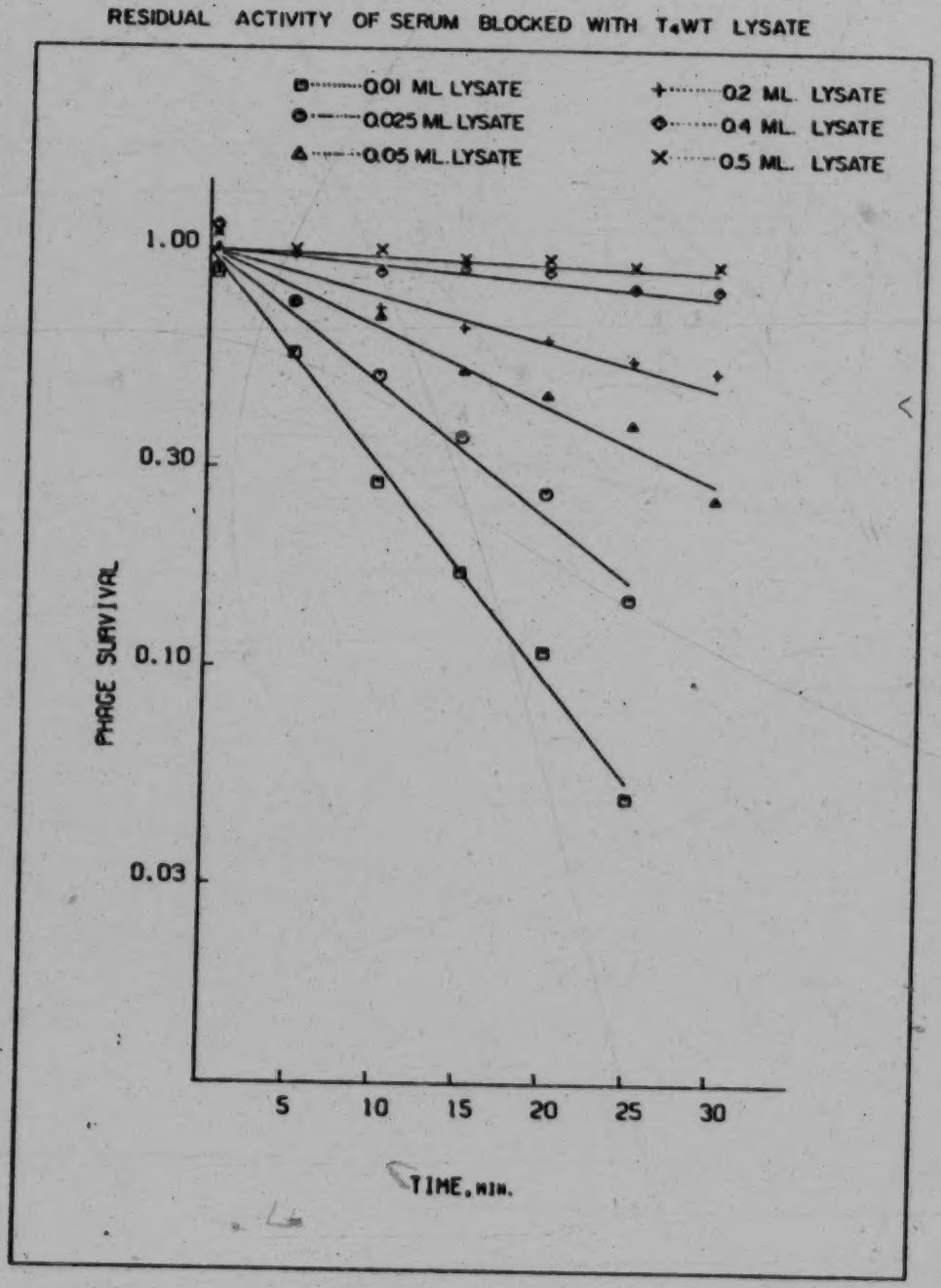

FIGURE 19. Residual anti-T4 activity after blocking with wild type T4 lysate. Curves were fit as in Figure 17.

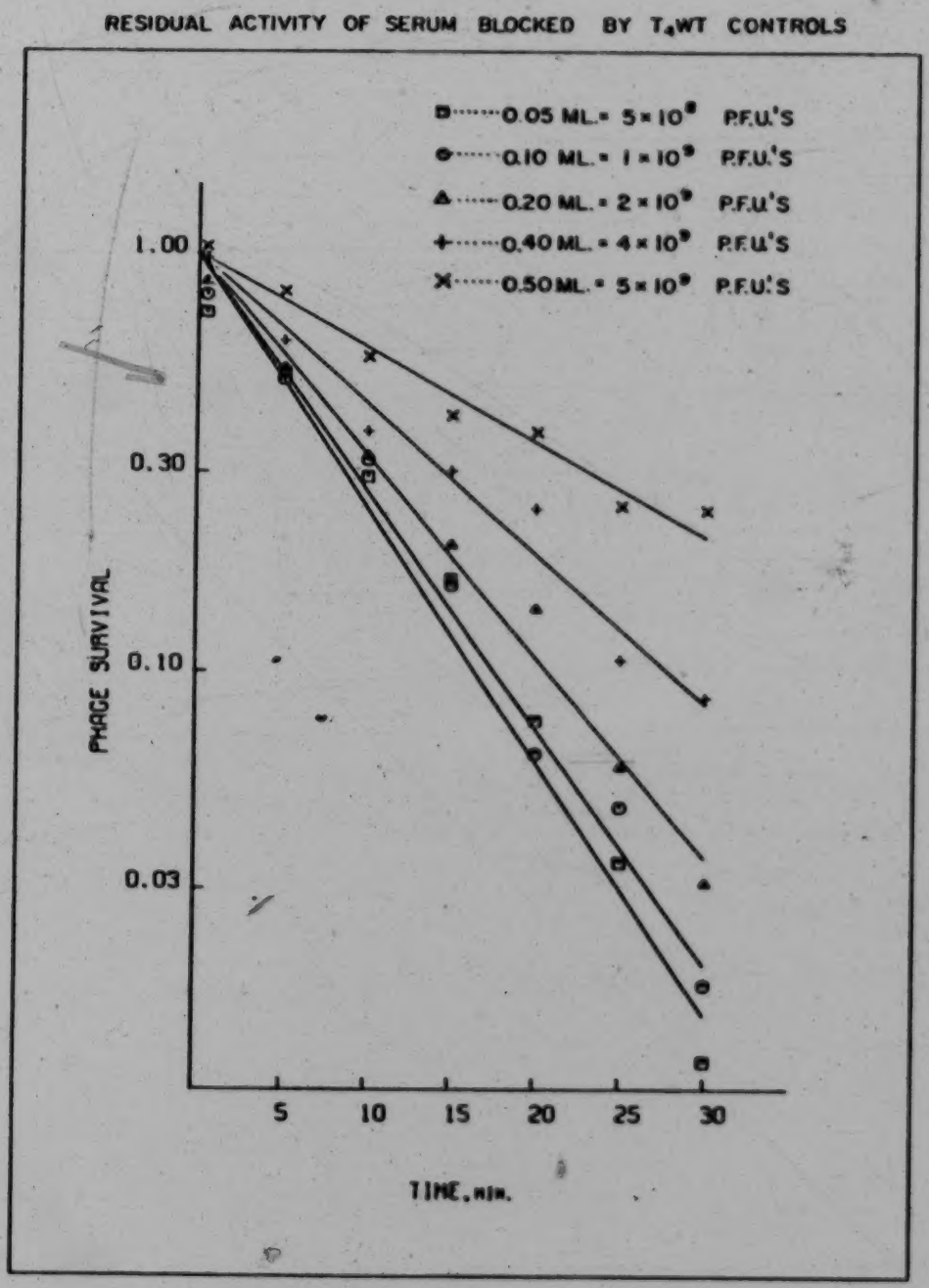

FIGURE 20. Residual anti-T4 activity after blocking with wild type T4. Phage at the same M.O.I. used for lysate in Figure 19 was added to medium containing no E. coli B/1. Indicated volumes were then added to anti-T4, and residual activities determined as before. P.F.U. counts were estimated from dilution factors only. Curves drawn as in Figure 17.

Sera blocked with lysates of the different amber mutants appeared to have different T4-neutralizing capabilities. H34 blocks the serum least efficiently at the lowest concentrations used (0.01 and 0.025 ml) when compared to other lysates, but this could be a result of the sampling errors introduced using these small volumes. The differences observed in the residual anti-T4 activity approach the precision limits of experimentation. Most of the lysates block neutralizing activity monotonically with increased concentrations. Edgar and Lielausis (1965) found changes in the slopes of the neutralizing curves of absorbed anti-T4, and suggested such non-linear kinetics were a result of contaminating residual fibers of input phage. The linearity of both wild type controls, notably as shown in Figure 19, does not agree with their observations. No corrections were made for residual fiber antigens remaining in lysates for unadsorbed phage, since extremes of this parameter showed insignificant blocking.

Non-linear kinetics were observed, however, at some of the higher concentrations of H34 and X4E lysates used in the absorptions, but first-order solutions of the data could be employed to determine residual neutralizing titers. Edgar and Lielausis (1965) showed there were neglible changes in these non-exponential curves when exponential inactivation was assumed. None of the characteristic "shoulders", found by Edgar and Lielausis (1965) and King and Wood (1969) in

their blocked sera, were observed in any of these absorption experiments. These "shoulders" are characteristic of multi-hit kinetics.

Results of the blocking experiments are summarized in Figure 21. Certain qualitative correlations among the fiber antigens and their roles in neutralization are evident, since major differences of slopes of the serum blocking activities can be seen. These observations will be interpreted later in the discussion upon the finding of cross-reacting fiber antigens being present in some of the lysates.

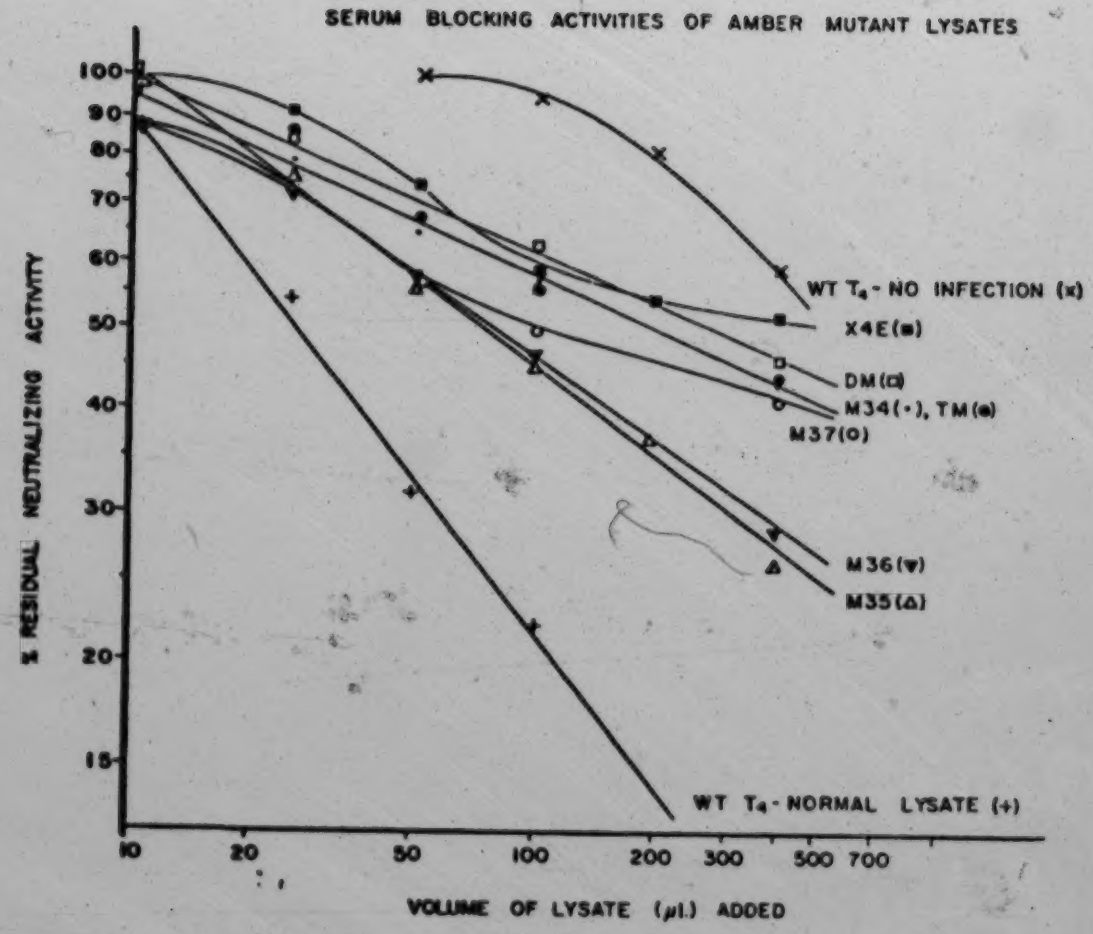

FIGURE 21. Summary of blocking activities of all ambers and T4 controls. Each point represents the linear slope of each of the curves in Figures 16 through 20, as well as data not presented for other amber mutants shown. Lines and curves fitted arbitrarily by eye.

DISCUSSION

The model for phage adsorption used in these studies was based upon formation of an obligatory reversible-complex prior to establishment of the irreversibly infected bacterium (Puck, et.al. , 1951, Stent and Wollman, 1952, Simon and Anderson, 1967). As outlined previously (pg 39, equation 7), such a model for adsorption can be described in the following scheme

$$P + B \underset{K^3}{\overset{K^1}{\rightleftharpoons}} P \cdot B \xrightarrow{K^2} B^*$$

This model need not reflect the actual adsorption process, as most likely there are numerous other interactions from initial contact to final infection. The above description, however, represents the rate-limiting steps for this interpretation.

For example, the model could be more rigourous in handling the individual adsorption of each of the six tail fibers, but if the adsorption of the first tail fiber to the cell wall is the rate limiting step for the adsorption process, this model still applies. Likewise, if K^2 represents the average probability that all six tail fibers have dissociated, then the above model remains representative of the process. Assumptions such as these greatly simplify the solutions of the differential equations describing this model. These equations and their solutions

are given in Appendix A.

This study has made extensive use of the conditional lethal amber mutant, *am* N122. When this mutant adsorbs to its restrictive host, *E. coli* B/1, any phage reaching the irreversible stage in infection (i.e., B*) is lost to the assay, since it is unable to form progeny. Plaques formed, therefore, are due to either free phage left unadsorbed at the time of sampling, or to phage which have dissociated from the [restrictive host-phage] complex.

Such dissociation can occur in two time periods in the assay protocol. The first is in the dilution tube immediately after sampling; the second is on the plate during incubation. The first time period is minimized to a few seconds, and should, therefore, not represent a source of error in the calculation of free phage left unadsorbed at the time of sampling. The second time period has been shown to be of about two hours duration (Stemke, *et. al.*, in press). Corrections for the generation of free phage on the plate for up to two hours have been included in the kinetic manipulations.

Other workers have examined the effects of bacterial concentration on phage adsorption kinetics (Gamow, 1969, Stent and Wollman, 1952). In this study, the rate constants best fitting the adsorption data were consistent for all but the highest bacterial concentrations examined. Such

deviations have previously been observed for numerous other models, and are not significant as the adsorption assays for the remainder of the experiments were carried out at acceptable bacterial concentrations (Gamow, 1969).

Phage T4 are neutralized with one-hit kinetics when IgG or whole anti-T4 serum is used as the inactivating agent (Delbruck, 1945; Jerne and Skovsted, 1953; Stemke and Lennox, 1967). The equation describing this relationship is

$$S = 1 - e^{-KT/D} \qquad (1)$$

A linear exponential decrease in phage survival with time is observed upon incubation of phage with either of these neutralizing agents. The single-hit kinetics shown in Figure 22 (o) arise from the monogamous binding of the divalent IgG molecules to critical site(s) on the phage. Since time of incubation and dosage are directly proportional, relationships such as those shown in Figure 22 can be used to correlate phage survival in both IgG and Fab' mediated neutralization.

Kinetics of phage neutralization by Fab' are also shown in Figure 22(■). Phage survival in this case is characterized by a "shoulder", and follows the multi-target equation

$$S = 1 - (1 - e^{-KT/D})^n \qquad (3)$$

with n being the ordinate extrapolate of the linear portion

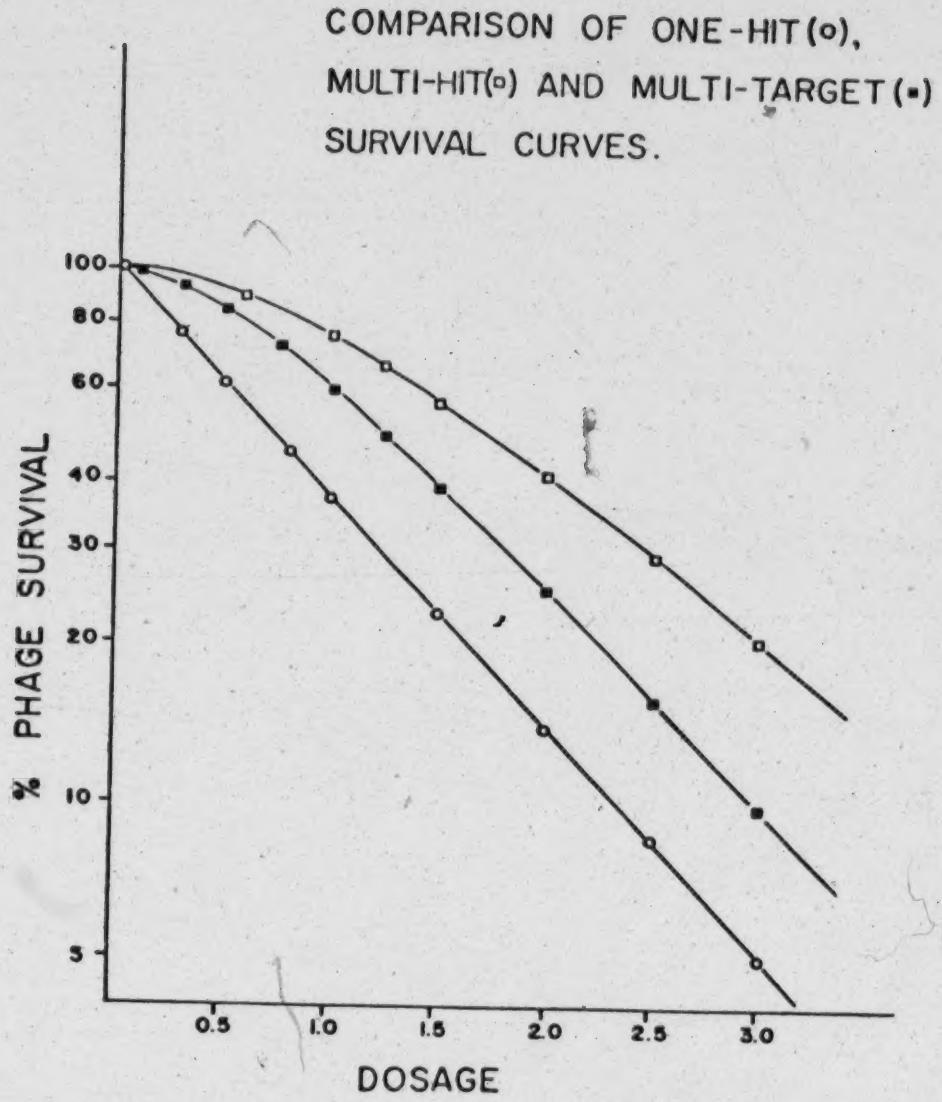

FIGURE 22. Predicted survival curves of one-hit (o), multi-hit (□), and multi-target (▪) phage neutralization models. The one hit model is followed by IgG neutralization of phage. Fab' neutralization follows the multi-target equation given in the text, but use of the multi-hit system facilitates calculations by permitting class distributions to be predicted from the Poisson function.

of the survival curve (Stemke, 1969). The value for 'n' in equation (3) represents the number of combinations of Fab' with phage critical sites necessary to completely inactivate the phage. These interactions are of necessity independent, as opposed to the monogamous binding of both active sites of the IgG molecule.

The interaction of a single monovalent fragment with the phage tail fiber is assumed to modify the adsorption profile of the untreated phage. Such a modification is normally manifest as a decreased initial rate of adsorption, along with a lower percentage of the phage population finally being removed from the non-permissive bacterial suspension. Such adsorption profile changes are directly proportional to Fab' dosage (see Figure 5, pg 46). In these experiments employing Fab' to inactivate the phage, the summation of the characteristics of the different predicted classes of adsorbers has allowed consistent fitting to the experimental data.

The two mechanisms described by equations (1) and (3) imply the existence of different classes of phage resulting from treatment with the neutralizing agents. In the case of IgG treatment, only one adsorbing class of phage remain after treatment , and this surviving fraction is assumed to be composed of "normal" adsorbers only. Those phage with one hit of IgG are unable to adsorb to the bacteria. In the case of the multi-target hypothesis for Fab' neutralization,

the surviving fraction would be composed of 2 adsorbing classes of phage; those with no Fab' molecules bound (P^0 class), and those with one hit (P^1 class). Those phage with two (or more) Fab' molecules bound to critical sites are unable to adsorb (hence, neutralized).

Total survivors, then, in this second proposal are comprised of the P^0 fraction (o) and the P^1 fraction (●) shown on Figure 23. The sum of these two classes yields the points indicated on the multi-hit survival curve (□) in Figure 22. The P^2 class is shown for completeness and represents those phage which have been neutralized.

As an alternative to the concept of two adsorbing classes of phage, these neutralization kinetics involving Fab' and phage could be explained by dissociation of the fragment permitting normal adsorption to occur. Other workers have found neglible effects for such dissociation in divalent antibody neutralization, but the univalent nature of Fab' might favour [complex] dissociation (Krummel and Uhr, 1969, Stemke, 1969).

As in dissociation of untreated phage in the original restrictive host complex formation, any [phage-Fab'] complex which dissociates on the plate within two hours could still give rise to a plaque. Therefore, such dissociation could not be directly measured in the simple neutralization assays, and secondary evidence had to be obtained from

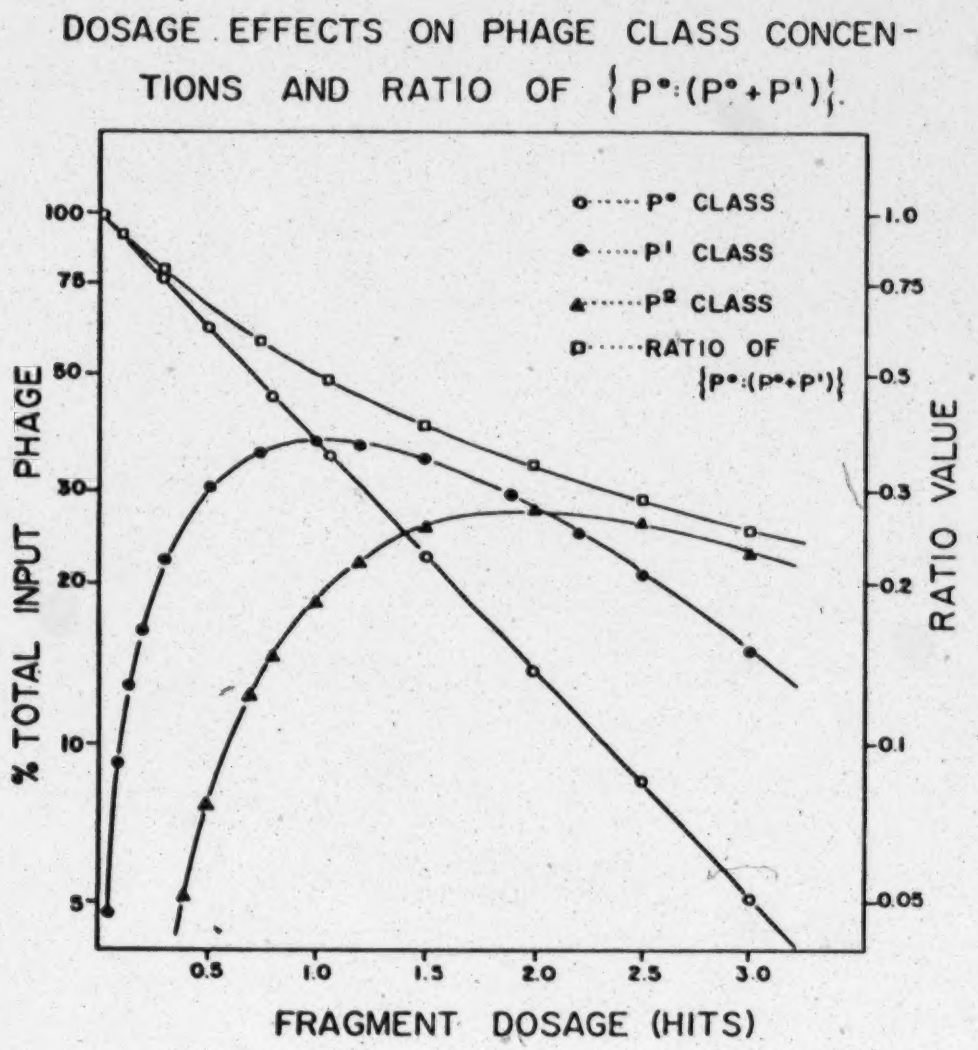

FIGURE 23. Relative concentrations of P^0, P^1 and P^2 classes of phage at different dosages of Fab'. Also shown is the change in the value of the ratio $P^0:(P^0+P^1)$ with increasing dosages. Hit values were calculated as in Materials and Methods. Phage classes are those predicted from a Poisson distribution of Fab' over the input phage population.

experiments in which adsorption differences could reflect the effects of this dissociation. The results presented in Figures 6 and 7 (Pages 50-51) indicate [Fab'-phage] dissociation does occur. The time scale itself indicates the degree of dissociation when compared to the kinetics of adsorption of the partially neutralized phage. The significance of [Fab'-phage] dissociation within 20 minutes was questionable, although measurable differences in adsorption characteristics were evident over 10 hours.

If dissociation was to account for the observed changes in adsorption of phage given different dosages of Fab', one could hypothesize that Fab' neutralized with one hit kinetics, and that only those phage with no Fab' molecules bound could adsorb. Thus, the rate of [Fab'-phage] dissociation (represented by Kd) would be indicative of the rate of regeneration of the sole adsorbing class. Assuming that untreated phage, or those phage with Fab' bound to non-critical sites, possessed the same adsorption characteristics as before, the model was established to include the effects of this Kd.

The equations and their solutions for this dissociation model have been developed in Appendix A. Essentially, it was found that for [Fab'-phage] dissociation to fully account for the observed changes in adsorption, the experimentally determined Kd had to be increased 8 to 20 times (see Table III, pg 57). Thus, such dissociation can

be neglected in the Fab' neutralization scheme outlined above.

The assumption that a single Fab' hit modifies the functioning of a single fiber follows from the proposed model. Further evidence in support of this hypothesis could be obtained if such adsorption changes were to be generated in an independent manner.

Tail fibers are added to fiberless T4 particles via a random mechanism (Wood and Henninger, 1969, Ward, et.al., 1970). By examining the complementation of fiberless T4 particles with active fibers in vitro, a second means of altering the adsorption characteristics of phage was established.

When fiberless T4 particles were activated in vitro with a lysate containing tail fibers, PFU increases similiar in magnitude to those reported by Wood and Henninger (1969) were observed. By examining the adsorption characteristics of these complemented phage, it was possible to establish a model compatible with that of the proposed inactivation model. The utilization of adsorption profile changes is probably more indicative than titer increase for the true activation process involved with fiber addition to particles, either in vitro or in vivo.

Adsorption characteristics of the complemented phage particles are similiar to those of the partially neutralized

phage. Hypothesizing again two different adsorbing classes of phage (C^0 and C^1) and using the same rate constants for each of these populations as for the Fab' treated phage (i.e., the P^0 and P^1 classes), good fits were consistently obtained for the experimental data.

The changes from a slow to a fast adsorbing phage population could represent phage particles passing through various stages of activation, each class having a different number of functionally active fibers. Adsorption of the phage could only occur after each particle had obtained a critical minimum number of fibers.

Although exact fiber counts of these complemented phage particles were not established as thought possible by electron microscopy, division of these particles into adsorbing classes possessing 4, 5 or 6 fibers can be justified (Wood and Henninger, 1969; Gamow and Kozloff 1968; Ward, et.al. , 1970). From the adsorption profile of these complemented phage, it is possible to calculate a "hit equivalent" value. Such a term is useful only for the correlation of the two mechanisms in that it determines the relative concentration of fast and slow adsorbers in the activation process, as in the Fab' inactivation process. Since the titer of the activated phage does not change significantly after 60 minutes, normalized values of total phage population can be used. Deviations caused by the normalization of data (to uniform input phage counts) at

times earlier than 60 minutes in the activation scheme are evident in the treatment of adsorption profiles in Figure 13 (page 64).

From this "hit-equivalent" ratio, and assuming only two adsorbing classes, as opposed to Wood and Henninger's proposal of different efficiencies or probabilities of infection, it is possible to calculate the relative concentration of a C^0 class of adsorbers. The "C0" designation is used to represent those phage which are fully adsorbable with wild type characteristics. Such a class could have 5 or 6 fibers attached, but such a distinction is not possible at this level of model simulation.

One further point in this activation model is the apparent discrepancy in the adsorption characteristics of the standard am N122 and the final complemented particles (see Figure 12, page 62, "500 min. sample"). These adsorption profile differences suggest the complemented particles are slightly more active than the am N122 mutant. Computer solutions to the rate constants for this final complemented phage adsorption profile are comparable to those of am N122, except for a two-fold increase in K^1.

These differences in activity have been observed in other mutants as well, and are discussed later in this section. Long term storage effects on am N122 can influence its adsorption profile, and such effects could generate the

differences between the "500 min sample" of complemented phage and the standard *am* N122. This follows from the adsorption profile of the complemented particles being determined within minutes of fiber addition. Also, the complemented phage were not subject to high speed centrifugation as the *am* N122 mutants were in their purification.

The linearity of the "hit-equivalent" value with time, as well as its derivation into a linear C^0 generation rate, shown in Figure 13, pg 64, supports others workers' evidence for single fiber addition (Wood and Henninger, 1969; Ward, *et. al.*, 1970). This linearity suggests that fiber addition is a diffusion controlled process with no dependency on homotrophic cooperativity effects nor differential rates of attachment from first fiber to last. These data do not exclude the possibility of a separate activation step, independent of final fiber attachment, being responsible for the changes in adsorption characteristics.

Although other workers have successfully employed the ferritin-labelling technique previously described, few positive results were obtained in the present study. Lack of success can generally be attributed to insufficient specificity within the system. The techniques available might have yielded sufficient evidence to support the hypothetical situations predicted for the adsorption data,

had they been successful. Favourable evidence, even for the fiber counts on wild type T4 and fiberless T4 particles could have been used to correlate the activation process with the neutralization model.

Individual roles of the fiber antigens may be beyond the resolution of the ferritin-labelling technique. Evidence for binding of the anti-rabbit IgG to individual fiber antigens would require homogeneous antibody preparations, specific for each fiber antigen to be examined. Non-specific protein binding to the grid surface may tend to obliterate the non-covalent IgG-fiber antigen interactions as well. The technique would undoubtably suffer from extremes in salt concentrations on the grid surface (during sample preparation and drying) with respect to the neutralization reaction, and any correlation between kinetic and electron microscopic observations would have been seriously limited. The resolution required for locating specific antigens on the fibers by the technique of ferritin-labelled antibodies might also be limited by the size of the ferritin conjugate.

Others have been able, however, to locate fiber antigens using specific-antibody techniques (Yanagida and Ahmed-Zadeh, 1970, Hoglund, 1967). The antibody concentrations employed in those studies were much too high to correlate their observations with neutralization data. The antigenic regions of interest on each fiber are of the

order of a few hundred Angstroms or less. Coupled with the size of the conjugate, individual neutralizing antibodies might be located using this technique at the low concentrations required for kinetic interpretations of neutralization.

Functional differences of the fiber antigens in the neutralization process were investigated by examination of any adsorption differences among the various amber mutants raised under permissive conditions. Initially, adsorption characteristics of the amber mutants were determined to correlate the mutation site with adsorption function. These results, shown in Figures 14 and 15 (pages 66-67), and described by their rate constants in Table IV (page 68), can be interpreted on such a functional level.

The amber mutants X4e, M35, M36, and M23-10 all adsorb less efficiently than <u>am</u> N122. M36 and X4e adsorb with similiar kinetics, both being the slowest of normal adsorbers examined. Since gene 36 involves the hinge region of the fiber, an amino acid substitution in this region of the protein could influence proper functioning of these fibers in adsorption. A specific example could be when the fibers change shape and act to relocate the phage baseplate in closer proximity to the cell wall. Similiarly, the mutation in gene 35 (which acts to modify the BC half fiber prior to attachment to the A half-fiber) could influence the hinge region of the completed fiber.

The M34 stock amber mutant adsorbed slower than the am N122 standard. One explanation for this could be that the amino acid substitution in the 34 gene product results in interference with the attachment of the proximal half-fiber to the baseplate following fiber completion. Interference with some role in the triggering mechanism responsible for the initiation of sheath contraction could also arise from the amber coded insertion.

The M37 mutant adsorbs significantly faster than am N122. Since the location of this amber mutation (N91) within gene 37 has not been found in a search of the literature, it would be reasonable to predict that its resulting amino acid insertion in the product of gene 37 is at a non-critical site, and the stock mutant possesses "constitutive" properties which permit it to adsorb more efficiently. One explanation for the difference in adsorption characteristics could be that the stock M37 population has a higher percentage of phage possessing their optimal fiber complement, as opposed to a lower percentage within the am N122 stock, due to aging and storage effects. Such effects have not been investigated within these mutants, however.

Examination of the computer solutions to the adsorption profiles for the various amber mutants leads to many of the same explanations for the differences observed in the rates

of their adsorption. The slow adsorbers are characterized by a 10-fold decrease in the initial binding rate, K^1, suggestive of misaligned fibers or incomplete fibers attached to the baseplate, as opposed to an incomplete complement of fibers, which would be characterized by an increase in K^2. Those stock mutants with adsorption profiles only slightly slower than the am N122 control show a slight increase in K^2, suggestive of less stable phage-bacterial intermediate complexes.

The rapid adsorption characteristics of M37 can be interpreted from the 10-fold decrease in K^2 (a decrease in the rate of desorption of the phage from the host bacterium) as a more stable complex which is resistant to dissociation. Slight modifications to the fibers resulting in a more efficient binding process could be responsible, or, perhaps as suggested before, the binding efficiency would be higher through the interactions of more fibers on a higher percentage of phage.

These differences in adsorption characteristics of the various mutants likely arise from the differences in position of the termination codon in each mutant. Similiar to the different adsorption functions of each antigen, then, neutralization functions are probably different among the fiber antigens. Further insight into the actual mechanism of neutralization would require examination of the individual roles of the fiber antigens. The method of

investigation in this study has been limited to the determination of the serum blocking power (SBP) of lysates from mutant-infected E. coli B/1.

Historically, SBP has been used as an indication of fiber antigen concentration (Burnet, 1933; Edgar and Lielausis, 1965; King, 1968). Upon examination of numerous parameters involved in antibody-antigen reactions, it becomes apparent that this blocking power does not necessarily reflect the absolute antigen concentration within the lysate.

Molecular size and accessibility of the antigen is of prime importance to individual antigen-antibody binding site interactions. Also of importance are the various affinity coefficients of antibodies involved specifically with neutralization. The immunogenicity of each fiber antigen, therefore, plays a significant role in determining the characteristics of the neutralizing antiserum which is "blocked" with the lysates.

Therefore, several questions can be raised concerning the actual type of fiber-antibody reactions which lead to neutralization. For example, if a large number of low-affinity antibodies (monovalent, for simplicity) bind to a fiber, could they have the same effect as a single high-affinity molecule specifically bound at a more critical or sensitive region? Also, does the binding of low affinity

antibody to a critical antigenic region influence the binding of other antibodies to either critical sites on other fibers or non-critical sites on the same fiber? Arising from this last question is the importance of divalent IgG binding to one or two fibers, since both combining sites are monospecific for the same determinant.

It is not yet clear if a distinction can be made as to a structure being more susceptible to neutralization based on its function as opposed to its accessibility. The hinge region of the fiber (B antigen) would be a prime target functionally in a hypothetical situation due to the stereochemical hindrance imposed by a single fragment. However, the larger proximal half-fiber (A antigen) would probably bind many more antibody fragments of the same relative affinity as the anti-B fragments due to the larger size and accessibility of the gene 34 product. Both could feasably cause the same degree of neutralization, but would demonstrate very different kinetics if observed independently.

Thus, in any given instant in neutralization, the probability of an antibody binding to the larger antigen would be greater than that of an interaction with a smaller antigen. Arising from these differences in interactions between phage and neutralizing antibodies are the multi-hit versus the multi-target theories presented in Figure 22, page 90. The multi-hit theory is based upon numerous

antibody interactions. The multi-target theory arises from the distinction of differences in antigenicity of each of the fiber antigens. Thus, a multi-hit theory implies the number of neutralizing antibodies bound to the phage, and a multi-target theory implies the number of targets (i.e., fiber antigens) which must be involved.

The only means of examining fiber antigen levels in these lysates has been through blocking levels. Since there is no direct assay for the amounts of gene products in the lysates apart from the blocking activity, antigen levels had to be determined through indirect means. It was necessary to examine by biological and biochemical means any differences of the amber mutants studied in their efficiencies of transcriptional and translational processes, and to correlate this with the fiber antigen concentrations in the lysates which were being used to block the anti-T4 serum.

Just as efficiencies of suppressor activity are different in permissive host bacteria (Su+), efficiencies of adsorption and coefficients of transmission are different in amber mutants (Krieg, 1967). That is, differences in efficiency of the transcriptional processes of the amber mutant can be observed as differences of growth rates and specific "activities" of the different mutants. As such, they can be expected to exhibit different rates of protein synthesis, hence different antigen concentrations under

identical growth conditions.

In the Su+ host, both incomplete and complete polypeptide chains are synthesized. The efficiency of complete polypeptide synthesis is determined by the relative frequencies of termination and substitution.

Likewise, in the Su- host (*E. coli* B/1), these problems arise in the effective termination of the polypeptides. To some extent, the reversion rate offers a relative indication of the background "contaminating" fiber antigen concentration in the deficient lysates arising from leakiness.

In the case of the amber phage mutants, by controlling the effective adsorption multiplicity (i.e., the actual number of infected host bacteria, rather than input phage per bacterium), and using the same host preparation, the burst size (on permissive host) should give a means of comparison of the general rates of antigen synthesis of the various amber mutants in the restrictive host. It was possible to eliminate the problems in determining antigen concentrations in the lysates by establishing uniform bacterial concentrations prior to infection, and uniform infected cell numbers for each of the mutants. Thus, by effectively "normalizing" infection for all of the mutants, it was possible to interpret uniform lysozyme activities in each of the amber lysates (table V, page 73) as an

independent indication of uniform protein synthesis. This suggests that fiber antigen biosynthesis in the mutants is uniform as well, and that the lysate blocking experiments summarized in Figure 21 (page 86) could be interpreted on an empirical basis.

Major differences of slopes of these serum blocking activities were evident. Obvious differences in the wild type lysate blocking activity and the amber mutants is indicative of the larger amounts of antigen produced by the more efficient wild type infection. Lower fiber antigen production in the amber mutants is most likely due to effects of polarity. Such effects will be discussed later.

Intermediate slopes of M35 (△) and M36 (▽) lysates suggest insignificant roles in neutralization for these two products, since their absence (in the lysates) has the least influence on decreasing the serum blocking activity of all the lysates.

The remaining curves and straight lines of M34(.) and M37 (o) and all multiple mutants are difficult to differentiate quantitatively. The X4e mutant lysate fails to block neutralizing activity (i.e., highest residual K values after absorption with this lysate), suggesting this mutant's defective antigens play the largest role in neutralization. These observations agree with others' conclusions that this mutant fails to produce any fiber

antigens (Edgar and Lielausis, 1965).

M34 seems to have a slightly lower activity in blocking anti-T4 when compared to M37, suggesting that the gene 34 product plays the larger role in neutralization. The double and triple amber mutants have intermediate values when compared to X4e and M37, in this series of blocking curves, which would not be expected since they are comprised of various combinations of the M34 and M37 mutants. One would expect lower amounts of blocking antigen being produced due to the presence of two or three termination sites. No explanation for this observation can be offered at this time.

Maximal wild type fiber contamination remaining in lysates from phage left unadsorbed to bacterial host cells was determined from simple dilutions using the same volumes as for the lysates. From the differences in position of this control curve and the activity curves of the mutants in Figure 21, no corrections had to be applied to the residual neutralizing activity values.

Edgar and Lielausis (1965) suggested input fibers accounted for about 1% of the blocking activity of the lysates, and such input fibers were responsible for the non-linear neutralization curves of serum blocked with higher concentrations of fiber antigens. Data presented in this thesis (Figure 20, pg 83) at relatively high input fiber

concentrations does not support their conclusion. Also, their observation of "shoulders" in neutralization curves of S36 and S37 (antisera absorbed with the respective defective lysate) indicate 4- or 5-hit kinetics from back extrapolation of their neutralization curves. Neutralization curves of similiarly blocked sera in this study again differ from their results. These differences are most likely due to the different absorption and precipitin protocols employed. Their lysate-antiserum incubations were carried out at 48°C for 24 hours; conditions for precipitation in this study were an initial one-hour incubation at 37°C, then 24 hours at 0-4°C, then high speed centrifugation. Alteration of fiber antigenicity under the two different conditions is a distinct possibility, and could lead to the different residual neutralizing activities observed. More likely, the removal of specific antibodies (through centrifugation of the complexes) in this protocol leads to the differences.

Two major factors have prevented definitive conclusions from being established in the question of neutralizable antigens and their involvement in the phage inactivation. Of primary concern is the significance of polar effects of amber mutations found in the mutants investigated. The amber mutation, if strongly polar, depresses the synthesis of gene products co-transcribed distally (Snustad, 1968, Zipser, 1969). Two important polar regions of the T4

genetic map are both in the fiber cluster, with a strong gradient existing between genes 34 and 35 and genes 36 through 38 (Stahl, et.al. , 1970; Beckendorf and Wilson, 1972).

Of significance to this problem is the high degree of re-initiation which must occur in these two co-transcribed cistrons, whose operators are located on the proximal region of each (Beckendorf and Wilson 1972). Of major consequence, then, is the unanswered question: To what degree can reinitiation of transcription occur, leading to polypeptides coded distal to the amber site? The sensitivity of the serum blocking tests, in order to differentiate fiber antigen roles in neutralization, does not permit any valid conclusions to be drawn from these experiments utilizing amber mutant lysates in which re-initiation after termination may or may not have occurred.

Also of concern, more obvious than the first problem, is that of incomplete amber polypeptide fragments remaining in the lysate at the time of assay. The relative size of these fragments can be estimated from their map position, except for the polarity effects imposed as outlined previously. Different lengths of fragments can arise from a secondary effect of the termination, that of non-specific enzyme degrading systems which could possibly act on the amber fragment after termination but prior to assay (Goldschmidt, 1970).

From evidence published on a B-galactosidase amber mutant of E. coli (Goldschmidt, 1970), half lives of the incomplete polypeptide fragments are about 7 minutes. Thus, depending again on the map position, concentration of these contaminating amber fragments in the lysate can vary as to exact time of infection, transcription, and lysis. Arising from this aspect is the problem of asynchronous infection throughout the bacterial population.

From the estimated half-life of the the B-galactosidase fragments of 7 minutes, about 5% of the initial fragment concentration would still be present, allowing for about 3 half-lives between transcription of the nonsense codon and lysis.

Goldschmidt also hypothesized differential rates of synthesis of the fragments as well as the preferential (though not specific) enzyme degrading system for amber fragments. Thus, concentration of each fiber antigen and components thereof could be dependent also on this relatively unknown parameter. If the differential rates of synthesis of the amber fragments were countered by the enzymatic degradation prior to lysis, it would still be possible to interpret the blocking data presented before.

King, in 1971, could find no evidence for amber fragments in lysates using disc gel electrophoretic analysis (King and Laemmli, 1971). Others have found that amber

polypeptides did not absorb antibodies corresponding to their gene products (Yanagida and Ahmed-Zadeh, 1970; Edgar and Lielausis, 1965).

In the amber mutants examined, however, there is no evidence to suggest the fragments disappear entirely. Amber fragment isolation from mutant-infected cells has proven useful in demonstrating colinearity between genetic map position and gene product synthesis (Sarabhai, et.al., 1964; Wilson, et.al., 1972; Beckendorf, et.al., 1973). Different lengths of cross-reacting fragments would be indicated by the different position each amber mutation occupies in its respective gene. Further complications are apparent as to the actual time of translational interruption as distinct from asynchronous infection; the later the amber fragment termination, the larger the fragment produced but the shorter the time for degradation. The larger fragments would more closely resemble the wild-type structures as well, and probably be more resistant to degradation. Hence, amber mutations found late in a gene would yield a disproportionately larger fragment than those found early, even though degrading enzymes might be present.

In summary of these blocking experiments, then, the SBP of each lysate can be described as a complex monotonic function of crude lysate concentration. One must be aware of the inability to determine the absolute concentration of fiber antigens by this technique due to several factors.

Primarily, differences in antigenicity of each of the fiber antigens have not been established. It is also important to recognize the presence of contaminating amber polypeptide fragments in the blocking lysates. Each of these fragments is unpredictable in its concentration due to the effects of polar transcription, position of the amber lesion in its respective gene, possible differential rates of fragment synthesis, and the possible presence of a non-specific enzyme degrading system for these fragments.

Thus, it appears that lysates used in these blocking experiments are not specifically "pure" enough for the problem under investigation. Unless amber mutations located early in each gene, each with a well-defined and predictable polarity effect, are used in lysate blocking studies, no significant distinction in roles in neutralization can be determined from such a technique. To gain further insight into the mechanism, it would seem necessary to employ highly purified antibody preparations of uniform affinity, along with purified fiber antigen preparations as elements of investigation.

Nevertheless, genes 34 and 37 do seem responsible for the larger portion of the serum blocking activity of the lysates examined. This follows not only from the actual blocking data presented in the results section, but perhaps also from the larger molecular sizes of these antigens.

SUMMARY

These studies concern the mechanism of neutralization of phage T4 by specific antisera and univalent antibody fragments. The primary object has been the development of a model describing the effects of Fab' binding to T4 tail fibers, with its concomitant influence on normal phage adsorption kinetics. Through the use of a conditional lethal amber mutant adsorbing to its restrictive host, it has been possible to show that partially neutralized phage adsorb with kinetics consistent with those of a mixed population of slow and fast adsorbers. These observations support the two-target theory of phage inactivation by Fab'. Fab' dosage, defined from the degree of neutralization, can be used to predict different classes of phage with, respectively, no molecules bound (0-hit), one molecule bound (1-hit) and two, or more, molecules bound (neutralized). Experimental adsorption profiles could be consistently fit to predicted characteristics of the summation of the two adsorbing classes (P^0 and P^1 classes) over the range of Fab' dosages examined.

[Fab'-phage] dissociation was evident since partially neutralized phage preparations regained the adsorption characteristics of untreated phage over a 10 hour period. The apparent rate of dissociation could not, however, account for the observed changes in adsorption caused by Fab' neutralization, and such dissociation effects were

considered neglible.

Secondary evidence in support of a single Fab'-fiber interaction causing the adsorption changes was gained from *in vitro* complementation of fiberless T4 particles with active tail fibers. Using rate constants derived from the Fab' experiments, the adsorption data of the complemented phage particles suggested activation proceeded through classes differing by a single fiber. Results consistent with adsorption differences of the final two activation stages arising from functional differences again support the two-target theory of neutralization.

Individual roles of the numerous fiber antigens were examined in an attempt to further elucidate the molecular basis of phage inactivation. One approach was to locate the specific "target" of neutralizing antibodies to a specific region or regions of the tail fibers. For this purpose, numerous amber lysates, deficient in one or more fiber antigens, were reacted with antiserum and the residual neutralizing activity of the partially absorbed antiserum was determined. Unambiguous interpretation of the results could not be made, however. In part this may have been due to indeterminant quantities of cross-reacting amber polypeptide fragments in the lysates. However, antigens coded in genes 34 and 37 appear to play the largest role in blocking specific neutralizing antisera.

BIBLIOGRAPHY

1. Adams, M.H., The Bacteriophages, Interscience Publishers Inc., New York, 1959.

2. Barber, P., Rittenberg, M.B., 1969. Anti-trinitrophenyl (TNP) Antibody Detection By neutralization of TNP-coliphage T4. Immunochem. 6, 163-174.

3. Bayer, M.E., 1968. Adsorption of Bacteriophages to Adhesions Between Wall and Membrane of Escherichia coli. J. Virol. 2,346-356.

4. Beckendorf, S.K., 1973. Structure of the Distal Half of the Bacteriophage T4 Tail Fiber. J. Mol. Biol. 73, 37-53.

5. Beckendorf, S.K., Kim, J.S., Lielausis, I., 1973. Structure of Bacteriophage T4 Genes 37 and 38. J. Mol. Biol. 73, 17-35.

6. Beckendorf, S.K., Wilson, J.H., 1972. A Recombination Gradient in Bacteriophage T4 Gene 34. Virology 50, 315-321.

7. Blakeslee, D., Antczak, D.F., Rowlands, Jr., D.T., 1973. Detection of Antibodies Specific for PTC, DNS, and Myoglobin By Neutralization of Conjugated Bacteriophage T4. Immunochemistry 10, 61-63.

8. Blank, S.E., Leslie, G.A., Clem, L.W., 1972. Antibody Affinity and Valence In Viral Neutralization . J. Immun. 108, 665-673.

9. Bowman, Jr., B.U., Patnode, R.A., 1964. Neutralization of Bacteriophage Phi-X-174 By Specific Antiserum. J. Immun., 92, 507-514.

10. Brenner, S., Streisinger, G., Horne, R.W., Champe, S.P., Barnett, L., Benzer, S., Rees, M.W., 1970. Structural Components of Bacteriophage . J. Mol. Biol. 1, 281-292.

11. Brown, D.T., Anderson, T.F., 1969. Effect of Host Cell Wall Material On the Adsorbability Of Cofactor-requiring T4. J. Virol., 4, 94-108.

12. Burnet, F.M., 1933. A Specific Soluble Substance from Bacteriophages. Brit. J. Exp. Pathol., 14, 100.

13. Cann, J.R., Clark, E.W., 1954. On the Kinetics of Neutralization of Bacteriophage T2 By Specific Antiserum. J. Immun. 72, 463-477.

14. Childs, J.D., 1973. Superinfection Exclusion By Incomplete Genomes of Bacteriophage T4. J. Virol. 11, 1-8.

15. Day, E.D., Advanced Immunochemistry. The Williams and Wilkins Company, Baltimore. 1972.

16. Delbruck, M., 1945. Effects of Specific Antisera on the Growth of Bacterial Viruses. J. Bacteriol. 50, 137.

17. Depamphilus, M.L., 1971. Isolation of Bacteriophages T2 and T4 Attached to the Outer Membrane of Escherichia coli . J. Virol. 7, 683-686.

18. Dudley, M.A., Henkens, R.W., Rowlands, Jr., D.T., 1970. Kinetics of Neutralization of Bacteriophage f^2 By Rabbit Antibodies. Proc. Natl. Acad. Sci. U.S.A., 65, 88-95.

19. Edgar, R.S., Lielausis, I., 1965. Serological Studies With Mutants of Phage T4D Defective in Genes Determining Tail Fiber Structure. Genetics 52, 1187-1200.

20. Edgar, R.S., Lielausis, I., 1968. Some Steps in the Assembly of Bacteriophage T4. J. Mol. Biol. 32, 263-276.

21. Edgar, R.S., Wood, W.B., 1966. Morphogenesis of Bacteriophage T4 in Extracts of Mutant Infected Cells. Proc. Natl. Acad. Sci. U.S.A., 55, 498-505.

22. Eiserling, F.A., Bolle, A., Epstein, R.H., 1967. Electron Microscopic Study of the Structure of Mutants of Bacteriophage T4D Defective in Tail Fiber Genes. Virology 33, 405-412.

23. Eiserling, F.A., Dickson, R.C., 1972. Assembly of Viruses. Ann. Rev. Biochem. 41, 467.

24. Epstein, R.H., Bolle, A., Steinberg, C.M., Kellenberger, E., Boy de la Tour, E., Chevalley, R., Edgar, R.S., Susman, M., Denhardt, G.H., Lielausis, I., 1963. Physiological Studies of Conditional Lethal Mutants of Bacteriophage T4D. Cold Spring Harbor Symposia Quant. Biol. 28, 375-394.

25. Franklin, N.C., 1961. Serological Study of Tail Struc-

ture and Function in Coliphage T2 and T4. Virology 14, 417-429.

26. Gamow, R.I., 1969. Thermodynamic Treatment of Bacteriophage T4B Adsorption Kinetics . J. Virol. 4, 113-115.

27. Gamow, R.I., Kozloff, L.M., 1968. Chemically Induced Cofactor Requirment for Bacteriophage T4D. J. Virol. 2, 480-487.

28. Garen, A., 1968. Sense and Nonsense in the Gentic Code. Science, 160, 149-159.

29. Goldschmidt, R., 1970. In Vivo Degradation of Nonsense Fragments of Escherichia coli . Nature 228, 1151-1154.

30. Goodman, J.W., Donch, J.J., 1964. Neutralization of Bacteriophage By Intact and Degraded Rabbit Antibody . J. Immun. 93, 96-100.

31. Haimovich, J., Sela, M., 1969. Inactivation of Bacteriophage T4, of Poly-d-alanyl Bacteriophage and of Penicilloyl Bacteriophage By Immunospecifically Isolated IgM and IgG Antibodies. J. Immun. 103, 45-55.

32. Hale, E.M., Hirata, A.A., Brosenback, R., Overby, L.R., 1969. Antiserum Neutralization of Bacteriophage QB : A Mathematical Analysis. J. Immunol. 102, 206-214.

33. Hershey, A.D., 1941. The Absolute Rate of Phage-Antiphage Reaction. J. Immunol. 41, 299-319.

34. Hoglund, S., 1967. Electron Microscopic Investigations of the Interaction Between the T2-Phage and Its IgG- and IgM-antibodies. Virology 32, 662-677.

35. Hornick, C.L., Karush, F., 1969. The Interaction of Hapten-Coupled Bacteriophage Phi-X-174 With Antihapten Antibody . Israel J. Med. Sci. 5, 163-170.

36. Imada, S., Tsugita, A., 1970. Morphogenesis of the Tail Fiber of Bacteriophage T4. II. Isolation and Characterization of a Component. (The Genes 35-36-37-38 Directing Half Fiber). Molec. Gen. Genet. 109, 338-355.

37. Imada, S., Tsugita, A., 1972a. Morphogenesis of the Tail Fiber of Bacteriophage T4. IV. Isolation and Characterization of a Component. (The Genes 36-37-38 Directing Component). Molec. Gen. Genet. 117, 319-

336.

38. Imada, S., Tsugita, A., 1972b. Morphogenesis of the Tail Fiber of Bacteriophage T4. V. In Vitro Complementation Between The Gene 36 Product and The Genes 37-38 Directed Component. Molec. Gen. Genet. 119, 185-190.

39. Jerne, N.K., Skovsted, L., 1953. The Rate of Inactivation of Bacteriophage T4 in Specific Antiserum. Ann. Inst. Pasteur., 84, 73-89.

40. Kaplan, S., 1973. In Vivo Translation of Amber and Ochre Codons in Escherichia coli . Molec. Gen. Genet. 120, 191-200.

41. Karush, F. 1970. Affinity and the Immune Response. Annals New York Academy of Sciences 169, 56-64.

42. King, J., 1968. Assembly of the Tail of Bacteriophage T4. J. Mol. Biol. 32, 231-262.

43. King, J., Laemmli, U.K., 1971. Polypeptides of the Tail Fibers of Bacteriophage T4. J. Mol. Biol. 62, 465-477.

44. King, J., Wood, W.B., 1969. Assembly of Bacteriophage T4 Tail Fibers: The Sequence of Gene Product Interaction. J. Mol. Biol. 39, 583-601.

45. Klinman, N.R., Long, C.A., Karush, F., 1967. The Role of Antibody Bivalence in the Neutralization of Bacteriophage . J. Immun. 99, 1128-1133.

46. Krieg, R.H., 1967. Ph.D. Thesis, University of California, Berkely. Genetic Factors of Escherichia coli Determining Suppression of the Amber Mutant Phenotype of T4 Bacteriophage. University Microfilms, Inc., Ann Arbor, Michigan.

47. Krummel, W.M., Uhr, J.W., 1969. A Mathematical and Experimental Study of the Kinetics of Neutralization of Bacteriophage Phi-X-174 By Antibodies. J. Immun. 102, 772-785.

48. Lanni, F., Lanni, Y.T., 1953. Antigenic Structure of Bacteriophage. Cold Spring Harbor Symposia Quant. Biol. 18, 159-168.

49. Makela, O., 1966. Assay of Anti-Hapten Antibody with the Aid of Hapten-Coupled Bacteriophage . Immunology 10, 81-86.

50. Michael, J.G., 1968. The Surface Antigens and Phage

Receptors in Escherichia coli B. Proc Soc. Exp. Biol. Med. 128, 434-438.

51. Muschel, L.H., Toussaint, A.J., 1962. Studies On the Bacteriophage Neutralizing Activity Of Serums. J. Immun. 89, 35-40.

52. Nagano, Y., Oda, M., Konishi, Y., 1956. Influence du Serum Antiphagique sur L'Adsorption due Bacteriophage par le Bacille Sensible. Ann. Inst. Pasteur 91, 641-652.

53. Notani, G.W., 1973. Regulation of Bacteriophage T4 Gene Expression. J. Mol. Biol. 73, 231-249.

54. Puck, T.T., Garen, A., Cline, J., 1951. The Mechanism of Virus Attachment to Host Cells. J. Exp. Med. 93, 65-68.

55. Sabelnikov, A.G., 1972. Spectrophotometric Determinations of Phage Concentrations in Lysates. Anal. Biochem. 48, 629-632.

56. Sarabhai, A.S., Stretton, O.W., Brenner, S., Bolle, A., 1964. Colinearity of Gene with Polypeptide Chain. Nature 201, 13.

57. Shinomiya, T., Imada, S., Tsugita, A., 1971. Morphogenesis of the Tail Fiber of Bacteriophage T4. III. Isolation of The Gene 35 Product and The Genes 36,37 and 38 Product. Molec. Gen. Genet. 111, 368-372.

58. Simon, L.D., Anderson, T.P., 1967. The Infection of Escherichia coli By T2 and T4 Bacteriophages as Seen in the Electron Microscope. I. Attachment and Penetration. Virology 32, 279-297.

59. Snustad, D.P., 1968. Dominance Interactions in Escherichia coli Cells Mixedly Infected With Bacteriophage T4D Wild-Type and Amber Mutants and Their Possible Implications as to Type of Gene-Product Function: Catalytic Vs. Stoichiometric. Virology 35, 550-563.

60. Stahl, F.W., Crasemann, J.M., Yegian, C., Stahl, M.M., Nakata, A., 1970. Co-Transcribed Cistrons in Bacteriophage T4. Genetics 64, 157-170.

61. Stemke, G.W., 1969. Mechanism of Bacteriophage T4 Neutralization By Rabbit Immunoglobulin and Its Proteolytic Digestion Fragments. J. Immun. 103, 596-606.

62. Stemke, G.W., Lennox, E.S., 1967. Bacteriophage Neut-

ralizing Activity of Fragments Derived From Rabbit Immunoglobulin By Papain Digestion. J. Immun. 98 94-101.

63. Stemke, G.W., Knight, W.S., Butz, E., Gates, D., in press. The Mechanism of Bacteriophage T4 Neutralization: Effects of Univalent Antibody Fragments on T4 Adsorption Kinetics. Accepted for publication in Can. J. Microbiol.

64. Stent, G.S. Molecular Biology of Bacterial Viruses. 1963. W.H. Freeman and Company.

65. Stent, G.S., Wollman, E.L., 1952. On the Two-Step Nature of Bacteriophage Adsorption. Biochim. Biophys. Acta 8, 260.

66. Takata, R., Tsugita, A., 1970. Morphogenesis of the Tail Fiber of Bacteriophage T4: Isolation and Characterization of a Component (The Gene 34 Product). J. Mol. Biol. 54, 45-57.

67. Terzaghi, E., 1971. Alternative Pathways of Tail Fiber Assembly in Bacteriophage T4? J. Mol. Biol. 59, 319-327.

68. To, C.M., Kellenberger, E., Eisenstark, A., 1969. Disassembly of T-Even Bacteriophage Into Structural Parts and Subunits. J. Mol. Biol. 46, 493-511.

69. Tsugita, A., Inouye, M., Terzaghi, E., Streisinger, G., 1968. Purification of Bacteriophage T4 Lysozyme. J. Biol. Chem. 243, 391-397.

70. Vargues, R., Vallet, M., 1973. Problemes De Cinetique Immunologique: Application a la Virologie. Bulletin De L'Institut Pasteur, 71 147-164.

71. Ward, S., Dickson, R.C., 1971. Assembly of Bacteriophage T4 Tail Fibers. III. Genetic Control of the Major Tail Fiber Polypeptides. J. Mol. Biol. 62, 479-492.

72. Ward, S., Luftig, R.B., Wilson, J.H., Eddleman, H., Lyle, H., Wood, W.B., 1970. Assembly of Bacteriophage T4 Tail Fibers. II. Isolation and Characterization of Tail Fiber Precursors. J. Mol. Biol. 54, 15-31.

73. Wildy, P., Anderson, T.F., 1964. Clumping of Susceptible Bacteria By Bacteriophage Tail Fibers. J. Gen. Microbiol. 34, 273-283.

74. Wilhelm, J.M., Haselkorn, R., 1971a. *In Vitro* Synthesis

Of T4 Proteins: The Products of Genes 9, 18, 19, 23, 24, and 38. Virology 43, 198-208.

75. Wilhelm, J.M., Haselkorn, R., 1971b. In Vitro Synthesis of T4 Proteins: Control Of transcription of Gene 57. Virology 43, 209-213.

76. Wilson, J.H., Kim, J.S., Abelson, J.N., 1972. Bacteriophage T4 Transfer RNA. III Clustering of the Genes for the T4 Transfer RNA's. J. Mol. Biol., 71, 547-556.

77. Wilson, J.H., Luftig, R.B., Wood, W.B., 1970. Interaction of Bacteriophage T4 Tail Fiber Components With a Lipopolysaccharide Fraction From Escherichia coli . J. Mol. Biol. 51, 423-434.

78. Witte, O.N., Slobin, L.I., 1972. Neutralization of Haptenated Bacteriophage f2 By Anti-hapten Antibodies: Direct Evidence for a Critical Site. J. Immun. 108, 927-936.

79. Wood, W.B., Edgar, R.S., King, J., Lielausis, I, Henninger, M., 1968. Biosynthesis and Function of Supramolecular Structures. Bacteriophage Assembly. Fed. Proc. 27, 1160-1166.

80. Wood, W.B., Henninger, M., 1969. Attachment of Tail Fibers in Bacteriophage T4 Assembly: Some Properties of the Reaction In Vitro and Its Genetic Control. J. Mol. Biol. 39, 603, 618.

81. Worthington Enzyme Manual, 1972. Worthington Biochemical Corporation, Freehold, New Jersey.

82. Yamamoto, K.R., Alberts, B.M., Benzinger, R., Lawhorne, L., Treiber, G., 1970. Rapid Bacteriophage Sedimentation in the Presence of Polyethylene Glycol and its Application to Large Scale Virus Purification. Virology 40, 734-744.

83. Yanagida, M., Ahmed-Zadeh, C., 1970. Determination of Gene Product Positions in Bacteriophage T4 By Specific Antibody Association. J. Mol. Biol. 51, 411-421.

84. Zipser, D. 1969. Polar Mutations and Operon Function. Nature 221, 21-25.

APPENDIX A

1. First Hypothesis - Two Adsorbing Classes of Phage.

The model describing the adsorption of the two classes of phage resulting from Fab' neutralization has been developed throughout the text of this thesis. Such a scheme can be represented as:

$$\phi_0 + B \underset{K^{12}}{\overset{K^{11}}{\rightleftharpoons}} [\phi_0 \cdot B] \xrightarrow{K^{13}} B^* \qquad (1)$$

$$\phi_1 + B \underset{K^{22}}{\overset{K^{21}}{\rightleftharpoons}} [\phi_1 \cdot B] \xrightarrow{K^{23}} B^* \quad . \qquad (2)$$

Calculations of the concentrations of free phage (either ϕ_0 or ϕ_1) and of the complexes follow the same mathematical derivations for both equations (1) and (2). Adjusting the rate constants describing the two equations to experimental data allows for the different concentrations of the two surviving types of phage to be calculated. These rate constants were best fit to the data by minimizing the value F , where

$$F = \sum [1 - \frac{DP(c)}{DP(e)}]^2 \quad .$$

DP(c) represents a calculated data point of total survivors at time 't' , and DP(e) is the experimental value of the total number of survivors at that same time, (i.e., the number of plaques at time t). The ratio of the initial number of the two different adsorbing classes could also be fit to the experimental data. Adjustments to the initial rate

constant estimation were by 10% and 3% positive or negative increments.

The best fit curve to the data was generated by calculating survivor concentrations (i.e., $\{\phi_0 + \phi_1\}$) at thirty second intervals for the duration of the experiment, using the best fit rate constants. The following mathematical derivations show the calculations involved in determining concentrations of either ϕ_0 or ϕ_1 and $[\phi_0 \cdot B]$ or $[\phi_1 \cdot B]$ at any time, t .

The above equations (1) and (2) can be summarized into one adsorption scheme;

$$\phi + B \underset{K_2}{\overset{K_1}{\rightleftharpoons}} [\phi \cdot B] \xrightarrow{K_3} B^* \qquad (3)$$

which can be used to represent the two adsorbing classes (differing only by the adsorption rate constant values) of phage in either the Fab' treatment (i.e., P^0 and P^1), or the <u>in vitro</u> complementation experiments (i.e., the C^0 and C^1 classes).

The differential equations describing the above scheme (3) are:

$$\left.\begin{aligned} \frac{d}{dt}[\phi] &= -K_1[\phi][B] + K_2[\phi \cdot B] \\ \frac{d}{dt}[\phi \cdot B] &= K_1[\phi][B] - (K_2 + K_3)[\phi \cdot B] \quad . \end{aligned}\right\} \qquad (i)$$

Let $[\phi] = x$; $[\phi \cdot B] = y$; and $[B] = B$. Therefore,

$$\left.\begin{aligned} \frac{dx}{dt} &= -K_1 Bx + K_2 y \\ \text{and} \\ \frac{dy}{dt} &= K_1 Bx - (K_2+K_3)y \end{aligned}\right\} \quad (ii)$$

or, if

$$X = \begin{vmatrix} x \\ y \end{vmatrix} \quad \text{and} \quad A = \begin{vmatrix} -K_1 & K_2 \\ K_1 & -(K_2+K_3) \end{vmatrix} . \quad (iii)$$

Then,

$$\frac{dX}{dt} = AX \quad .$$

To determine the eigenvalues of A, solve

$$A - \lambda I = 0 \quad (iv)$$

i.e.,

$$\begin{vmatrix} -(K_1 B + \lambda) & K_2 \\ K_1 B & -(K_2+K_3+\lambda) \end{vmatrix} = 0$$

or,

$$K_1K_2B + K_1K_3B + K_1B\lambda + \lambda(K_2+K_3+\lambda) - K_1K_2B = 0 \quad .$$

Therefore,

$$\left.\begin{aligned} \lambda_1 &= \frac{-(K_1B+K_2+K_3) - SR}{2} \\ \lambda_2 &= \frac{-(K_1B+K_2+K_3) + SR}{2} \quad , \end{aligned}\right\} \quad (v)$$

where

$$SR = \sqrt{(K_1B+K_2+K_3)^2 - 4 \cdot K_1 BK_3} \quad .$$

Then,

$$X = c_1 \Omega_1 e^{\lambda_1 t} + c_2 \Omega_2 e^{\lambda_2 t} \qquad \text{(vi)}$$

where Ω_1 and Ω_2 are eigenvectors corresponding to the eigenvalues. To determine the eigenvectors, substitute λ_1 and λ_2 into

$$(A - \lambda I) \cdot \Omega = 0 \quad .$$

If $\Omega = \begin{vmatrix} p \\ q \end{vmatrix}$, and $\lambda = \lambda_1$, then

$$[K_1Bp] - [K_2+K_3+\lambda_1]q = 0 \quad ,$$

or,

$$p = \frac{(K_2+K_3+\lambda_1)q}{K_1B} = \frac{-(K_1B+\lambda_2)q}{K_1B} \quad .$$

Let $q = \frac{K_1B}{\lambda_1-\lambda_2}$, then $p = \frac{-(K_1B+\lambda_2)}{\lambda_1-\lambda_2}$. If $\lambda = \lambda_2$, then $p = \frac{(K_2+K_3+\lambda_2)q}{K_1B}$. Or, if $q = \frac{-K_1B}{\lambda_1-\lambda_2}$, then $p = \frac{(K_1B+\lambda_1)}{\lambda_1-\lambda_2}$. Therefore,

$$\Omega_1 = \begin{pmatrix} \frac{-(K_1B+\lambda_2)}{\lambda_1-\lambda_2} \\ \frac{K_1B}{\lambda_1-\lambda_2} \end{pmatrix} \quad \text{and} \quad \Omega_2 = \begin{pmatrix} \frac{K_1B+\lambda_1}{\lambda_1-\lambda_2} \\ \frac{-K_1B}{\lambda_1-\lambda_2} \end{pmatrix} \qquad \text{(vii)}$$

Thus, substituting into equation (vi),

$$\left.\begin{aligned} [\phi] = x &= -c_1 \frac{(K_1B+\lambda_2)}{\lambda_1-\lambda_2} e^{\lambda_1 t} + c_2 \frac{(K_1B+\lambda_1)}{\lambda_1-\lambda_2} e^{\lambda_2 t} \\ [\phi \cdot B] = y &= c_1 \frac{K_1B}{\lambda_1-\lambda_2} e^{\lambda_1 t} - c_2 \frac{K_1B}{\lambda_1-\lambda_2} e^{\lambda_2 t} \end{aligned}\right\} \quad \text{(viii)}$$

At $t = 0$, $[\phi \cdot B] = 0$, and $c_1 = c_2 = N_0$. Thus

$$\left.\begin{aligned} [\phi] &= \frac{-N_0(K_1B+\lambda_2)}{\lambda_1-\lambda_2} e^{\lambda_1 t} + \frac{N_0(K_1B+\lambda_1)}{\lambda_1-\lambda_2} e^{\lambda_2 t} \\ [\phi \cdot B] &= \frac{N_0 \cdot K_1B}{\lambda_1-\lambda_2} e^{\lambda_1 t} - \frac{N_0 \cdot K_1B}{\lambda_1-\lambda_2} e^{\lambda_2 t} \end{aligned}\right\} \quad \text{(ix)}$$

Let

$$\left.\begin{aligned} A &= (K_1B+\lambda_2)/(\lambda_1-\lambda_2) \\ B &= (K_1B+\lambda_1)/(\lambda_1-\lambda_2) \\ C &= K_1B/(\lambda_1-\lambda_2) \end{aligned}\right\} \quad \text{(x)}$$

Therefore,

$$\left.\begin{aligned} [\phi] &= N_0[-A \cdot e^{\lambda_1 t} + B \cdot e^{\lambda_2 t}] \\ \text{and} \\ [\phi \cdot B] &= N_0 C[e^{\lambda_1 t} - e^{\lambda_2 t}] \end{aligned}\right\} \quad \text{(xi)}$$

At $t = 0$, $[\phi] = X_0$. Therefore, $X_0 = N_0[B-A]$, or $N_0 = X_0/[B-A]$

so that

$$[\phi] = \frac{X_0}{B-A}\,[-A\cdot e^{\lambda_1 t} + B\cdot e^{\lambda_2 t}] \quad . \qquad \text{(xii)}$$

2. Second Hypothesis - One Adsorbing Class of Phage. (Fab' Dissociation Model)

The model describing phage being unable to adsorb with only one Fab' fragment bound can be summarized in the following scheme.

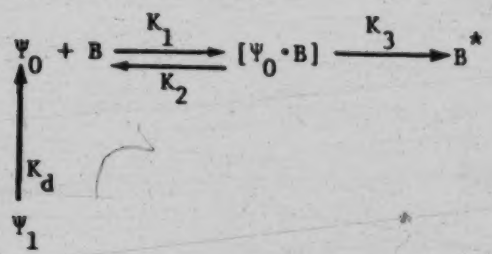

(4)

where Ψ_0 and Ψ_1 represent the 'zero-hit' and 'one-hit' classes of phage. Note that Ψ_1 is not able to adsorb, but decays to an adsorbable 'zero-hit' phage class via the dissociation of the Fab' molecule.

The differential equations describing this model (4) are:

$$\left.\begin{aligned} \frac{d}{dt}[\Psi_0] &= -K_1[B][\Psi_0] + K_2[\Psi_0\cdot B] + K_d[\Psi_1] \\ \frac{d}{dt}[\Psi_0\cdot B] &= K_1[B][\Psi_0] - (K_2+K_3)[\Psi_0\cdot B] \\ \frac{d}{dt}[\Psi_1] &= -K_d[\Psi_1] \quad . \end{aligned}\right\} \qquad \text{(xiii)}$$

If $[\Psi_0] = X$, $[\Psi_0 \cdot B] = Y$, and $[\Psi_1] = Z$, then

$$\left.\begin{aligned} \frac{dX}{dt} &= -K_1 B \cdot X + K_2 Y + K_d Z \\ \frac{dY}{dt} &= K_1 B \cdot X - (K_2 + K_3) Y \\ \frac{dZ}{dt} &= -K_d Z \end{aligned}\right\} \quad \text{(xiv)}$$

Let

$$A^* = \begin{pmatrix} -K_1 B & K_2 & K_d \\ K_1 B & -(K_2+K_3) & 0 \\ 0 & 0 & -K_d \end{pmatrix} .$$

Therefore, the eigenvalues are determined by solving

$$|A^* - \lambda I| = 0 ,$$

i.e.,

$$\begin{pmatrix} -(K_1 B+\lambda) & K_2 & K_d \\ K_1 B & -(K_2+K_3+\lambda) & 0 \\ 0 & 0 & -(K_d+\lambda) \end{pmatrix} = 0 \quad \text{(xv)}$$

or,

$$(K_d+\lambda) \begin{pmatrix} -(K_1 B+\lambda) & K_2 \\ K_1 B & -(K_2+K_3+\lambda) \end{pmatrix} = 0 .$$

Thus, the eigenvalues are:

$$\lambda = \lambda_1, \lambda_2 \quad , \quad \text{as before in system (3)}$$

and

$$\lambda = \lambda_3 = -K_d \quad .$$

Eigenvectors, then, corresponding to $\lambda = \lambda_1$, require the solution to

$$[A^* - \lambda I]\Omega = 0 \quad , \quad \text{where} \quad \Omega = \begin{vmatrix} p \\ q \\ r \end{vmatrix} \quad . \qquad \text{(xvi)}$$

Therefore,

$$\left.\begin{aligned} -(K_1 B+\lambda_1)p + K_2 q + K_d r &= 0 \\ (K_1 B)p - (K_2+K_3+\lambda_1)q &= 0 \\ -(K_d+\lambda_1)r &= 0 \quad . \end{aligned}\right\} \qquad \text{(xvii)}$$

But $\lambda_1 \neq -K_d$, and $r = 0$ from the third equation above. The equations for p and q become

$$\left.\begin{aligned} -(K_1 B+\lambda_1)p + K_2 q &= 0 \\ K_1 B p - (K_2+K_3+\lambda_1)q &= 0 \end{aligned}\right\} \qquad \text{(xviii)}$$

which are the same equations as in system (3), so that

$$\Omega_1 = \begin{vmatrix} \frac{-(K_1B+\lambda_2)}{\lambda_1-\lambda_2} \\ \frac{K_1B}{\lambda_1-\lambda_2} \\ 0 \end{vmatrix} \quad \text{and, similarly for } \lambda = \lambda_2 , \quad \Omega_2 = \begin{vmatrix} \frac{K_1B+\lambda_1}{\lambda_1-\lambda_2} \\ \frac{-K_1B}{\lambda_1-\lambda_2} \\ 0 \end{vmatrix} . \qquad \text{(xix)}$$

For $\lambda = \lambda_3 = -K_d$, the equations are

$$-(K_1B+\lambda_3)p + K_2q + K_dr = 0 ,$$

$$(K_1B)p - (K_2+K_3+\lambda_3)q = 0 ,$$

and

$$p = \frac{(K_2+K_3+\lambda_1)q}{K_1B} + \frac{(\lambda_3-\lambda_1)q}{K_1B} . \qquad \text{(xx)}$$

Let $q = \frac{K_1B}{\lambda_1-\lambda_2}$, and since $K_2 + K_3 + \lambda_1 = -(K_1B+\lambda_2)$,

$$p = \frac{-(K_1B+\lambda_2)}{\lambda_1-\lambda_2} + \frac{\lambda_3-\lambda_1}{\lambda_1-\lambda_2} . \qquad \text{(xxi)}$$

Substituting for p and q to determine r ,

$$\frac{(K_1B+\lambda_3)[K_1B+\lambda_2+\lambda_1-\lambda_3]}{(\lambda_1-\lambda_2)} + \frac{B\cdot K_1K_2}{(\lambda_1-\lambda_2)} + K_dr = 0$$

or

$$r = \frac{-[K_1B+\lambda_3][K_1B+\lambda_2+\lambda_1-\lambda_3] + B\cdot K_1K_2}{K_d(\lambda_1-\lambda_2)} . \qquad \text{(xxii)}$$

Therefore,

$$\left.\begin{aligned}
[\Psi_0] &= -c_1 \frac{(K_1B+\lambda_2)}{\lambda_1-\lambda_2} e^{\lambda_1 t} + c_2 \frac{(K_1B+\lambda_1)}{\lambda_1-\lambda_2} e^{\lambda_2 t} \\
&\quad - c_3 \frac{(K_1B+\lambda_2)}{\lambda_1-\lambda_2} e^{\lambda_3 t} - c_3 \frac{(K_d+\lambda_1)}{\lambda_1-\lambda_2} e^{\lambda_3 t} \\
[\Psi_0 \cdot B] &= c_1 \frac{K_1B}{\lambda_1-\lambda_2} e^{\lambda_1 t} - c_2 \frac{K_1B}{\lambda_1-\lambda_2} e^{\lambda_2 t} + c_3 \frac{K_1B}{\lambda_1-\lambda_2} e^{\lambda_3 t} \\
[\Psi_1] &= \frac{c_3[(K_d-K_1B)(K_1B+\lambda_2+\lambda_1+K_d) - BK_1K_2]}{K_d(\lambda_1-\lambda_2)} e^{-K_d t}
\end{aligned}\right\} \quad \text{(xxiii)}$$

Defining,

$$\left.\begin{aligned}
A &= (K_1B+\lambda_2)/(\lambda_1-\lambda_2) \\
B &= (K_1B+\lambda_1)/(\lambda_1-\lambda_2) \\
C &= K_1B/(\lambda_1-\lambda_2) \\
D &= (K_d+\lambda_1)/(\lambda_1-\lambda_2) \\
E &= \frac{(K_d-K_1B)(K_1B+\lambda_2+\lambda_1+K_d) - K_1BK_2}{K_d(\lambda_1-\lambda_2)} \quad .
\end{aligned}\right\} \quad \text{(xxiv)}$$

Then equations(xxiii) become

$$\left.\begin{aligned}
[\Psi_0] &= -Ac_1 \cdot e^{\lambda_1 t} + Bc_2 \cdot e^{\lambda_2 t} - (A+D)c_3 \cdot e^{\lambda_3 t} \\
[\Psi_0 \cdot B] &= C[c_1 \cdot e^{\lambda_1 t} - c_2 \cdot e^{\lambda_2 t} + c_3 \cdot e^{\lambda_3 t}] \\
[\Psi_1] &= Ec_3 \cdot e^{-K_d t} \quad .
\end{aligned}\right\} \quad \text{(xxv)}$$

Applying the initial conditions in order to determine the coefficients c_1 , c_2 , and c_3 , at $t = 0$, $[\Psi_0 \cdot B] = 0$, and $c_1 - c_2 + c_3 = 0$. Also, at $t = 0$, $[\Psi_0] = X_0$, $[\Psi_1] = Z_0$. Therefore, $c_3 = Z_0/E$, and $X_0 = -A \cdot c_1 + B \cdot c_2 - (A+D) \cdot c_3$. Since $c_2 = c_1 + c_3$,

$$X_0 = -A \cdot c_1 + B \cdot (c_1 + c_3) - (A+D) \cdot c_3 \quad .$$

Solving for c_1 in terms of c_3 ,

$$c_1 = [X_0 + c_3 \cdot (A+D-B)]/(B-A) \quad . \qquad \text{(xxvi)}$$

3. Simulated Phage Adsorption Profiles.

The following data can be assumed from best fitting values obtained from the experimental data presented in the Results section of this thesis. (All data on a sec^{-1} basis).

$$[K_1 B] = [0.347 \times 10^{-10}] \times [2.5 \times 10^{8}] = 0.0088$$

$$K_2 = 0.00051 \qquad K_2' = 0.13$$

$$K_3 = 0.0025$$

$$K_d = 0.00003$$

(Note that K_2' represents the reversible decay constant for $[\phi \cdot B]$ from the model incorporating two adsorbing populations. K_d represents the decay of $[\Psi_1]$ to $[\Psi_0]$. Thus, the two rate constants are mutually

exclusive in concept.)

The first hypothesis (schemes 1 and 2) was used to generate best fit adsorption profiles of phage survivors from the above applicable rate constants. If X_0 and X_0' are the initial concentrations of ϕ_0 and ϕ_1, then, at time t,

$$[\phi_0] = \frac{X_0 \cdot [-A \cdot e^{\lambda_1 t} + B \cdot e^{\lambda_2 t}]}{(B-A)}$$

and

$$[\phi_1] = \frac{X_0' \cdot [-A' \cdot e^{\lambda'_1 t} + B' \cdot e^{\lambda'_2 t}]}{(B'-A')} .$$

But $X_0 = \alpha \cdot P_0$ and $X_0' = (1-\alpha) \cdot P_0$, where P_0 is the total initial phage population that is viable, and α is the fraction of survivors retaining the adsorption characteristics of the untreated phage. Therefore,

$$[\phi_0] + [\phi_1] = P_0 \left[\frac{\alpha[-A \cdot e^{\lambda_1 t} + B \cdot e^{\lambda_2 t}]}{(B-A)} + \frac{(1-\alpha) \cdot [-A' \cdot e^{\lambda'_1 t} + B' \cdot e^{\lambda'_2 t}]}{(B'-A')} \right].$$

Thus, a normalized concentration of $[\phi_0] + [\phi_1]$, at any time, t, can be calculated from this expression, since all of the coefficients can be numerically solved from the rate constants.

It has been shown that, for the second hypothesis of Fab' dissociation, at any time, t,

$$[\Psi_0] = -c_1 \cdot A \cdot e^{\lambda_1 t} + c_2 \cdot B \cdot e^{\lambda_2 t} - c_3 \cdot (A+D) \cdot e^{\lambda_3 t}$$

and

$$[\Psi_1] = c_3 \cdot E \cdot e^{-K_d t} .$$

If X_0 and Z_0 are the initial values of $[\Psi_0]$ and $[\Psi_1]$, then

$$c_3 = Z_0/E$$

$$c_1 = [X_0 + Z_0(A+D-B)/E]/(B-A)$$

and

$$c_2 = c_1 + c_3 \quad .$$

By normalizing again to the initial total population, i.e., setting $X_0 = \alpha \cdot P_0$ and $Z_0 = (1-\alpha) \cdot P_0$, as in hypothesis 1, it is possible to generate a simulated adsorption curve for $[\Psi_0]$. By adjusting the value of K_d employed in the simulated adsorption curves, until coincident curves of the first and second hypothesis were obtained, it is possible to obtain an estimate of the value of the rate of dissociation of the Fab' phage complex which would be required to explain the actual adsorption data by a one-hit theory of neutralization.